

***In Vivo* Analysis of Parvins,
A Family of Focal Adhesion Proteins**

INAUGURAL-DISSERTATION

zur

Erlangung des Doktorgrades

der Mathematisch-Naturwissenschaftlichen Fakultät

der Universität zu Köln



Vorgelegt von

Haiyan Chu

Aus Jiangsu, China

Köln, Februar 2005

Referees/Berichtererstatter Prof. Dr. Angelika Anna Noegel
 Prof. Dr. Jens Brüning

Date of oral examination/ 03.05.2005
Tag der mündlichen Prüfung

The present research work was carried out under the supervision of Prof. Dr. Angelika Anna Noegel at the University of Cologne and the direction of Prof. Dr. Reinhard Fässler in the Max Planck Institute of Biochemistry, Martinsried, Germany, from January 2002 to January 2005.

Diese Arbeit wurde von Januar 2002 bis Januar 2005 unter der Betreuung von Frau Prof. Dr. Angelika Anna Noegel, Universität Köln und der Leitung von Herrn Prof. Dr. Reinhard Fässler am Max-Planck-Institut für Biochemie, Martinsried, Deutschland durchgeführt.

Table of Contents

	Pages
Table of Contents.....	1-4
List of abbreviations.....	5-6
1 Introduction.....	7-17
1.1 Cell-matrix adhesion	7-8
1.2 ILK, PINCH, parvin and IPP ternary complexes.....	8-15
1.2.1 ILK.....	8-9
1.2.2 PINCH.....	10
1.2.3 Parvin family.....	10-13
1.2.4 The cellular functions of IPP complexes.....	13-15
1.3 Hematopoiesis and the immune response.....	15-17
1.4 Aim of the thesis.....	17
(5 Figures: Figure 1-1to 1-5)	
2 Materials and Methods.....	18-32
2.1 Construction of targeting vectors.....	18-21
2.1.1 Plasmid DNA miniprep and maxiprep, PAC screening and maxiprep	18
2.1.2 Preparation of chemically competent cells.....	19
2.1.3 DNA digestion and purification.....	19
2.1.4 DNA linkers, phosphorylation and annealing of oligonucleotides	19-20
2.1.5 DNA ligation and competent cell transformation.....	20
2.1.6 Southern analysis and colony hybridisation.....	20-21
2.1.7 DNA sequencing.....	21
2.2 Generation of knockout mice.....	21-25
2.2.1 Preparation of feeder cell line.....	21
2.2.2 ES cell culture.....	22
2.2.3 Linearization of targeting vector.....	22
2.2.4 Electroporation of targeting DNA into ES cells.....	22-23
2.2.5 Selection and picking of G-418 positive ES clones.....	23
2.2.6 Identification of recombinant ES clones.....	23-24
2.2.7 Generation of chimeric mice and breeding scheme.....	24
2.2.8 Mice genotyping.....	24-25

2.3	<i>In vivo and in vitro</i> assays.....	25-32
2.3.1	Generation and purification of peptide antibodies.....	25
2.3.2	Peptide blocking experiment.....	25-26
2.3.3	Western analysis.....	26
2.3.4	Immunoprecipitation.....	26-27
2.3.5	DNA mutagenesis and <i>in vitro</i> translation.....	27
2.3.6	Northern analysis and RT-PCR.....	27-28
2.3.7	DNA transfection.....	28-29
2.3.8	Immunofluorescence staining of cultured cells.....	29
2.3.9	Immunostaining of tissue sections.....	29
2.3.10	Magnetic cell sorting	29-30
2.3.11	Generation of BM-derived dendritic cells and macrophages.....	30
2.3.12	Flow cell cytometry analysis (FACS).....	30-31
2.3.13	Immunization.....	31-32
2.4	Reagents and antibodies.....	32
2.5	Statistics.....	32
3	Results.....	33-75
3.1	Generation and characterization of parvin peptide polyclonal antibodies.....	33-39
3.1.1	Generation of α -, β - and γ -parvin peptide antibodies.....	33
3.1.2	Characterization of α -, β - and γ -parvin peptide antibodies.....	33-39
3.1.2.1	α -, β - and γ -parvin antibodies specifically work on Western blot.....	33-35
3.1.2.2	α -parvin antibody works on cell immunostaining.....	35-36
3.1.2.3	α -parvin antibody works on tissue immunostaining.....	36-37
3.1.2.4	α - and γ -parvin antibodies work for immunoprecipitation.....	37-38
3.1.3	Summary.....	38-39
(8 Figures: Figure 3.1-1 to 3.1-8; 1 Table: Table 3.1-1)		
3.2	<i>In vivo</i> analysis of γ-parvin.....	40-63
3.2.1	γ -parvin is expressed in lymphatic tissues, specifically in B cells, T cells, dendritic cells and macrophages.....	40-43
3.2.2	γ -parvin forms complexes with ILK and PINCH1.....	43
3.2.3	Subcellular localization of γ -parvin in fibroblasts.....	43-46
3.2.4	Generation of γ -parvin knockout mice.....	46-53

3.2.4.1	γ -parvin gene structure, alternative splicing and the gene targeting strategy.....	46-49
3.2.4.2	Construction of γ -parvin targeting vector.....	49-52
3.2.4.3	Genotyping strategy for γ -parvin.....	52
3.2.4.4	Generation of γ -parvin chimeric mice.....	52-53
3.2.4.5	Gene deletion of γ -parvin.....	53
3.2.5	Phenotypic analysis of γ -parvin null mice.....	54-63
3.2.5.1	γ -parvin null mice are viable and fertile and show normal Mendelian distribution	54
3.2.5.2	ILK and PINCH1 are downregulated in γ -parvin null hematopoietic cells.....	54-56
3.2.5.3	γ -parvin null mice exhibit normal architecture of lymphoid organs.....	56-58
3.2.5.4	γ -parvin mice show normal hematopoiesis.....	59-61
3.2.5.5	γ -parvin null dendritic cells can mature normally <i>in vitro</i>	61-62
3.2.5.6	γ -parvin null mice display normal T-cell dependent antibody response.....	62-63

(19 Figures: Figure 3.2-1 to 3.2-19; 1 Table: Table 3.2-1)

3.3	<i>In vivo</i> analysis of α-parvin.....	64-75
3.3.1	α -parvin exon 2 deletion.....	64-70
3.3.1.1	α -parvin knockout strategy.....	64
3.3.1.2	Construction of α -parvin targeting vector	64-67
3.3.1.3	Genotyping strategy of wildtype and recombinant alleles.....	67
3.3.1.4	Generation of α -parvin chimeric mice.....	67-68
3.3.1.5	Exon 2 deletion of α -parvin	68-70
3.3.2	Preliminary phenotypic analysis of α -parvin exon 2 deletion mice.....	70-72
3.3.2.1	α -parvin exon 2 deletion mice are smaller.....	70-71
3.3.2.2	α -parvin exon 2 deletion protein can localize to FA.....	71-72
3.3.3	Generation of α -parvin null mice.....	72-74
3.3.4	α -parvin null mice are embryonic lethal.....	75

(13 Figures: Figure 3.3-1 to 3.3-13; 1 Table: Table 3.3-1)

4	Discussions and perspectives.....	76-85
4.1	Parvin peptide antibodies.....	76-77
4.2	Expression profile of parvins and their associated proteins ILK and PINCH1 in the hematopoietic system.....	77-78

4.3	Subcellular localization of γ-parvin in fibroblasts.....	78-79
4.4	ILK-PINCH-parvin complexes.....	79-80
4.5	γ-parvin is dispensable for normal hematopoiesis.....	80-81
4.6	γ-parvin is dispensable for T-cell dependent antibody response.....	81-82
4.7	α-parvin is critical for mouse embryo development.....	82-83
4.8	Intact α-parvin is indispensable for normal embryo development.....	83-84
4.9	Distinct roles of parvin paralogues.....	84-85
5	Summary/Zusammenfassung.....	86-88
6	Acknowledgements.....	89
7	References list	90-95
	Statement/Erklärung.....	96
	Curriculum Vitae/Lebenslauf.....	97-98

List of abbreviations

aa, amino acid(s)

bp, base pairs

BM, bone marrow

BSA, bovine serum albumin

cDNA, complementary DNA

DC, dendritic cell

DEPC, diethylpyrocarbonate

DMEM, Dulbecco's modified eagle media

DTT, dithiothreitol

ECM, extracellular matrix

EDTA, ethylenediaminetetraacetic acid

ELISA, enzyme-linked immunosorbent assay

ERK, extracellular signal-regulated kinase

ES cell, embryonic stem cell

EST, expressed sequence tag

FA, focal adhesion site(s)

F-actin, filamentous actin

FAK, focal adhesion kinase

FBS, fetal bovine serum

FITC, fluorescein isothiocyanate,

g, gram

GAPDH, glyceraldehyde 3-phosphate dehydrogenase

GM-CSF, granulocyte/macrophage colony-stimulating factor

GSK-3 β , glycogen synthase kinase-3 β

h, hour

HRP, horseradish peroxidase

Ig, immunoglobulin

IGF, insulin-like growth factor

ILK, integrin-linked kinase

IPP complexes, ILK-PINCH-parvin complexes

kb, kilobase(s)

KLH, keyhole limpet hemocyanin

LD motif, leucine-rich sequences (LDXLLXXL)
LIM, lin-11, isl-1, mec-3
LN, lymph node
LPS, lipopolysaccharide
M, molar
M-CSF, macrophage colony-stimulating factor
MEKK1, mitogen-activated protein/extracellular signal-regulated kinase kinase 1
min, minute
NP-CG, nitrophenyl-chicken gamma globulin
PAC, P1-derived artificial chromosome
PAGE, polyacrylamide gel electrophoresis
 α -parvin, α -parvin/actopaxin/CH-ILKBP
 β -parvin, β -parvin/affixin;
PAT, Paralysed Arrested elongation at Two-fold
PALS, periarteriolar lymphoid sheath
PAS/AGM, para-aortic splanchnopleura/aorta-gonad mesonephros region
PBS, phosphate-buffered saline
PCR, polymerase chain reaction
PDGF, platelet-derived growth factor
PI3K, phosphatidylinositol-3 kinase
PINCH, particularly interesting new cysteine-histidine rich protein
PIP₃, phosphatidylinositol 3,4,5-triphosphate
 α -PIX, Pak-interacting exchange factor, also called Cool2 (cloned out of library)
PKB/AKT, protein kinase B/AKT
PP, Peyer's patches
PMSF, phenylmethylsulfonyl fluoride
RNase, ribonuclease
RT, room temperature
RT-PCR, reverse transcription-polymerase chain reaction
s, seconds(s)
SDS, sodium dodecyl sulfate
Tris, tris(hydroxymethyl)aminomethane

1. Introduction

Integrins are the major cellular receptors for cell adhesion to extracellular matrix (ECM) proteins and are also important for cell-cell adhesions. Integrin mediated signaling regulates many aspects of cell behaviour.

1.1 Cell-matrix adhesion

Cell interactions with ECM (e.g., fibronectin, vitronectin and various collagens) are mediated by transmembrane cell adhesion receptors. Cell-ECM adhesions are crucial for various biological processes, including cell adhesion, migration, proliferation, differentiation, cell survival and they contribute to embryogenesis, wound healing, and inflammation (Hynes, 2002; Lee and Juliano, 2004). The adhesions with the ECM are mainly mediated by integrins, which connect the ECM to the actin cytoskeleton at the cell interior. Cell adhesion leads to integrin clustering and formation of classical focal adhesions and variants (focal complexes, fibrillar adhesions and podosomes) (Geiger et al., 2001).

Focal adhesions (FAs) are flat and elongated cellular structures that localize near the periphery of the cell. FAs mediate strong cell adhesion to the substrate and anchor bundles of actin microfilaments through a plaque containing many FA associated molecules (Geiger et al., 2001). FA associated proteins include cytoskeletal proteins (e.g. talin, tensin, vinculin, paxillin, α -actinin and α/β -parvin), signalling molecules such as tyrosine kinases (e.g. Src, FAK, PYK2, Csk), serine/threonine kinases (e.g. ILK, PKC, PAK), modulators of small GTPases and other enzymes (PI3 kinase). FA associated proteins can bind to integrins (e.g. ILK, FAK) or actin (e.g. α -parvin, vinculin) and thereby link integrins to the cytoskeleton. Some proteins can directly act as integrin-actin linkers (e.g. talin, familin, α -actinin). Many adaptor proteins interact with integrin-bound and actin-bound components (e.g. PINCH) to link them to each other (Zamir and Geiger, 2001).

FAs serve two significant functions. First they act as an ECM-actin cytoskeleton connection to transmit force or tension at adhesion sites to maintain strong attachments to the underlying ECM. Second, they function as a signalling center (Sastry and Burridge, 2000). The core components of FAs are integrins. Each integrin consists of two transmembrane subunits, called α and β subunits. Integrin engagement leads to the recruitment and activation of signalling proteins such as FAK (Miranti and Brugge, 2002; Playford and Schaller, 2004). Phosphorylation of FAK recruits SH2-containing proteins including Src and Fyn and subsequently a variety of proteins that transduce signals to many

downstream pathways (Cary et al., 1998; Roy et al., 2002; Webb et al., 2004). Rho GTPases control signal transduction pathways that link cell surface receptors to a variety of intracellular responses, although they do not interact with integrin directly (Guo and Giancotti, 2004).

1.2 ILK, PINCH, parvin and IPP ternary complexes

ILK, PINCH and parvin are multidomain proteins that are widely expressed in human and mouse tissues, and are well conserved in evolution (Zhang et al., 2002; Wu, 2004). ILK binds PINCH and parvin and *ILK-PINCH-parvin* form ternary complexes (IPP complexes; Tu, et al., 2001; Wu, 2001; Wu 2004). The complexes act as structural and functional linkers between ECM and the actin cytoskeleton through integrin-binding ILK and actin-binding- parvin proteins (Figure 1-1).

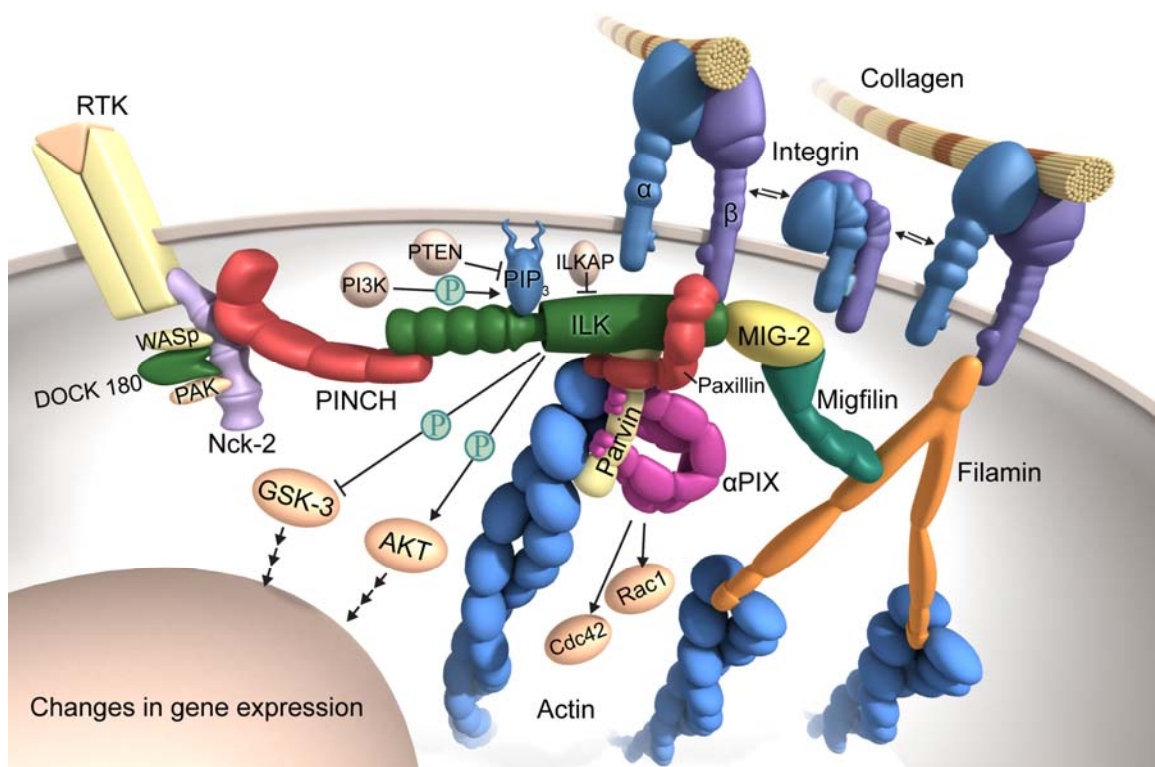


Figure 1-1 ILK-PINCH-parvin complexes localize to focal adhesion sites through the interaction of ILK with the β 1 or β 3 integrin tail. The activation of ILK by PI3K leads to the phosphorylation of PKB/Akt and GSK3 β (from Grashoff et al., 2004).

1.2.1 ILK

ILK was discovered as a serine/threonine protein kinase that interacts with the cytoplasmic tails of $\beta 1$ and $\beta 3$ integrins (Hannigan et al., 1996). ILK is composed of three conserved domains (Figure 1-2). The N-terminal domain contains four ankyrin repeats that bind to the LIM protein PINCH (Tu et al., 1999) and interact with ILKAP, a PP2C phosphatase that negatively regulates ILK kinase activity (Leung-Hagesteijn et al., 2001). The pleckstrin homology (PH)-like motif of ILK binds PIP₃, the product of PI3K (Huang and Wu, 1999). The C-terminal kinase catalytic domain of ILK binds to paxillin and the CH2 domains of α - and β -parvins leading to the FA localization of parvins (Wu and Dedhar, 2001, Tu et al., 2001; Yamaji et al., 2001). Additionally, Pat-4, ILK homologue in *C. elegans*, binds to UNC-112, which in turn binds to filamin-binding protein migfilin. UNC-112 is essential for localization of Pat4/ILK to integrin-containing muscle attachment sites (Mackinnon et al., 2002; Tu et al., 2003).



Figure 1-2 Functional domains of ILK and its binding partners. There are four ANK repeats at the N-terminus of ILK and the first ANK repeat mediates the binding to PINCH1/PINCH2. The PH motif binds PIP₃. The C-terminal kinase domain binds to α -/ β -parvins. Integrin $\beta 1$ binds to the C-terminus of ILK. A paxillin binding site (PBS) lies in the C-terminus of ILK and is important for paxillin binding.

The kinase activity of ILK was shown by its ability to phosphorylate peptides and model substrate myelin basic protein *in vitro* (Hannigan et al., 1996), and to induce phosphorylation of the protein kinases PKB/Akt at Ser473 and GSK-3 β at Ser9 in cells overexpressing ILK (Delcommenne et al., 1998). PKB/Akt is a Ser/Thr kinase implicated in cell proliferation and growth factor signaling and is a key signalling intermediate in the survival pathway (Lawlor and Alessi, 2001; Cantley, 2002). GSK-3 β is inactivated by phosphorylation mediated by ILK (Delcommenne et al., 1998; Cohen and Frame, 2001). However, recently it was shown that the kinase activity of ILK is not required for PKB/Akt and GSK-3 β signaling in several vertebrate cell types nor is it necessary for invertebrate development. As the defects in ILK null flies and worms could be fully rescued with ILK mutants that lacked kinase activity (Zervas et al., 2001; Mackinnon et al., 2002). Furthermore, ILK-null fibroblastoid cell lines and ILK-null chondrocytes have severe

adhesion and proliferation defects but normal phosphorylation of PKB/Akt and GSK-3 β (Sakai et al., 2003; Grashoff et al., 2003).

Several adaptor proteins such as PINCH and parvin that bind ILK directly or indirectly, regulate the actin cytoskeleton (Brakebusch and Fässler, 2003).

1.2.2 PINCH

PINCHs are LIM-only adapter proteins. There are two PINCH proteins, PINCH1 and PINCH2 in mammals and they are encoded by different genes and share significant sequence similarity (Zhang et al., 2002a; Braun et al., 2003). PINCH binds to the first N-terminal ANK repeat domain of ILK through the LIM1 domain and links cell-adhesion mediated integrin signalling to growth factor receptors via an interaction with Nck-2 (Tu et al., 1999; Figure 1-3). Nck-2 interacts with growth factor receptor tyrosine kinases such as epidermal growth factor receptor (EGFR) or platelet-derived growth factor receptor (PDGFR), and recruits a large number of proteins including actin modulators such as Dock180 and the p21-activated kinase (PAK) (Velyvis et al., 2003). The interaction of ILK with PINCH plays a crucial role in the regulation of cell shape and migration (Tu et al., 1999; Zhang et al., 2002b).

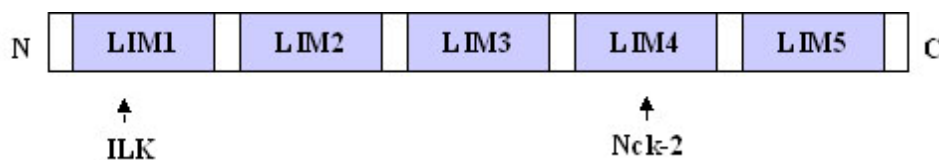


Figure 1-3 The domain structure of PINCHs and their binding partners. PINCHs are 37kD proteins that contain five LIM domains. The LIM domain is a cysteine-rich protein binding motif consisting of around 50 amino acids which can fold into two-zinc fingers. PINCH binds to ILK through its LIM1 domain and the LIM4 mediates binding to Nck-2.

1.2.3 Parvin family

The founding member of the parvin family, α -parvin, also known as CH-ILKBP/actopaxin, was identified independently in several laboratories (Nikolopoulos and Turner, 2000; Olski et al., 2001; Tu et al., 2001). Subsequently two other paralogues of α -parvin, β -parvin (affixin) and γ -parvin, were also identified (Olski et al., 2001; Yamaji et al., 2001). Mammalian α -, β - and γ -parvins are encoded by different genes. The mouse α -parvin gene is located on chromosome 7. β -parvin is located on chromosome 15 and γ -parvin is also present on chromosome 15 around 12 kb downstream of β -parvin. Mouse parvin genes

show similar gene structures as those found in humans (Table 3.2-1; Olski et al., 2001). β - and γ -parvin likely diverged from a common ancestral gene as lower organisms including *C. elegans* and *D. melanogaster* only have a single α -parvin-like gene (Olski et al., 2001; Tu et al., 2001; Yamaji et al., 2001; Lin et al., 2003).

Parvins are composed of a single actin-binding domain (ABD) preceded by an N-terminal stretch (Figure 1-4). The ABD contains two calponin homology (CH) domains in tandem. The N-termini of α - and β -parvins contain two putative nuclear localization signals (NLSs) and three potential SH3-binding sites (Olski et al., 2001). α -parvin contains a paxillin binding site (PBS) within the CH2 domain, which is important for binding to both paxillin and ILK (Olski et al., 2001; Nikolopoulos and Turner, 2002).

Parvins are highly conserved between human and mouse. Mouse α -parvin is a 42.1 kD protein composed of 372 amino acids (aa), sharing 98.9% identity with human α -parvin at the amino acid level. Human and mouse β -parvins share high homology to α -parvin. Human and mouse γ -parvins are composed of 331 amino acids and are more distantly related to α -parvin (Olski et al., 2001).

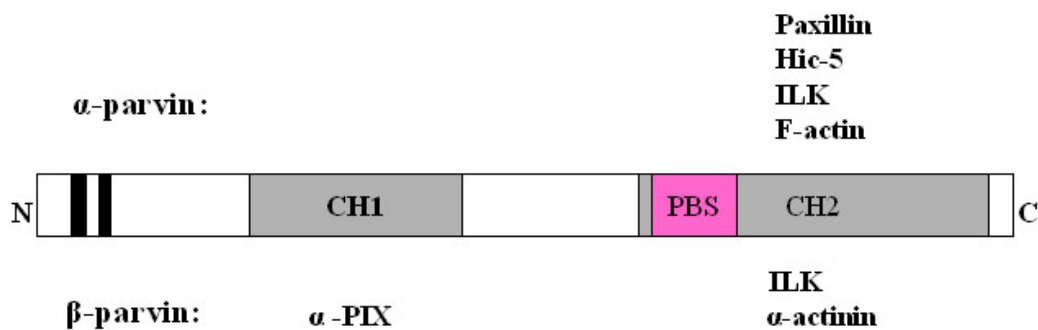


Figure 1-4 Schematic representation of the domain structure of α - and β -parvin and their binding partners. There are two putative NLSs (black boxes) at the N-termini of the proteins. A paxillin binding site (PBS; 273-290) (purple box) locates in the CH2 domain of α -parvin. γ -parvin has similar protein structure with a shorter N-terminus and lacks the NLSs.

In human and mouse there are single α -parvin proteins (Nikolopoulos and Turner, 2000; Olski et al., 2001; Tu et al., 2001). There are four β -parvin isoforms expressed in humans arising from alternative splicing or alternate initiation sites, called CLINT (397 aa), β -parvin(l) (365 aa), β -parvin(s) (351 aa) and β -parvin(ss) (314 aa), in order of decreasing length (Yamaji et al., 2001; Mongroo et al., 2004). CLINT is only found in human. The N-terminal sequence of CLINT arises from two unique 5' exons (Mongroo et al., 2004). The three shorter β -parvin isoforms, β -parvin(l), β -parvin(s) and β -parvin(ss), are generated by different promoter usage (Yamaji et al., 2001). α -parvin is widely expressed (Nikolopoulos

and Turner, 2000; Olski et al., 2001; Tu et al., 2001; Yamaji et al., 2001). β -parvin is also widely expressed with higher expression levels in heart and skeletal muscles (Yamaji et al., 2001) and β -parvin(ss) is the major isoform in spleen tissue and in platelets (Yamaji et al., 2002). γ -parvin seems to be predominantly expressed in lymphoid organs (Korenbaum et al., 2001).

α -parvin directly binds to F-actin, paxillin, Hic-5 (hydrogen peroxide-inducible clone-5), and ILK (Nikolopoulos and Turner, 2000; Olski et al., 2001; Tu et al., 2001). β -Parvin directly binds to ILK, α -actinin and α -PIX (Yamaji et al., 2001; Rosenberger et al., 2003; Yamaji et al., 2004; Mishima et al., 2004). α -PIX activates Rac and Cdc42 and has been implicated in X-linked non-specific mental retardation (Kutsche et al., 2000). β -Parvin probably binds F-actin although this has never been shown directly (Yamaji et al., 2001; Brakebusch and Fässler, 2003). No γ -parvin binding partners have been identified so far.

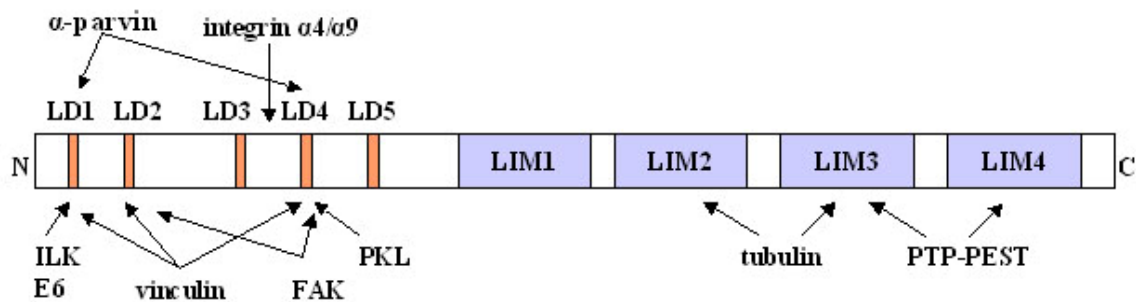


Figure 1-5 Domain structure and binding partners of paxillin. Paxillin is composed of N-terminal leucine-rich LD motifs and C-terminal LIM domains that mediate protein-protein interaction. Paxillin binding partners include structural proteins (parvin, vinculin, tubulin) and signalling molecules (FAK, PTP-PEST) (Brown and Turner, 2004).

Paxillin is a multidomain protein that localizes to FAs and functions as a molecular adaptor or scaffold protein that provides multiple docking sites at the plasma membrane and is involved in the integration of growth factor- and adhesion-mediated signal transduction pathways (Turner 2000; Figure 1-5). While most integrin-associated proteins interact with the cytoplasmic tails of β integrins, paxillin interacts with α integrins $\alpha 4$ and $\alpha 9$ (Liu et al., 2001; 2002). Paxillin LD motifs bind to several proteins associated with remodelling of the actin cytoskeleton, such as α -parvin and ILK. For example, α -parvin directly binds to paxillin LD1 and LD4 motifs (Nikolopoulos and Turner, 2000). Additionally, the paxillin LD1 motif also mediates interactions with ILK, vinculin and the papillomavirus protein E6 (Wood et al., 1994; Tong and Howley, 1997; Nikolopoulos and Turner, 2002). An α -parvin PBS mutant (V282G/L285R), incapable of binding paxillin *in vitro*, cannot target to FAs

and ectopic expression of the PBS mutant results in reduction in cell adhesion, which suggests an important role for α -parvin in integrin-dependent remodelling of the actin cytoskeleton during cell motility and cell adhesion (Nikolopoulos and Turner, 2000). Hic-5 is a LIM protein with striking similarity to paxillin that shuttles between FAs and nucleus (Shibanuma et al., 2003) and is implicated in integrin-mediated signalling through an interaction with FAK (Nishiya et al., 2001).

α -actinin consists of an N-terminal ABD containing two CH domains, a central region with four spectrin-like repeats and a C-terminal calmodulin-like domain. Two α -actinin molecules form a dimer. α -actinin binds to β integrins as well as cytoplasmic proteins including vinculin, zyxin and paladin and crosslinks actin filaments to actin bundles and networks and serves as an important scaffold protein (Otey and Carpen, 2004; Ronty et al., 2004). α -actinin binds to the β -parvin CH2 domain in an integrin mediated adhesion-dependent and in an ILK kinase activity-dependent manner (Yamaji et al., 2004). In CHO cells, β -parvin colocalizes with α -actinin and ILK at FAs and at the tip of the leading edge, whereas in skeletal muscle cells they colocalize at the sarcolemma (Yamaji et al., 2001).

α - and β -parvins bind to the C-terminal kinase domain of ILK through their CH2 domains and colocalize with ILK to FAs (Tu et al., 2001; Yamaji et al., 2001). The CH2 domain of α -parvin mediates the FA localization of the protein through its interaction with both paxillin and ILK (Nikolopoulos and Turner, 2000; Tu et al., 2001). An α -parvin point mutation (F271D) that inhibits ILK-binding impairs the FA localization of α -parvin (Tu et al., 2001). The α -parvin CH2 domain alone is sufficient for FA targeting and α -parvin mutants lacking the CH2 domain do not localize to FAs (Tu et al., 2001; Olski et al., 2001). The functional interactions between ILK, α -parvin and paxillin have also been shown to be mutually important for the localization of these proteins to FAs (Nikolopoulos and Turner, 2001; Attwell et al., 2003).

Phosphorylation of α -parvin N-terminus has been implicated in the actin cytoskeleton reorganization processes, such as cell adhesion, migration and mitosis (Yamaji et al., 2001; Curtis et al., 2002; Clark et al., 2004). The N-terminus of α -parvin contains six putative cdc2 phosphorylation sites. The first two consensus phosphorylation sites are phosphorylated by cyclin B1/cdc2 kinase during mitosis and after mitosis there is adhesion-independent dephosphorylation, which suggests that α -parvin dephosphorylation precedes cell spreading and the reformation of FAs (Curtis et al., 2002). Recently, it was shown that Erk may contribute to the cell adhesion/spreading-induced phosphorylation of the N-terminus of α -parvin and the phosphorylation regulates cell spreading and migration (Clarke

et al 2004). β -parvin can be phosphorylated on its CH2 domain by ILK *in vitro*, although the biological significance of the phosphorylation is not known (Yamaji et al., 2001).

1.2.4 The cellular functions of IPP complexes

Multiple IPP ternary complexes may be present in the same cell. α - and β -parvin are co-expressed in certain cell types (Zhang et al., 2004). PINCH1 and PINCH2 are also often present in the same cell (Zhang et al., 2002a). Both α - and β -parvins bind to ILK and form ternary complexes with ILK and PINCH (Tu et al., 2001; Zhang et al., 2004). The binding of α - and β -parvin to ILK is mutually exclusive. Similarly, one ILK molecule cannot bind to two PINCH molecules simultaneously (Zhang et al., 2002; Zhang et al., 2004).

IPP complexes formation is essential for their recruitment to FAs, and the complexes formation precedes the recruitment into FAs (Zhang et al., 2002c). Disruption of the IPP complexes significantly impairs cell shape modulation, cell motility and fibronectin matrix deposition (Zhang et al., 2002d; Guo and Wu, 2002). Different IPP complexes have been suggested to play distinct roles, although they may share certain common functions (Wu, 2004). Each component of the PINCH1-ILK- α -parvin complex has been shown to be important to protect cells from apoptosis (Fukuda et al., 2003a). For example, α -parvin has been shown to regulate cell survival by facilitating membrane translocation, but not the phosphorylation, of PKB/Akt. The membrane targeting of PKB/Akt is an early and obligatory step in the activation of PKB/Akt. Cells that were depleted of α -parvin by RNAi undergo extensive apoptosis despite the presence of cell-ECM contacts and soluble growth factors. While PINCH1-ILK- β -parvin complexes were suggested to play a proapoptotic role (Zhang et al., 2004). The IPP complexes stabilize the individual proteins of the complexes and the mutual dependence of the IPP components is well conserved in both mammals and invertebrates (Fukuda et al., 2003b; Lin et al., 2003).

Rho GTPases (Cdc42, Rac, and Rho) act as molecular switches to control signal transduction pathways by cycling between a GDP-bound inactive form and a GTP-bound active form and they interact with downstream targets to elicit a variety of intracellular responses, including the regulation of actin dynamics (Etienne-Manneville and Hall, 2002). ILK, PINCH, α - and β -parvin have been shown to provide a signaling pathway that links integrin signaling to Cdc42/Rac activation. The loss of PINCH1 or ILK, significantly reduced the activation of Rac (Fukuda et al., 2003b), while loss of α -parvin, but not β -parvin, markedly stimulated Rac activation and enhanced lamellipodium formation (Zhang et al., 2004). β -parvin binds to α PIX, a Rac/Cdc42-specific guanine nucleotide exchange

factor, and they co-localize at the cell periphery to lamellipodia and ruffles in cells adhered to fibronectin (Rosenberger et al., 2003). Over-expression of the α PIX-binding β -parvin CH1 domain induced significant actin reorganization in MDCK cells by activating Cdc42/Rac, and disrupted epithelial cell polarity (Mishima et al., 2004).

In vivo genetic studies of PINCH, ILK and parvin have widened our knowledge of their functions. In invertebrates *C. elegans* and *Drosophila*, mutations in PAT-4/ILK, UNC-97/PINCH lead to embryonic lethal with defects in dense body and M line assembly due to the disruption of the integrin–actin linkage (Hobert et al., 1999; Zervas et al., 2001; Mackinnon et al., 2002; Clark et al., 2003). PAT-6, the parvin homologue in *C. elegans*, localizes to body muscle attachments, which are the analogs of focal adhesions. PAT-6 null mutant worm show similar muscle attachment defects. The proper polarization and recruitment of PAT-6/parvin to muscle attachments requires perlecan, integrin, ILK and UNC-112 (Lin et al., 2003). Loss of function of ILK has also been studied in mammals. ILK null mice die during early embryogenesis and the ILK-null cells exhibit altered actin cytoskeleton organization, impaired cell–ECM adhesion and spreading, and reduced proliferation (Sakai et al., 2003; Grashoff et al., 2003; Terpstra et al., 2003). Thus, the cellular phenotypes induced by gene inactivation are remarkably similar to those resulting from disruption of the IPP complexes, which suggests that the formation of the IPP complexes is likely essential for many biological functions (Wu, 2004).

1.3 Hematopoiesis and the immune response

Cell-cell and cell-matrix adhesions of hematopoietic cells are important to control their migration, retention, self-renewal, and differentiation (Prosper and Verfaillie, 2001). Integrins are important cell surface receptors mediating several of these interactions. α - and β -parvins have been implicated in integrin-mediated cell-adhesion and migration (Yamaji et al., 2002; Fukuda et al., 2003b).

All blood cells derive from hematopoietic stem cells (HSC), which have the potential to self-renew and to develop the clonal precursors of all known differentiated blood cell types (Morrison et al., 1995). Hematopoiesis begins in the mouse on day 7 of gestation in the yolk sac outside the embryo proper and in the para-aortic splanchnopleura (PAS)/aortagonad mesonephros (AGM) region in the embryo. Around embryonic stage 8.5 (E8.5), when circulation starts, the HSC are present in the fetal blood and at E10 start to colonize the fetal liver (Weissman, 1994). Later, hematopoietic progenitors seed bone marrow (BM), thymus, spleen and other lymphoid organs.

HSC give rise to lymphoid, myeloid and erythroid precursor cells. These different lineage-committed cells express characteristic markers on their surface. In thymus, the T cell precursors are part of CD4CD8 double negative (DN) population and they do not express molecules characteristic for mature T cells like CD4, CD8 or the T cell receptor complex. During the development of B cells, the first lineage specific marker is B220 (CD45R) and this molecule is expressed at all stages through to activated B cells. B220 expression increases during differentiation. While immature B cells express medium levels B220 (B220^m), mature B cells produce high amounts of B220 (B220^h). CD19 is expressed from the pro B cell stage throughout B cell development. IgM is present on immature B cells after the V, D, J rearrangements of the genes of the immunoglobulin heavy and light chains. In early mature cells a change in RNA processing of the heavy-chain primary transcript leads to production of two mRNAs encoding IgM and IgD. These cells leave the BM and can be activated by their specific foreign antigen in secondary lymphoid organs, where the expression of IgD increases. Activated B cells proliferate, and differentiate into antibody-secreting plasma cells and long-lived memory cells (Janeway et al., 2001).

During the immune response, the macrophages and neutrophils of the innate immune system provide a first line of defense against pathogens. When the innate host defenses are bypassed, evaded, or overwhelmed, an adaptive immune response is required. Adaptive immunity refers to antigen-specific defense mechanisms designed to remove a specific antigen. Three major cell types participate in the acquired immune response: T cell, B cell, and antigen-presenting cells (APC), particularly dendritic cells (DC). An adaptive immune response is initiated when circulating naïve T cells encounter their corresponding antigen in secondary lymphoid tissues presented by APCs. The processed antigen is noncovalently bound to the major histocompatibility complex (MHC) class I and/or MHC class II molecules on the APC. The antigen binding to T-cell receptors (TCRs) activate the T lymphocytes, and lead to their proliferation and differentiation into effector cells. Once activated, some T cells migrate to the sites of infection and help other phagocytic cells destroy the antigen. Other T cells remain in the peripheral lymphoid organ and help B cells respond to the antigen.

Immunological memory is generated during the primary response in part because the proliferation of antigen-stimulated naïve cells creates memory cells through clonal expansion, and in part because memory cells are able to respond more sensitively and rapidly to the same antigen than naïve cells. Thus, immunologic memory in the antibody system is generated by a T-cell-dependent response and carried by long-lived memory B

cells in germinal centers of lymphoid follicles that recognize antigen by high-affinity antibodies. In the early stage of an immune response, plasma cells secrete antibody of the IgM class, while class switching may occur. Class switching occurs in mature B cells and is dependent on antigenic stimulation of the cell if antigen-activated mature B cells receive the cytokines released by activated T cells. During the second immune response, IgG antibodies appear at higher concentration, and great persistence, than IgM (Janeway et al., 2001). Mice deficient in CD40, OCA-B, and Vav1 are unable to switch isotype and can produce only IgM (Kawabe et al., 1994; Kim et al., 1996; Gulbranson-Judge et al., 1999).

1.4 Aim of the thesis

The physiological functions of mammalian parvins are unknown. The aim of my PhD project is to study the functions of parvins *in vivo* using parvin mutant mouse models generated by genetic approaches. The phenotypes of parvin loss-of-function mutants were analysed. This thesis mainly focuses on α - and γ -parvin.

2 Materials and Methods

2.1 Construction of targeting vectors

2.1.1 Plasmid DNA miniprep and maxiprep, PAC screening and maxiprep

Plasmid DNA miniprep

Minipreps were carried out according to a modified QIAGEN[®] protocol as follows. A single fresh bacterial colony was picked and cultured in 2 ml LB medium (1L: 10g NaCl, 10g tryptone peptone, 5g yeast extract) containing appropriate antibiotic (ampicillin 100µg/ml or kanamycin 25µg/ml or chloramphenicol 25µg/ml) at 37°C overnight with vigorous shaking. The next morning, bacteria were harvested and the pellet was resuspended in 200 µl buffer P1 (50mM Tris.HCl, pH 8.0; 10mM EDTA) with 100µg/ml RNase. The bacteria pellet was lysed in 200µl buffer P2 (200 mM NaOH, 1%SDS) and incubated for 5 min at RT. The lysate was neutralized with 200µl chilled buffer P3 (3.0 M potassium acetate, pH5.5) on ice for 5 min and centrifuged for 5 min at 13000 rpm in a tabletop microcentrifuge. The supernatant was taken out and mixed with an equal volume of isopropanol to precipitate DNA. DNA was collected by centrifugation at 13000 rpm for 5 min and the pellet was washed with 400 µl 70% ethanol and air-dried. DNA pellet was dissolved in 50-100µl H₂O.

Plasmid DNA maxiprep

Plasmid DNA was prepared using the QIAGEN[®] plasmid maxiprep kit according to the procedure described by the manufacturer.

PAC screening and maxiprep

129/Sv mouse PAC(P1-derived artificial chromosome) library RPCI21 (from the Human Genome Mapping Project Center, Cambridge, United Kingdom, 10 membranes) was hybridised with mouse α -, β - and γ -parvin cDNA probes derived from EST clones (from I.M.A.G.E, UK-HGRP RC) to screen parvin genomic containing clones. The hybridisation procedures were followed as Materials and Methods 2.1.6. Five positive PAC clones were ordered for each parvin gene.

A single fresh bacterial colony was cultured in 500 ml LB medium at 37°C with antibiotic overnight. Bacterial cells were harvested by centrifugation at 6000 x g for 15 min at 4°C. The pellet was resuspended in 10 ml buffer P1 and lysed with 10 ml buffer P2 and incubated at RT for 5 min. The lysate was incubated with 10 ml chilled buffer P3 on ice for

10 min and centrifuged at 6000 x g for 15 min. The supernatant was taken out and an equal volume of isopropanol was added and incubated at RT for 30 min to precipitate DNA. DNA was pelleted by centrifugation at 4°C for 20 min at 15000 x g and resuspended in 5 ml H₂O. Contaminant RNA was precipitated from the DNA solution by incubating the solution with 5 ml 5M LiCl on ice for 30 min followed by centrifugation at 4°C for 10 min at 20000 x g. DNA supernatant was taken out and incubated with an equal volume of isopropanol at RT for 30 min. DNA was pelleted by centrifugation at 4°C for 20 min at 12000 rpm and washed with 70% ethanol, then resuspended in 700 µl H₂O with 10 µl 10 mg/ml RNase and incubated at 37°C for 1h to remove the remaining RNA. The solution was extracted with 700 µl Phenol/chloroform and DNA was reprecipitated with 70 µl NaAc (3M, pH 5,5) and 700 µl isopropanol. The DNA pellet was washed with 70% ethanol, air-dried and dissolved in 100-200 µl H₂O.

2.1.2 Preparation of chemically competent cells

Fifty microliters of competent DH5α cells were incubated in 5ml LB medium with 0.02 M MgSO₄ and 0.01M KCl and cultured at 37°C overnight. The next day, the 1ml overnight culture was cultured in 150ml prewarmed LB with 0.02M MgSO₄/0.01M KCl and grown for around 1.75 h at 37°C until the culture reached an OD₆₀₀ density of 0.3 to 0.4. The culture was kept on ice for 10 min and spun down for 10min at 6000 rpm at 4°C. The pellet was resuspended in 37.5ml TFBI (25 mM KAc, 50mM MnCl₂, 100 mM RbCl, and 10 mM CaCl₂; pH 5.8; sterilely filtered; with sterile glycerol added to 15%) and kept on ice for 10 min before spinning down at 6000 rpm for 10 min at 4°C. The pellet was resuspended in 4ml TFBII (10mM MOPS pH 7.0; 75mM CaCl₂, 10mM RbCl, 15% glycerol, autoclaved) and cells were aliquoted in 50 µl or 100 µl on dry-ice/isopropanol and kept at -80°C.

2.1.3 Plasmid DNA digestion and purification

Plasmids and vectors were digested with enzymes from New England Biolab. MspI, an isoschizomer of SexAI that cleaves DNA methylated by dcm methylase C (m⁵)CWGG was purchased from SibEnzyme, Ltd. Digested DNA fragments were separated on an agarose gel and visualized by ultraviolet light. The DNA fragments were isolated from an agarose gel and purified with QIAquick[®] or QIAEX[®] II Gel Extraction Kit (QIAGEN) according to the procedure described by the manufacturer. Recovery of the DNA fragments was checked on an agarose gel.

2.1.4 DNA linkers and oligonucleotides phosphorylation and annealing

Sall, PstI, BamHI, NotI phosphorylated DNA linkers were purchased from New England Biolab. Alternatively, the complementary oligonucleotides containing appropriate restriction enzyme sites were phosphorylated and annealed as follows: 1µl 100 pmol/µl oligonucleotides A and Oligonucleotides B were mixed with 1µl 10 x T4 polynucleotide kinase buffer, 1µl 10mM ATP, 5µl H₂O and 1µl T4 DNA polynucleotide kinase and incubated at 37°C for 1h. Seventeen microliters H₂O and 3µl 0.5M NaCl were added and incubated at 80°C for 10min on a heating block. The heating block was switched off and the samples were taken out of the block until the temperature decreased below 30°C.

2.1.5 DNA ligation and transformation

Vector DNAs were digested and dephosphorylated with calf intestinal phosphatase (CIP) in order to reduce vector self-ligation. DNA polymerase I Large Klenow fragment (New England BioLabs) was used to fill in sticky DNA ends. Targeted DNA fragments were ligated to the vectors with T4 DNA ligase (New England BioLabs) in 20µl volume reactions. For Pfu DNA polymerase amplified PCR fragment cloning, DNA fragments were ligated to a blunt-end vector directly. For cloning of Taq DNA polymerase amplified PCR fragments, T-Vector was made by digesting pBlueScript[®] II KS vector with EcoRV and incubated with Taq DNA polymerase in the presence of dTTP at 37°C for 30 min to obtain an extra T at the end of linearized vector fragments.

The ligations were transformed to chemically competent *E. coli* strain DH5α or dam mutant DM110 cells (demethylated mutant). Four microliter ligations were added to 100ul competent cells and incubated on ice for 45 min, heat-shocked at 42°C for 90 sec and incubated for 5 min on ice. The transformants were cultured in 1ml LB medium without antibiotics at 37°C for 30-40 min in a bacteria shaker and plated onto LB plates containing antibiotics with or without blue/white selection.

2.1.6 Southern analysis and colony hybridization

DNA was digested with appropriate enzymes and separated in an ethidium bromide-containing agarose gel. The gel was photographed under UV light. DNA fragments were depurinated in 0.25 M HCl for 10 min, denatured in 0.5 M NaOH/1.5 M NaCl for 20 min 2 times and neutralized with neutralizing buffer (0.5 M Tris.HCl pH 7.0, 1.5 M NaCl) for 20 min 2 times. The DNA fragments were transferred to nylon membrane with 10 X SSC overnight and UV-crosslinked (autocrosslinker; UV Stratalinker 2400, STRATAGENE).

DNA probes were labelled using a random priming DNA labelling kit (rediprimer™ II kit, Amersham Pharmacia Biotech). Unincorporated nucleotides were removed by centrifugation of probe through a G-50 Sepharose column. The blot was prehybridized in church buffer (1L: 10g BSA, 500ml NaPi, 350 ml 20% SDS, 2ml 0.5M EDTA, 10ml 10mg/ml single-strand DNA) at 65°C for 1h and hybridized with probes of 1×10^6 dpm/ml church buffer at 65°C overnight. The blot was then washed with 1% SDS/40mM NaPi 2 times for 20 min and exposed to X-ray film.

For low-efficiency cloning, colony hybridization was used to screen positive clones. The bacteria were picked from one LB plate and scratched onto a second gridded LB plate and the same position of a gridded circular nylon. Both plates were incubated at 37° to regrow the bacteria. The next morning, the bacterial DNA on the membrane was lysed in denature solutions for 5 min and then in neutralization solution for 5min and crosslinked. The membrane was hybridized with radioactivity labelled probes as that for Southern blot. The positive colonies were recovered from the 1st LB plate.

2.1.7 DNA sequencing

Seven hundred micrograms plasmid DNAs or DNA fragments were sequenced with 2µl Big Dye Terminator premixture, 1µl 10 pmol/µl primers in 10 µl volumes. Sequencing cycling program: 95°C 30 sec, 50°C 30 sec, 60°C 4 min, cycling 25 times and samples were kept at 4°C. DNA was precipitated with 0.1 volume 3M NaAc pH5.5 and 2.5 volume 99.9% ethanol and incubated -20⁰C for 20 min. DNA was centrifuged at max speed at 13000 rpm for 10 min and washed with 70% ethanol. The sequencings were performed by Medigenomix (Martinsried, Germany) and viewed with Chromas version1.45.

2.2 Generation of knockout mice (Talts et al)

2.2.1 Feeder cell preparation

Feeder cells were prepared from embryonic stage (E) 14.5 embryos containing a neomycin resistant gene. Embryos were isolated sterilely from the uterus of the pregnant mice. The head, liver, kidneys and spleen of embryos were removed under the stereoscope. The remaining embryonic tissue was cut into small pieces and digested in a 50ml Falcon tube with 1x trypsin-EDTA (1mL/embryo) for 10 min at 37 °C. The tissue was further dissociated by pipetting with a 5ml pipette and incubated 10 min at 37 °C. This procedure was then repeated with a 2-ml pipette and incubated for 5-10 min at 37 °C. Following this

incubation, an equal volume of EF medium (DMEM with 10% FBS) was added to inactivate the trypsin activity. Non-dissociated tissue was allowed to sediment for 1-2 min and the supernatant containing single cells was seeded onto 10-cm dishes (1 dish per embryo). After the cells reached confluence (2 days later), they were trypsinized and plated onto two 175-cm flasks/ per 10cm-petridish. Cells were grown to confluence and then for an additional 3 days to obtain super-confluent cells. Cells were harvested by trypsinization and 10% of the cells were reseeded back onto the 175cm-flasks. The other 90% of harvested cells were centrifuged at 900g for 5 min and the cell pellets were X-irradiated at a dose of 6000 Rad for 5.4 min at the Max-Planck Institute of Neurobiology. Irradiated cells were frozen in freezing medium (70% DMEM, 20% FBS, 10% DMSO) in Nunc CryoTubesTM. with cells from each 175cm² flask frozen into 3 vials. The reseeded cells were grown until they reached super confluence then irradiated and frozen as before. The day after freezing, a vial of cells was thawed and cultured to control efficiency of irradiation and contamination.

2.2.2 ES cell culture

The mouse R1 embryonic stem (ES) cell line, originally from the András Nagy lab in Toronto, Canada, was established from a 129/Sv x 129/Sv-CP F1 3.5-day male blastocyst. The 15th passage R1 ES cells were cultured in ES cell medium supplemented with 20% FBS tested for ES cell use. ES cell medium consisted of DMEM high glucose+ Na-pyruvate+2mM L-Glutamate (Gibco), 0.1 mM 2-mercaptoethanol, 1X non-essential amino acids of 100x stock solution (Gibco), and 1000U/mL leukemia inhibitory factor (LIF). One ampoule of ES R1 cells was thawed and seeded onto a 25cm² flask together with feeder cells in ES medium without antibiotics. The ES medium was changed every day and cells were trypsinized every second day onto 75 cm² or 175cm² flasks 2 to 3 times until enough cells were available for electroporation.

2.2.3 Linearization of targeting vector

One hundred micrograms of targeting construct DNA was digested with NotI in a volume of 200 µl for 1.5 h after which 1µl of digested DNA was separated in an agarose gel and compared with undigested DNA to control the complete linearization. The DNA solution was extracted with 200 µl phenol/chloroform, and followed with 200 µl chloroform /isoamylalcohol (24:1). The DNA was then precipitated with 0.1 volume of 3M Na-acetate pH 5.2 and 2.5 volumes of 99.5% ethanol. A coiled DNA thread was visible after vigorous

shaking. The DNA string was washed with 70% ethanol once and transferred to a capped 1.5 ml tube containing 1ml 70% ethanol and stored at -20°C .

2.2.4 Electroporation of construct DNA into ES cells

ES cells were washed with 1XPBS twice and harvested by trypsinization. The cells were counted and 5×10^7 ES cells were washed twice with 10ml PBS to remove remaining serum. At the same time, six 10-cm dishes were seeded with feeder cells in 7ml ES medium/dish.

The linearized construct DNA was spun down and the 70% ethanol was removed. DNA was air-dried in the hood for 10 to 15 min and dissolved in 700 μl PBS. The DNA/PBS solution was vortexed vigorously for 15-20 min until DNA completely dissolved and was no longer visible. The PBS/DNA solution was added to the 5×10^7 ES cell pellet and gently mixed. The DNA/ES cell mixture was transferred to a Gene Pulser[®] Cuvette (0.4 cm electrode gap, Bio-Rad Laboratories) being careful to avoid air bubbles. The cuvette was incubated at room temperature for 1 min before electroporation (electroporation parameters: 0.8kv, 3 μF , time constant 0.1ms). The cells were taken out from the cuvette with a glass pipette filled with 1ml ES medium and transferred to a 15 ml falcon tube with 10 ml ES medium. The electroporated ES cells were equally distributed to six 10cm-dishes with preseeded feeder cells.

2.2.5 Selection and picking of G418-resistant clones

Selection with 500 $\mu\text{g/ml}$ G418 began on the day following electroporation and was carried out for 6-8 days until picking. ES medium was changed every day during selection. One day before picking, fifteen 24-well tissue culture plates were seeded with feeder cells in 1ml G418-containing ES medium. G418-resistant clones were picked onto a 96-well microtiterplate filled with 150 μl trypsin-EDTA and incubated at 37°C for 5 min. And the ES clones were dissociated into single cells by pipetting up and down several times and transferred to the wells with feeder cells. The medium was changed on the next day to remove the trypsin-EDTA. Approximately 3 days after picking, all clones on one 24-well plate were frozen at the same time. ES Clones were trypsinized and resuspended in 1 ml freezing medium. Half of this was frozen and the remaining half was left in the well, which was then filled with ES medium. The medium was replaced the next morning to prevent the toxic effect of DMSO in the freezing medium.

2.2.6 Identification of positive ES cell clones

The ES cells in 24-well plates were grown for 3-4 days until the medium turned yellow. The yellow medium was sucked away and ES cells were lysed in 0.5ml lysis buffer (100mM Tris-HCl at pH 8.5, 5mM EDTA pH 8.0, 0.2% SDS, 200mM NaCl, 100µg/ml proteinase K). The lysates were kept in lysis buffer for 8 h to 8 days until all samples were lysed. ES cell DNA was precipitated by adding 1 ml isopropanol to each well and the plates were shaken on an orbital shaker for 4-8 h at RT. DNA became visible as web-like structure. DNA was fished out and resolved in 150 µl TE buffer by incubation at 50-55⁰C for 10-12 h. 24 µl DNA was digested with an appropriate enzyme in 30 µl volumes for Southern analysis. Recombinant ES clones were identified with both external and internal probes on Southern blots.

2.2.7 Generation of chimeric mice and breeding scheme

Positive ES cell clones that showed equal density of wildtype and recombinant alleles on Southern blot were selected and cultured for blastocyst microinjections. For microinjection, ES cells were trypsinized and washed twice with ES medium. ES cells were microinjected into C57/B6 blastocysts (day 3.5) and transferred into the uterus of day 2.5 pseudopregnant foster mice. The microinjections were performed in the Department of Molecular Medicine or by the transgenic facility at Max-Planck-Institute of biochemistry in Martinsried. The pseudomothers gave birth to chimeric mice 17-19 days after uterus transfer of injected blastocysts. Using ES cells derived from 129/Sv mice, chimeric mice are recognized by agouti stripes. Highly chimeric male mice were mated to C57/B6 female mice for germ-line contribution of the ES cells. The heterozygous agouti offspring (if viable) were identified by Southern blotting. The heterozygous offspring were then mated to obtain homozygous mice.

2.2.8 Mouse genotyping

Mice were distinguished with numbered ear-tags and approximately 5mm piece of tails were clipped into tubes with corresponding numbers and incubated in 500 µl lysis buffer (50mM Tris-HCl, pH 7.5; 50 mM EDTA; 1% SDS; and 10 µg/ml Proteinase K) at 55⁰C overnight with vigorous shaking. Newborn mice were identified with a toe-clipping identification method. DNA was isolated using a phenol-chloroform extraction or a simplified DNA isolation method that omitted the phenol/chloroform extraction procedure (Laird et al., 1991). PCR analysis was used to identify wildtype, heterozygote and homozygote mice. All reactions were run on a T3 Thermocycler PCR machine (Biometra)

and analyzed using agarose gel electrophoresis. For DNA amplification, genomic DNA was initially denatured for 3 min at 95°C followed by 34 cycles at 95°C for 30 sec, annealing at 53°C for 30 sec and extended at 72°C for 30 sec.

The following primers were used for mouse PCR genotyping.

4 Primers were used for genotyping γ -parvin null mice:

Wildtype allele F 5'-GTT TGA AGA ACT GCA GAA GG-3'

R 5'-GTT GAT CCA TTC CAT CAG CA-3'

Recombinant allele F 5'- CTG GGT AAT AAG CGT TGG CAA T -3'

R 5'- CCA ACT GGT AAT GGT AGC GAC-3'

3 Primers were used for genotyping α -parvin exon 2 deletion mice:

F1 5'-GGA ATG AAC GCC ATC AAC CT-3' (for wildtype allele)

F2 (PGKf): 5'-GAT TAG ATA AAT GCC TGC TC-3' (for recombinant allele)

R1 5'-TGA AAG CAG CTT CGG CCT AAC-3'

3 Primers used for genotyping α -parvin null mice:

F1, F2 are same as those used for α -parvin exon 2 deletion mice

R2 5'-TTG CGT GAG TTT GGA TCG AC-3'

2.3 *In vivo* and *in vitro* assay methods

2.3.1 Generation and purification of peptide antibodies

Peptides of 14-16 amino acids from the N-terminal region of α -, β - and γ -parvins were synthesized and lyophilized in the department of Bioorganic chemistry in Max-Planck Institute. Two mg peptides were coupled to KLH (keyhole limpet hemocyanin, Imject[®] Maleimide Activated mc KLH, PIERCE). KLH is a carrier protein with a large molecule capable of stimulating its own immune response. For the initial immunization, one aliquot of 500 μ g peptide-hapten complexes in 500 μ l PBS was mixed with 500 μ l Inject Freund's Complete Adjuvant (Sigma) in an adaptor (B/BRAUN) between two syringes until emulsion developed. The emulsion was immediately injected subcutaneously to a rabbit with a non-pyrogenic needle (20G x 1/2). After the initial immunization, the animal was boosted with injection of another aliquot of immunogen. This was done 3 times with 2-week intervals. One week after the 3rd boost or 7 weeks after the initial immunization, the animal was bled. Antisera were characterized by Western blotting, cell/tissue immunostaining and immunoprecipitation assays. The antisera were further purified by using SulfoLink[®] kit (PIERCE).

2.3.2 Peptide blocking experiment

The specificity of peptide antisera to respective peptides was tested using a peptide blocking experiment. One microliter antiserum was mixed with corresponding peptides or control peptides. For example, 1 μ l α -parvin peptide antiserum was incubated with 12.5-20 μ g α -parvin peptide or control peptide (same amount of β -parvin or γ -parvin peptide) in 1ml 5% milk/TBS solution and mixed overnight at 4°C. The next morning, the antibody-peptide complex was spun down and removed. The “cleaned” antibody supernatant was diluted in 5% milk/TBS solution and applied to a Western blot. The protein band was abolished by incubation with the respective peptide, but not by control peptide.

2.3.3 Western analysis

Cells were lysed with lysis buffer (0.15 M NaCl, 5 mM EDTA, 1% TX-100; PH 7.4) in the presence of proteinase inhibitors (Pepstatin 1 μ M, Na₃VO₄ 1 μ M, Leupeptin 10 μ M; or proteinase inhibitor tablet, Roche). Alternatively, tissues were homogenized in RIPA buffer (0.15 M NaCl, 50 mM Tris.HCl pH 7.4, 5 mM EDTA, 0.1%SDS, 1% sodium deoxycholate, 1%TX-100 with proteinase inhibitors). Proteins were estimated with BCA™ Protein Assay kit (PIERCE).

Proteins (30 to 50 μ g was used for detection of γ -parvin) were denatured at 95°C with 15mg/ml freshly added DTT or 1% 2-mecaptoethanol and separated by 10% SDS-PAGE and transferred to PVDF membrane (Amersham Pharmacia Biotech) with 15% isopropanol. The blots were stained with 10% Ponceau S (Sigma) to record the ladder of the protein molecular weight marker (BD science, board range). The blots were blocked in 5% non-fat dry milk/TBS pH7.5/0.1%Tween20 (blocking solution) for 1 h at RT and probed with primary antibody in blocking solution for 1 h at RT or 4°C overnight. Blots were then washed with blocking solution 6 times for 5 min each and incubated with the secondary antibody diluted in blocking solution for 1 h at RT. The blots were washed with TBS 5 min 5 times and signal was detected with ECL+Plus™ kit (Amersham Pharmacia). Occasionally blots were stripped with stripping buffer (100 mM 2-mecaptoethanol, 2% SDS, 62.5mM Tris-HCl pH6.7) at 55°C for 30 min with occasional agitation. The blots were washed with TBS 6 times for 5min each to remove 2-ME after stripping and then reprobed using other antibodies.

2.3.4 Immunoprecipitation (IP) assay

Cells were lysed or tissues were homogenized in ice-cold IP buffer (150 mM NaCl, 1 mM EGTA, 1% TX-100, 100 mM NaF, 10% Glycerol, 50 mM HEPES pH7.5, 10 mM Na₄P₂O₇·10H₂O) with proteinase inhibitors. Fifteen milligrams Protein A (Sigma) was incubated in H₂O for 30 min and rinsed with IP buffer by centrifugation at 12000 g 20 sec 3 times and resuspended in 1ml IP buffer. Fifty to one-hundred microliters of Protein A was added to lysate of 500µg-1mg protein and mixed with 1µg parvin antibody by tumbling mixture end over end at 4°C overnight. The next day, the mixture was centrifuged and the pellet was washed with lysis buffer 3 times at 12000 x g at 4°C. The pelleted proteins were denatured in 20-40 µl 1X sample buffer and heated at 95°C for 5min and subjected to SDS-PAGE followed by Western blotting assay.

2.3.5 DNA mutagenesis and *in vitro* translation

LB plates carrying α -, β - and γ -parvin cDNA plasmids in pGEM[®]-T Easy vector were kindly provided by the laboratory of Dr. Angelika A. Noegel (Cologne university). The sequencing of newly maxipreped cDNA plasmids showed a single mutation in each parvin cDNA. The mutations were corrected with QuickChange[™] site-directed mutagenesis kit (STRATAGENE) according to the procedure described by the manufacturer.

Parvin cDNAs (with a stop codon at the 3' end) were amplified with Pfu/Vent[®] DNA polymerase and cloned into a modified pCS2⁺ mammalian SP6 promoter driving expression vector (from Max-Planck Institute of Biochemistry) with FseI and AscI restriction enzyme sites. *In vitro* translation reactions were performed with TNT[®] Coupled Transcription/Translation Systems using rabbit reticulocyte lysate (Promega) according to the supplier's instructions. The post-translation reactions were analyzed by Western blotting.

2.3.6 Northern analysis and RT-PCR

Total RNA was isolated from tissues using TRIzol reagent (GibCo) according to the procedure described by the manufacturer with mild modification. Briefly, tissue samples were homogenized in TRIzol, 50-100 mg tissue/ml TRIzol. Samples were incubated at RT for 5 min. Chloroform was added to the sample (at 0.2x the volume of TRIzol used) and vortexed vigorously and centrifuged at 12000 x g 4°C for 15min. The upper aqueous phase was extracted with 1 volume phenol pH 4.0/chloroform and centrifuged at 12000 x g for 15 min at 4°C. The RNA in the upper aqueous phase was precipitated with 0.5 volume isopropanol and centrifuged at 12000 x g for 15 min at 4°C. The RNA pellet was washed

with 70% ethanol/DEPC-H₂O, centrifuged at 12000 x g for 10 min at 4°C and air-dried. Finally, the RNA pellet was resolved in DEPC-H₂O and quantified at A260.

Six microliters of 15 µg total RNA was denatured in 14 µl denature solution (see below) at 56°C for 10 min and loaded with 2µl loading buffer (see below) onto an agarose-formaldehyde gel and electrophoresed in 1X MOPS buffer at 120V for 2h. The gel was photographed and 18S and 28S ribosomal RNA bands were used to assess the size of mRNA. RNA was transferred to a charged nylon membrane and the blot was probed with ³²P-labeled cDNA probe. The same blot was stripped and reprobed with a NADPH cDNA probe as a RNA loading control.

When RNA concentrations were too low, RNA was precipitated with 0.1 volume 4M LiCl, 2.5 volumes ethanol at -20°C for 1h or overnight.

Agarose-formaldehyde gel preparation: 2.25g agarose was dissolved in 115ml DEPC-H₂O then cooled to 50°C. The gel was then cast with 7.5 ml 20 X MOPS running buffer and 27 ml formaldehyde in a hood.

Solutions: RNA denature solution 140 µl: 20 X MOPS 5 µl, formaldehyde 35 µl, formamide 100 µl. RNA loading buffer: 10µl ethidium bromide, 50µl 10 X formaldehyde gel loading buffer. 10 X formaldehyde gel loading buffer: 50% glycerol, 10 mM EDTA pH 8.0, 0.25%(w/v) bromophenol blue. 20X MOPS gel running buffer: 0.8M MOPS, 0.2M NaAc, 20mM EDTA pH7.0.

For RT-PCR, 2.5 µg total RNA was reverse-transcribed using the SuperScript™ II RNase H⁻ reverse transcriptase (Invitrogen) according to the procedure described by the manufacturer. α-Parvin exon 2 deletion mice mRNA transcripts were analysed using primers derived from exon 1 and exon 3 sequences. F(E1f1): 5'-GCC TCA AAT GCC TGG AAT AA-3', R(E3r): 5'-CAT TGT CCG GAC CTC ATT CT-3'. Amplified products were separated on 2% ethidium bromide agarose gel, visualized by UV transillumination and photographed.

2.3.7 DNA transfection

Full-length γ-parvin cDNA was amplified to include a stop codon at 3' end and cloned into the pEGFP-C1 vector (Clontech) BamHI site to express GFP-γ-parvin fusion protein. To express N-terminal FLAG tagged γ-parvin, full-length γ-parvin cDNA was cloned into the BamHI site of pcDNA3.1-NFLAG vector (Sigma). To express C-terminal FLAG tagged γ-parvin, full-length γ-parvin cDNA without stop codon was cloned into the BamHI site of p3XFAG-CMV-14 vector (Sigma). The control vectors, GFP-γ-parvin, FLAG-γ-parvin, or

γ -parvin-3XFLAG plasmids were transfected to NIH/3T3 cells with PolyFect® Transfection reagent (QIAGEN) in 6-well plates or 10cm-dishes according to the manual. 30-40 h later, cells were trypsinized and reseeded onto fibronectin coated coverslips and fixed with 3-4%PFA after 6 h for immunostaining analysis. Alternatively, cells were directly lysed for Western blotting or immunoprecipitation assays.

2.3.8 Immunofluorescence staining of cultured cells

Coverslips (Ø120mm, MARIENFELD) were sterilized by ethanol immersion and flaming. The coverslips in 24-well were coated with 300ul 5-10 μ g/ μ l fibronectin and kept at 4°C overnight or at 37°C for 1h. Fibronectin was removed and coverslips were rinsed with PBS once and 1 ml medium was added to each well. Cells were grown on coverslips for 6 h before fixation with ice-cold 3% PFA for 20 min. PFA was washed away with 1.5 ml PBS/well, 5 min 3 times. For intracellular protein staining, cells were permeabilized with 0.2% TX-100/PBS for 30 min at RT. Cells were blocked with 5% goat serum/3% BSA in PBS at 37°C or RT for 1 h and incubated with primary antibodies for 1 h at RT or 4°C overnight. Primary antibodies were washed away and incubated with chrome-conjugated fluorescence second antibodies for 1h. For nucleus staining, cells were incubated with 0.1-0.2 μ g/ml DAPI for 5 min at RT. Cells were mounted with evanol and kept at 4°C or -20°C in dark.

2.3.9 Immunostaining of tissue sections

Tissues were frozen in cryomatrix (ThermoShandon, USA) with dry-ice/isopropanol and sectioned (MICROM, HM 500 OM) at 6-8 μ m thickness. Cryosections were air-dried at RT for 1h and isolated using a PAP pen. Tissues were fixed with ice-cold 4% PFA/PBS for 20 min. For immunofluorescence staining of tissue sections, the same procedures were followed as those for cell staining (2.3.8).

2.3.10 Magnetic cell sorting

B cells and T-cells were sorted using a magnetic cell sorting system according to the procedure described by the manufacturer (Miltenyi Biotec Inc. USA). Briefly, 1×10^7 splenic cells were resuspended in 90 μ l sorting buffer (PBS pH 7.2, 0.5% BSA, 2 mM EDTA) in a 15-ml Falcon tube and incubated with 10 μ l mouse FITC conjugated B220, CD4 or CD8 antibodies (BD Bioscience) on ice for 30 min in the dark. The unbound antibody was washed away with 10 ml sorting buffer by centrifugation at 500 x g for 5 min. 5×10^5 cells were taken out for FACS analysis control before sorting. The rest of the cells

were resuspended in 90 μ l buffer with 10 μ l anti-FITC MicroBeads for 15 min at 4-8⁰C. Unbound anti-FITC MicroBeads were washed away and cells were resuspended in 500 μ l buffer and applied to the column in the magnetic field. The column was washed with 500 μ l sorting buffer 3 times. Then the column was removed from the separator and placed in a 1.5ml Ependof tube. 1 ml sorting buffer was added to the column and the labelled cells were immediately flushed out by firmly pressing the supplied plunger. Sorted cells were counted and $2-5 \times 10^5$ cells (around 1/10 of sorted cells) were applied for FACS analysis used for evaluation of the purity of sorted cells. The sorted cells were lysed in 30-50 μ l lysis buffer for Western analysis of parvins, ILK and PINCH expression.

2.3.11 Generation of BM-derived dendritic cells and macrophages

Bone marrow-derived dendritic cells and macrophages were generated in Dr. Michael Sixt's lab in Max Planck Institute of Biochemistry, Martinsried. Briefly, on the day 0, bone marrow from 8-weeks-old control and γ -parvin^{-/-} littermate mice was flushed out and dispersed into single cells by pipetting up and down and seeded into 10cm-petri dishes in 9ml R10 medium (RPMI, 10% serum, 5% penicillin/streptomycin) plus 1ml conditioned medium from the GM-CSF-producing cell line for the generation of dendritic cells ($2-3 \times 10^6$ cells/dish). On the day 3, 8ml R10 plus 2ml GM-CSF were added into each dish. On the day 6, 10ml medium was replaced with 8ml R10 plus 2ml GM-CSF. And on the day 8, around 8×10^6 cultured non-adherent cells were pooled and cultured in a small cell culture dish and LPS (20ng/ml, Sigma) was added to stimulate the maturation of dendritic cells.

To generate macrophages, the same procedure was followed as above, except that 10% L929-conditioned medium, a source for M-CSF, was added into the medium to stimulate the growth of macrophages instead of GM-CSF. And the adherent cells were harvested on the day 7 by trypsinization.

The cells were analysed by FACS with antibodies (CD11c-FITC, MHC II-FITC or biotinylated, Gr-1-PE, F4/80-biotinylated, CD86-PE or biotinylated, CD40-biotinylated; BD Biosciences Pharmigen).

2.3.12 Flow cytometry analysis (FACS)

Lymph nodes, spleen, thymus, Peyer's patches and bone marrow were taken onto cell strainers (70um Nylon, BD FalconTM) with 10 ml cold PBS on a petri dish. Tissues were smashed on the strainer with the inner flat part of a 10 ml-syringe into single cells. Only hematopoietic cells could pass through the strainer. Single hematopoietic cells were

transferred into a 50ml Falcon tube through the strainer. The petri dish was rinsed with an additional 10ml PBS to collect all cells. Cells were spun down at 1300-1500 rpm 5 min at 4°C. The supernatant was removed and cells were resuspended in 5ml FACS buffer (1%BSA/PBS). Splenic cells and thymocytes were diluted in 5 ml FACS buffer, while cells from bone marrow, lymph nodes, and Peyer's patches were diluted in 2 ml or less of FACS buffer. Cells were counted and 1×10^6 cells were distributed into the wells of the round-bottom 96-well plates for staining. Cells were pelleted in 96-well plates and resuspended in 50µl primary antibody and incubated for 30 min on ice in the dark. The cells were washed once by adding 200 µl FACS buffer to the wells and centrifuged at 1300-1500 rpm 5 min at 4°C. Supernatants were sucked away and cells were resuspended in the secondary antibody and incubated for 10-30 min on ice in the dark. The secondary antibody was washed away with 200 µl FACS buffer as before and cells were resuspended in 200 µl FACS buffer and transferred into FACS tubes. 10 µl propidium iodide (PI, 50µg/ml) was added to each sample before FACS measurement to exclude dead cells.

Fluorochrome-conjugated and biotinylated antibodies used in FACS analysis were from BD Biosciences Pharmingen. Antibodies used: IgD-FITC (fluorescein isothiocyanate); B220-PE (phycoerythrin); IgM-Bio (biotinylated); CD4-FITC, CD3-PE, CD-8-Bio, Gr-1-Bio, Mac-1-Bio, Ter119-Bio, NK1.1-FITC, Dx5-Bio. Primary antibodies were diluted in FACS buffer (1:200) and the 2nd SA-Cy5 (Cy5-conjugated streptavidin) was diluted 1:500.

Samples were analysed on a BECTON DICKINSON FACSCalibur. The data were analysed with BD CellQuestTM Pro Software.

2.3.13 Immunization

NP₂₀-CG (nitrophenyl-chicken γ -globulin; from the laboratory of Dr. Ari Waisman, Cologne University) was diluted to 1 mg/ml with sterile PBS. One volume of alum (Imject[®] Alum, PIERCE) was added to NP₂₀-CG and incubated for 30 min at RT with vigorously vortex. Two-month-old control (+/+ or γ -parvin+/-) and γ -parvin-/- mice (n=5-6 in each group) were immunized intraperitoneally with 100 µg NP₂₀-CG (200 µl NP₂₀-CG-Alum emulsion). 50 µl blood was taken from eye with 50 µl capillary on the same day (day 0) before the immunization and on the day 7, 14, 21, and 28 after the immunization. Blood was taken on the day 42 again and 10 µg/mouse of NP₂₀-CG in PBS was administered intraperitoneally for secondary/memory responses and the blood was taken on the day 49, 56, 63 and 70.

Blood was let stand at RT for 2-3 h and centrifuged at 14000 rpm for 15 min and the sera were collected and kept at -20°. The anti-NP-CG (nitrophenyl-chicken gamma

globulin) antibody isotypes (IgM, IgG1, IgG2a, IgG3, Ig κ and Ig λ) were determined by means of ELISA carried out in the laboratory of Dr. Ari Waisman (Cologne University).

2.4 Reagents and antibodies

Primary antibodies; PINCH1 and PINCH2 peptide rabbit polyclonal antibodies were generated by Fabio Stanchi in Max Planck Institute of Biochemistry, Martinsried. Mouse ILK and paxillin monoclonal antibodies were from BD Transduction laboratory. α -tubulin tyrosinated Y/L rat monoclonal antibody referred to Kilimatin et al (1982). α -actin rabbit polyclonal antibody was from Sigma.

Secondary antibodies; Anti-rabbit/mouse/rat IgG(H+L)-HRP were from BD Biosciences. Anti-mouse IgG-FITC/Cy3, anti rabbit Cy3/FITC were from Jackson. FITC-conjugated phalloidin was from Sigma. Rabbit Anti-FLAG polyclonal antibodies were from Sigma.

2.5 Statistics

The statistics of FACS and ELISA data were performed with the Student's t-test. The P value of significance was set at 0.05.

3 Results

3.1 Generation and characterization of parvin peptide polyclonal antibodies

3.1.1 Generation of anti-parvin peptide polyclonal antibodies in rabbits

To generate mouse parvin-specific antibodies, N-terminal peptides were produced corresponding to α -parvin amino acid residues 5-19, β -parvin residues 3-16 and γ -parvin residues 2-17 with an additional cysteine (C) added to the N-terminus of the peptides (Figure 3.1-1). Rabbits were immunized with peptides coupled to carrier protein KLH (keyhole limpet hemocyanin). The antisera were characterized by Western blotting, immunoprecipitation and immunostaining assays.

```

 $\alpha$ -parvin1MATSPQKSPLVPKSPTPKSPPSRKKDSFLGKLGGTLARRKKAKEVSEFQEEGMNAINLPLSPISFELD69
 $\beta$ -parvin      1MSSAPPRSPTPRAP-KMKKDESFLGKLGGTLARRKKKTREVTDLQEEGKSAINSPMAPALVDIH62
 $\gamma$ -parvin                1MELEFLYDL-----LOLP-----KEVAO18

```

Figure 3.1-1 The alignment of N-terminal amino acid sequences of mouse α -, β - and γ -parvin. The peptide sequences synthesized for antibody generation are emphasized with bold letters.

3.1.2 Characterization of parvin peptide antibodies

3.1.2.1 anti- α -, β - and γ -parvin peptide antisera specifically recognize the corresponding proteins on Western blot

Spleen tissue lysate was used for characterization of the antibodies. α -parvin (42 kD), β -parvin (41.7 kD) and γ -parvin (37.5 kD) were recognized by peptide antisera at their calculated molecular weights (Figure 3.1-2). The specificity of the antibodies to respective peptides was tested by a peptide blocking experiment. The corresponding signal of parvin was blocked by preincubation of antibody with the corresponding peptide, but not by control peptide. For α - and γ -parvin, the peptides specifically blocked the parvin signals, while the β -parvin peptide not only blocked the β -parvin signal, but also blocked two additional non-specific proteins.

Parvin paralogues, especially α - and β -parvin, share high homology to each other (74% identity and 85% similarity). In order to investigate the specificity of antibodies between the three parvins, the full-length cDNAs of α -, β - and γ -parvin were cloned into a mammalian expression vector and translated *in vitro* using a SP6 promoter-driving *in vitro* transcription/translation system with rabbit reticulocyte lysate as described in Materials and Methods. The translation reactions were analysed by Western blotting together with spleen lysate as a positive endogenous protein control. Figure 3.1-3 shows that each parvin antibody specifically recognizes the respective protein with no cross-reaction with other parvin paralogues.

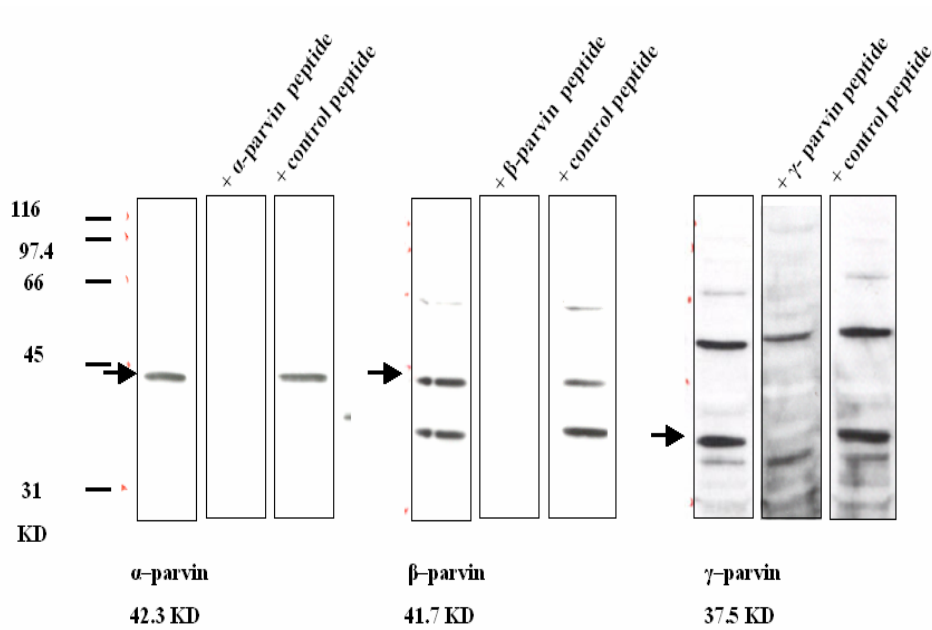


Figure 3.1-2 α -, β - and γ -parvin peptide antisera recognize corresponding parvin proteins at calculated molecular weights (the first column of each blot group, α -parvin 42 kD, β -parvin 41.7 kD, and γ -parvin 37.5 kD) in spleen lysate. The signals were specific to each peptide, which were blocked by corresponding peptides, but not by control peptides.

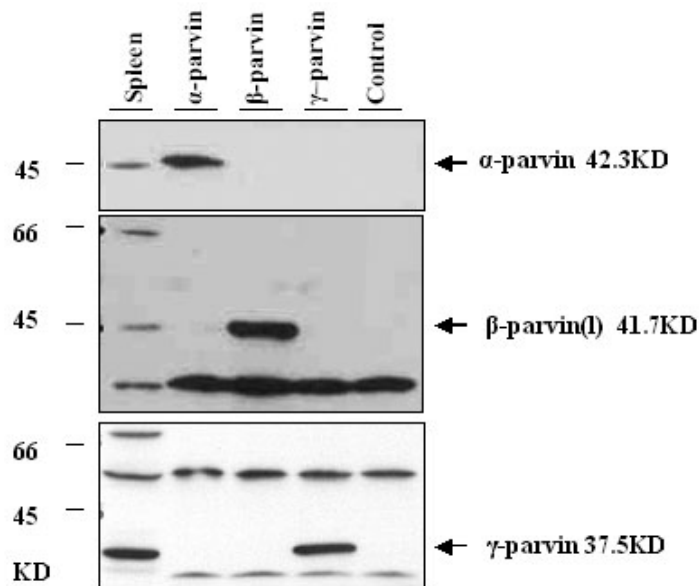


Figure 3.1-3 No cross-reactions between parvin peptide antisera. *In vitro* translated α -, β - and γ -parvin proteins were subjected to SDS-PAGE and probed with α -, β - and γ -parvin peptide antisera. Spleen lysate was used as an endogenous positive control for parvin proteins. No plasmid was added to the (negative) control *in vitro* translation reaction.

There are three β -parvin isoforms expressed in mouse using different promoter usage (Yamaji et al., 2001). The peptide used for β -parvin antibody generation is only present in β -parvin(l) while absent in the two shorter isoforms β -parvin(s) and β -parvin(ss). Therefore, the β -parvin antibody only recognizes β -parvin(l).

3.1.2.2 α -Parvin antibody works on cell immunostaining

MEF (mouse embryonic fibroblast) cells were used for the characterization of the parvin antibodies on cell immunostaining. The expression of parvins in MEF cells was examined by Western blotting. Both α - and β -parvin(l) are expressed in MEF cells and spleen tissue, and β -parvin(l) is expressed at a lower level in MEF cells than in spleen. γ -parvin is expressed in spleen but not in MEF cells (Figure 3.1-4).

α -parvin antiserum gave specific staining on MEF cells at the sites of focal adhesions. This signal could be specifically blocked by the α -parvin peptide, but not by control peptide (Figure 3.1-5). In contrast, β -parvin antiserum gave only non-specific background-like staining in MEF cells, similar to that of preimmune serum (data not shown). This may be due either to the low expression level of β -parvin(l) in MEF cells or the low binding affinity of the antibody. γ -parvin antiserum gave non-specific staining in nuclei of MEF cells (data not shown). Thus, only the α -parvin peptide antibody works for immunostaining on cultured cells.

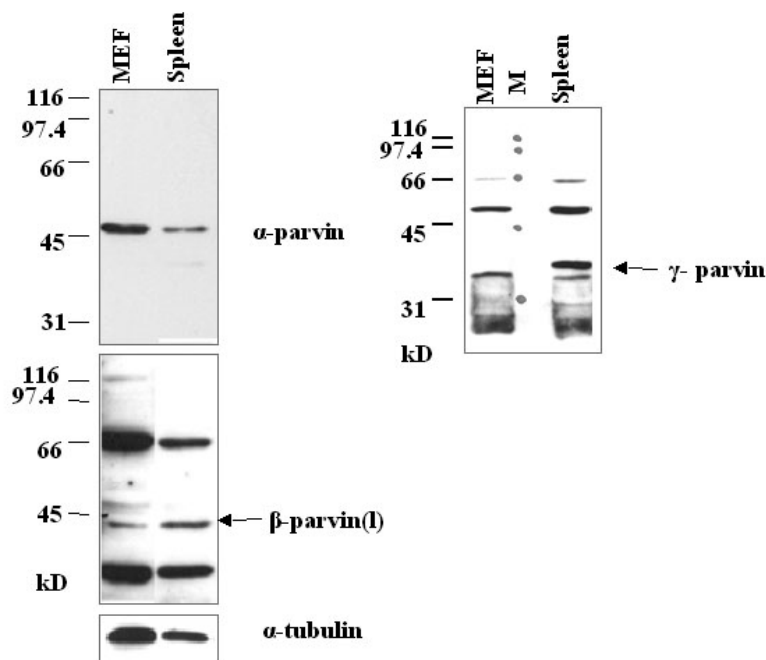


Figure. 3.1-4 α - and β -parvin(l), but not γ -parvin, are expressed in MEF cells. MEF cells and spleen lysates were analysed by Western blotting with anti- α -, anti- β - and anti- γ -parvin peptide antibodies. Anti- α -tubulin antibody was used as a loading control. M, molecular weight marker.

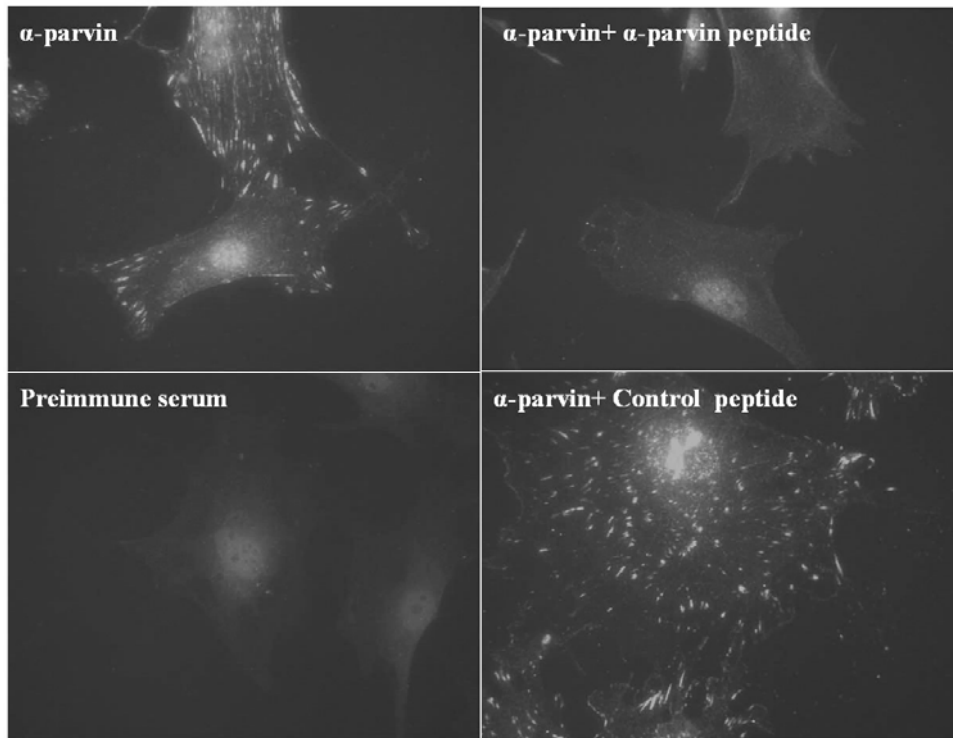


Figure 3.1-5 Immunostaining of α -parvin in cultured cells. α -parvin antiserum gave specific staining in MEF cells at FAs. The signals were specifically blocked by α -parvin peptide, but not by control peptide. The preimmune serums only gave background staining.

3.1.2.3 α -parvin antibody works on tissue immunostaining

The α -parvin peptide antiserum was further characterized for tissue immunostaining on cryosections. The antibody gave specific staining on skin and embryonic tissues of lung, cartilage and muscle (Figure 3.1-6), while the preimmune serum showed only background staining (data not shown). β -parvin antiserum also gave staining on tissues (data not shown), however the signal was not be reliable since the antibody recognized two additional non-specific proteins on Western blot (Figure 3.1-2).

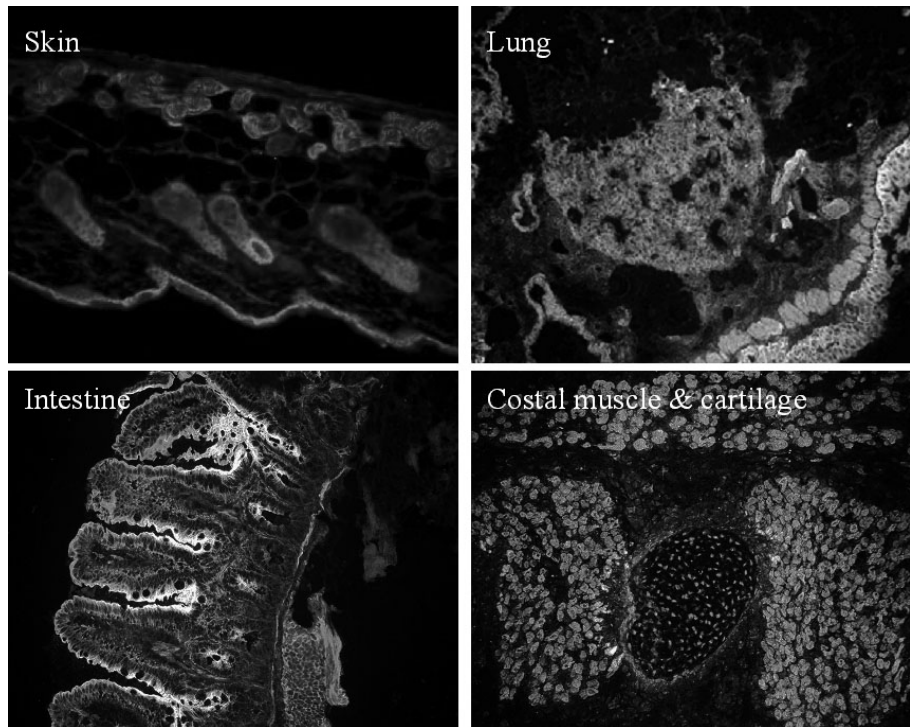


Figure 3.1-6 Immunostaining of α -parvin on tissue cryosections. α -parvin peptide antiserum gave specific signals on tissue cryosections, such as skin and embryonic tissues of lung, muscle and cartilage. Picture magnifications 200x.

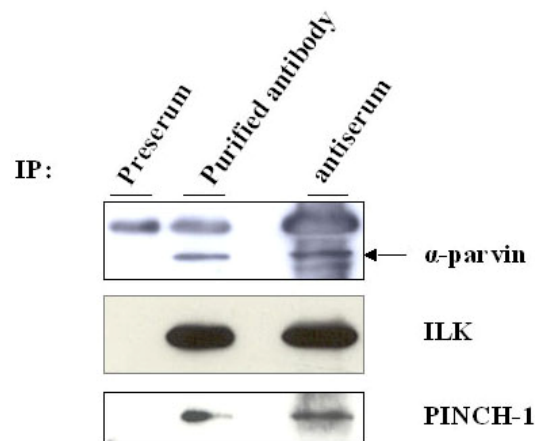


Figure 3.1-7 Coimmunoprecipitation of α -parvin with ILK and PINCH1 in MEF cells. MEF lysates were mixed with α -parvin peptide antiserum, purified antibody or preimmune serum as a control. The immunoprecipitates were analysed by Western blotting with α -parvin, ILK and PINCH1 antibodies.

3.1.2.4 α - and γ -parvin antibodies work for immunoprecipitation

Since α - and γ -parvin peptides specifically blocked the antibody binding to respective parvin proteins, the antisera were purified using the SulfoLink[®] kit. The purified antibodies gave the same patterns on Western blot as the unpurified antibodies (data not shown). The

antisera and purified antibodies were further characterized by immunoprecipitation (IP). Both α - and γ -parvin peptide antisera and purified antibodies could immunoprecipitate the corresponding proteins. Figure 3.1-7 shows that α -parvin, ILK and PINCH1 were detected in the immunoprecipitates with both the α -parvin peptide antiserum and purified antibody in MEF cell lysate. This is consistent with the published data that α -parvin forms complexes with ILK and PINCH1 (Tu et al., 2001; Guo and Wu, 2002; Zhang et al., 2002; Wu, 2004). γ -Parvin was also detected in both γ -parvin peptide purified antibody and antiserum immunoprecipitates from spleen lysate (Figure 3.1-8 and data not shown). Moreover, ILK and PINCH1 were also detected in the immunoprecipitate with the γ -parvin antibody, indicating that the ILK-PINCH-parvin ternary complex can be formed with all three parvin isoforms.

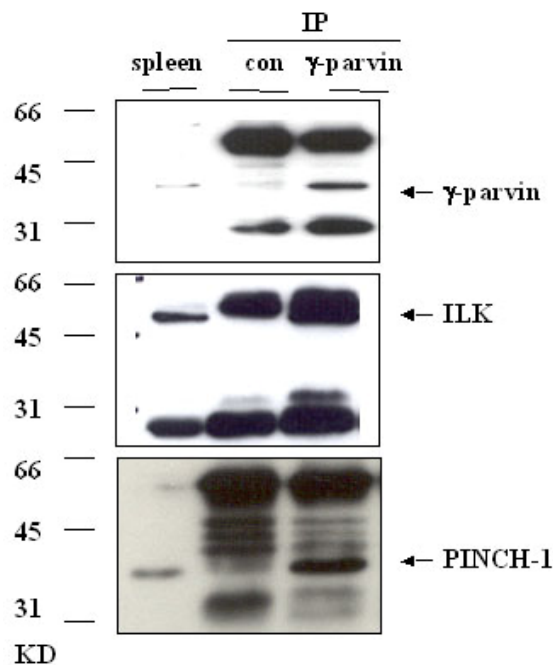


Figure 3.1-8 Coimmunoprecipitation of γ -parvin with ILK and PINCH-1 in spleen lysate. Spleen lysates were mixed with purified γ -parvin antibody or preimmune serum as a control. The immunoprecipitates were analysed by Western blotting with γ -parvin, ILK and PINCH1 antibodies. Con, preimmune serum.

3.1.3 Summary

The working conditions of parvin antibodies are summarized in Table 3.1-1. All three parvin peptide antibodies work on Western blot. They detect proteins of the correct sizes and the signals can be effectively blocked with the corresponding peptides. Additionally, both α - and γ -parvin antibodies can pull down the ternary complex proteins ILK and PINCH-1 in immunoprecipitation assays. Finally, the α -parvin antibody also works well for cell and tissue immunostaining.

Table 3.1-1 Working conditions of parvin peptide antibodies.

Antiserum	WB dilution	IP	Cell IM dilution	Tissue IM dilution
α-parvin	1:10000	+	1:4000	1:1000
β-parvin	1:5000	-	-	-
γ-parvin	1:5000	+	-	-

The dilutions of antibodies used for Western blotting (WB) and immunostaining (IM) are shown. +, working assay; -, non-working assay.

3.2 *In vivo* analysis of γ -parvin

3.2.1 γ -parvin is expressed in lymphoid tissues, specifically in B cells, T cells, dendritic cells and macrophages

The putative γ -parvin was identified as a parvin family member in 2001 (Olski et al., 2001). Little is known about γ -parvin except its mRNA expression profiles. Northern blots using embryonic and adult mouse tissues, adult human tissues, and various cell lines show that γ -parvin is predominantly expressed in hematopoietic/lymphoid organs (Olski et al., 2001; Korenbaum et al., 2001). I confirmed the γ -parvin mRNA expression pattern by Northern blotting using a 639-bp cDNA probe derived from an EST clone (Accession: BC011200) encompassing nucleotides 140-777 of the cDNA. In agreement with published data, a major transcript of around 2.8-kb was detected (data not shown and Figure 3.2-10B; Korenbaum et al., 2001).

Expression of the γ -parvin protein was confirmed by Western blotting with our anti- γ -parvin peptide polyclonal antibody as described in Results 3.1. The lysates of lymphoid tissues including BM, thymus, spleen, lymph nodes (LN) and Peyer's patches (PP), were resolved to SDS-PAGE and probed with antibodies to γ -parvin, α - and β -parvins, and ILK.

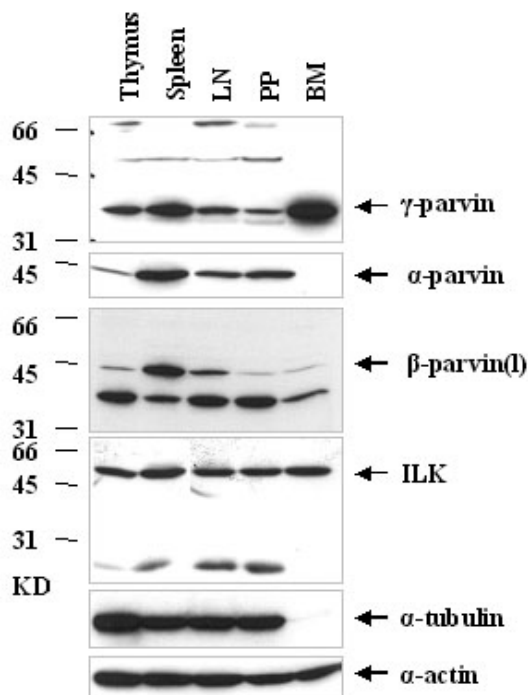


Figure 3.2-1 Expression of parvins and ILK in mouse lymphoid tissues on Western blot. α -tubulin and α -actin were used as protein loading controls.

The blots were stripped and reprobed with α -tubulin and α -actin antibodies as loading controls. γ -parvin was expressed in all five of these lymphoid tissues, with the highest expression level in BM. The other two members of the parvin family, α - and β -parvin, were also expressed in lymphoid tissues. However, very interestingly, α -parvin was not

detectable in BM lysate. Among these five lymphoid tissues, spleen tissue showed higher expression levels of both α - and β -parvins than the other lymphoid tissues. It seems that at least in BM and thymus, γ -parvin is the major parvin member expressed. ILK was expressed in all five lymphoid tissues at similar levels. Previously, it was shown that in some non-lymphoid tissues, such as lung, γ -parvin is moderately expressed, and several variant strong transcripts were detected in testis by Northern blot (Korenbaum et al, 2001). I found that γ -parvin was expressed at a very low level in the lung and was hardly detectable in testis lysate with the anti- γ -parvin antibody (data not shown). This may be due to the low expression level of the protein or the low detection sensitivity of my antibody.

Interestingly, anti-rat tyrosinated α -tubulin monoclonal antibody gave a very weak signal from the lysate derived from BM (Figure 3.2-1). While with anti-rabbit α -actin polyclonal antibody, I showed that similar amount of protein was loaded from BM compared to the other lymphoid organs. The full-length yeast α -tubulin was used as the antigen to generate the tyrosinated rat monoclonal antibody (Kilmartin et al., 1982). Hematopoietic cells in BM have a high divergence with regard to the tubulin protein (Josh and Cleveland, 1990). The failure to detect α -tubulin in BM may be due to the low cross-reactivity between tubulin species or the tyrosination difference arising from the sequence divergence (Wehland et al., 1984).

To further investigate cell-type specific expression of γ -parvin, B and T cells were sorted by FACS from adult mouse splenic cells using antibodies against the B cell marker B220 and T cell markers CD4 and CD8. Spleen single cell suspension was prepared as described in Materials and Methods. Only hematopoietic cells could pass through the cell strainer while the tissue stroma cells were removed. The purities of the sorted cells were examined by FACS analysis and the lysates derived from B220+, CD4+ and CD8+ cells were used for Western analysis. γ -parvin, but not α - and β -parvin(1), was expressed in B220+, CD4+ and CD8+ subpopulations (Figure 3.2-2). Consistent with the absence of α -parvin in BM lysate, α -parvin was not detected in B220+, CD4+ and CD8+ cell subpopulations, nor in spleen single cell preps (data not shown), suggesting that α -parvin was not expressed in hematopoietic cells. β -parvin(1) was expressed in spleen single cell preps but was absent in B220+, CD4+ and CD8+ subpopulations,

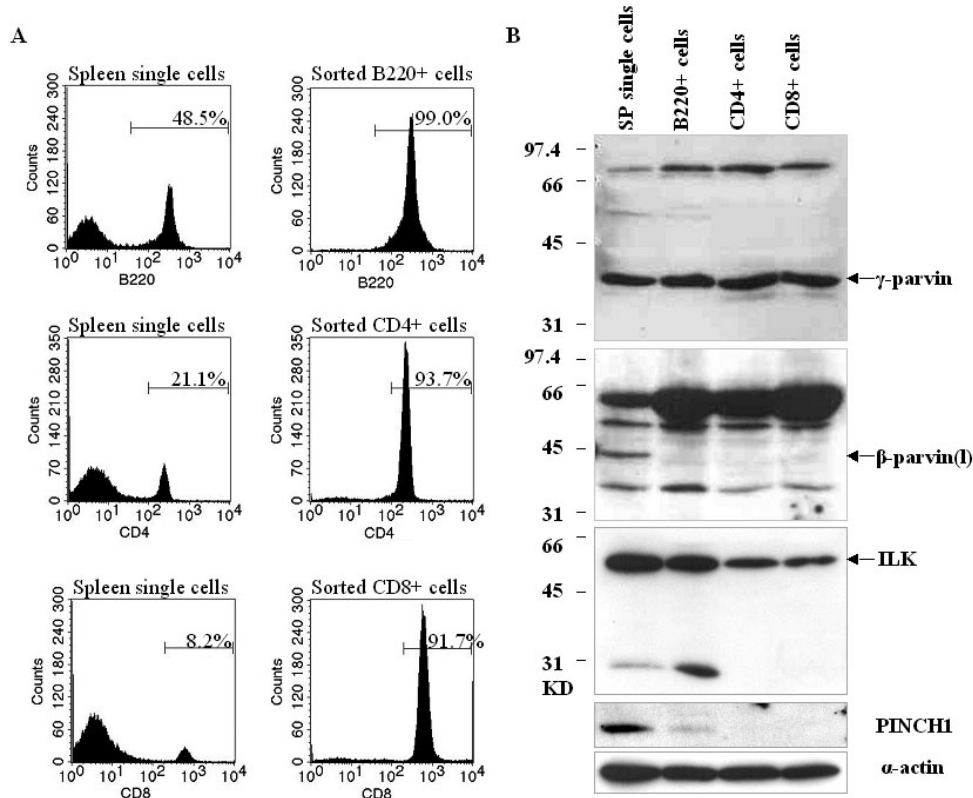


Figure 3.2-2 B220+, CD4+ and CD8+ cell-specific expression of parvins, ILK and PINCH1. (A) The purities of B220+, CD4+ and CD8+ cells were 48.0%, 21.1% and 8.2%, respectively, before sorting and reached 99.0%, 93.7% and 91.7%, respectively, after sorting. (B) Western blot of parvins, ILK and PINCH1 in splenic cells and sorted B220+, CD4+, CD8+ cells.

which indicated that β -parvin(l) was likely expressed in erythroid and/or myeloid lineages. ILK was expressed in B220+, CD4+ and CD8+ subpopulations and the expression levels were lower in CD4+ and CD8+ T cells compared to those in B220+ cells. PINCH1 was weakly expressed in B220+ cells. Consistent with its low expression in thymus (Figure 3.2-11), PINCH1 was not detectable in splenic CD4 and CD8+ T cells. PINCH2 was not detectable in lymphoid tissues of thymus or spleen (data not shown).

To further investigate whether γ -parvin was expressed in other cell types, such as the myeloid lineages, BM-derived macrophages and dendritic cells were generated as described in the Materials and Methods. The purities of cultured dendritic cells and macrophages were 85% and 98.7% respectively, as estimated by FACS using CD11c, MHCII and Gr-1 antibodies for dendritic cells and Mac-1, F4/80 for macrophages (Figure 3.2-12A and B). Both dendritic cells and macrophages expressed γ -parvin and the expression level of γ -parvin in macrophages was higher than that in dendritic cells (Figure 3-12C, lane 2 and 4).

β -parvin(l), but not α -parvin, was also expressed in dendritic cells and macrophages. Thus, γ -parvin was coexpressed with β -parvin(l) in dendritic cells and macrophages.

3.2.2 γ -Parvin is associated with ILK and PINCH1 and forms ILK-PINCH1- γ -parvin ternary complexes

It is known that both α - and β -parvins bind to ILK and PINCH1 and form ILK-PINCH-parvin (IPP) ternary complexes (Tu et al., 2001; Guo and Wu, 2002; Zhang et al., 2002). To investigate whether γ -parvin has such a property, spleen tissue lysate, which is abundant in γ -parvin protein, was immunoprecipitated with anti- γ -parvin purified antibody and preimmuneserum as a control. As shown in Figure 3.1-8, γ -parvin, ILK and PINCH1 were detected in the immunoprecipitates with γ -parvin antibody, but not with control preimmuneserum. Thus, like α - and β -parvin, γ -parvin also formed ternary complexes with ILK and PINCH1. The ILK-PINCH- γ -parvin (IPP) ternary complexes are present in spleen, suggesting the ILK-PINCH- γ -parvin complexes could be formed in at least B220+ cells, dendritic cells and macrophages, where all three proteins are expressed (Figure 3.2-12).

3.2.3 Subcellular localization of γ -parvin in fibroblasts

Both α - and β -parvins localize to FA sites (Olski et al, 2001; Yamaji et al., 2001). The formation of ILK-PINCH- α -parvin complexes is necessary for FA localisation of each component (Zhang et al., 2002c). The association of γ -parvin with ILK and PINCH1 in spleen makes it worthwhile to test whether γ -parvin also localizes to FA as α - and β -parvins do. To visualize the subcellular localization of γ -parvin, γ -parvin was tagged at the N-terminus with GFP. The control pEGFP vector and pEGFP- γ -parvin plasmid were transfected into NIH/3T3 fibroblasts. GFP- γ -parvin fusion proteins formed aggregate-like structures surrounding the nucleus. The expression of GFP and GFP- γ -parvin fusion proteins was confirmed with both γ -parvin antibody and GFP antibody by Western blot (Figure 3.2-3). Surprisingly, a small amount of GFP and γ -parvin were detected separately in the lysate of GFP-tagged γ -parvin transfected cells, indicating that some of the GFP- γ -parvin fusion protein was cleaved between GFP and the γ -parvin linker region. The instability/cleavage of the fusion protein may account for the formation of aggregates. Alternatively, N-terminal tagged-GFP may interfere with the interactions between γ -parvin and its binding partners or interacting proteins, which would then interfere with the proper subcellular localization of GFP- γ -parvin.

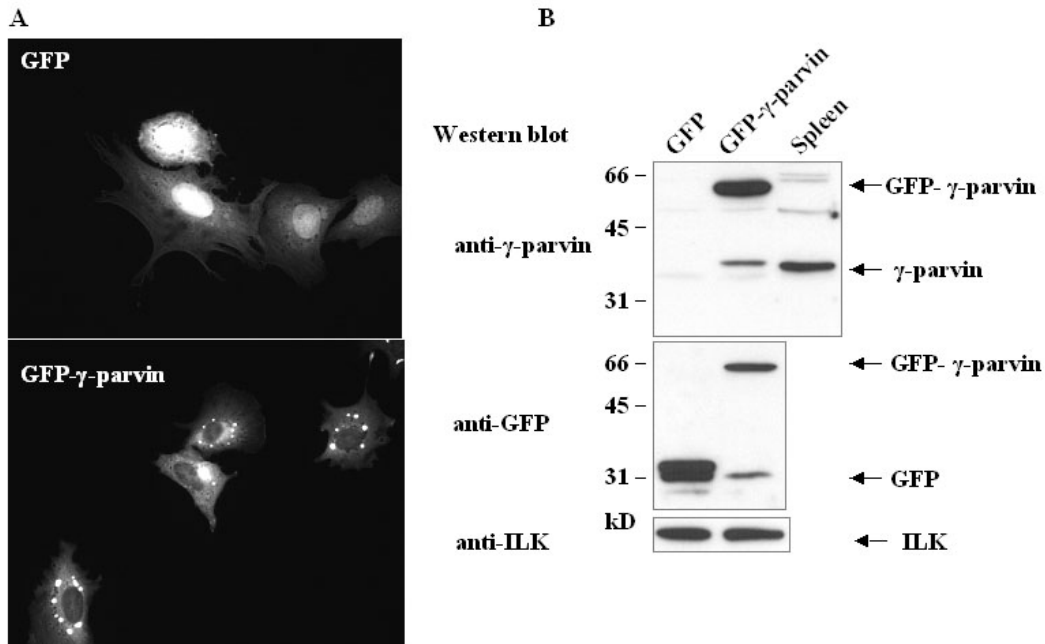


Figure 3.2-3 Subcellular localization of γ -parvin in fibroblasts. GFP and GFP- γ -parvin plasmids were transfected into NIH/3T3 cells. (A) GFP- γ -parvin formed aggregates in the cytoplasm and it was absent in focal adhesion-like structures, while GFP was distributed in both the cytoplasm and the nucleus. (B) Expression of GFP and γ -parvin fusion proteins. A small amount of GFP and γ -parvin were also detected in GFP- γ -parvin transfected cells by Western blotting. Spleen lysate was used as an endogenous γ -parvin protein control.

To exclude the possible interference of GFP-tag on the subcellular localization of γ -parvin, a short Flag epitope was tagged either to the N- or the C-terminus of the protein. The constructs were transfected into NIH/3T3 cells. Cells were then stained with rabbit anti-Flag antibody and mouse anti-ILK, anti-paxillin antibodies or FITC-phalloidin. Flag- γ -parvin displayed a cytoplasmic distribution and showed no colocalization of γ -parvin with ILK, paxillin or the tip of actin stress fibers (Figure 3.2-4). C-terminal Flag-tagged γ -parvin showed the same cytoplasmic distribution in NIH/3T3 cells (data not shown). The protein expression of Flag-tagged γ -parvins was confirmed by Western blot (Figure 3.2-5 and data not shown)

The absence of γ -parvin in FA structures in NIH3T3 cells is probably due to the very weak binding affinity of exogenously expressed γ -parvin with ILK compared to endogenous α - and β -parvins, which are expressed at high levels in 3T3 cells. To test this, lysates derived from C-terminal Flag vector and γ -parvin-Flag plasmid transfected cells were immunoprecipitated with γ -parvin antibody and the immunoprecipitates were subjected to SDS-PAGE and probed with γ -parvin and ILK antibodies. γ -parvin, but not ILK, was detected in the immunoprecipitates (Figure 3.2-5), suggesting that exogenously

expressed γ -parvin cannot compete with α - and β -parvin for binding to ILK and therefore fails to localize to FAs. γ -parvin might localize to FA structures in certain cell types under certain conditions. Cells that do not express α - and β -parvin (cells derived from α - and β -parvin double null mice) will be useful to further test this hypothesis.

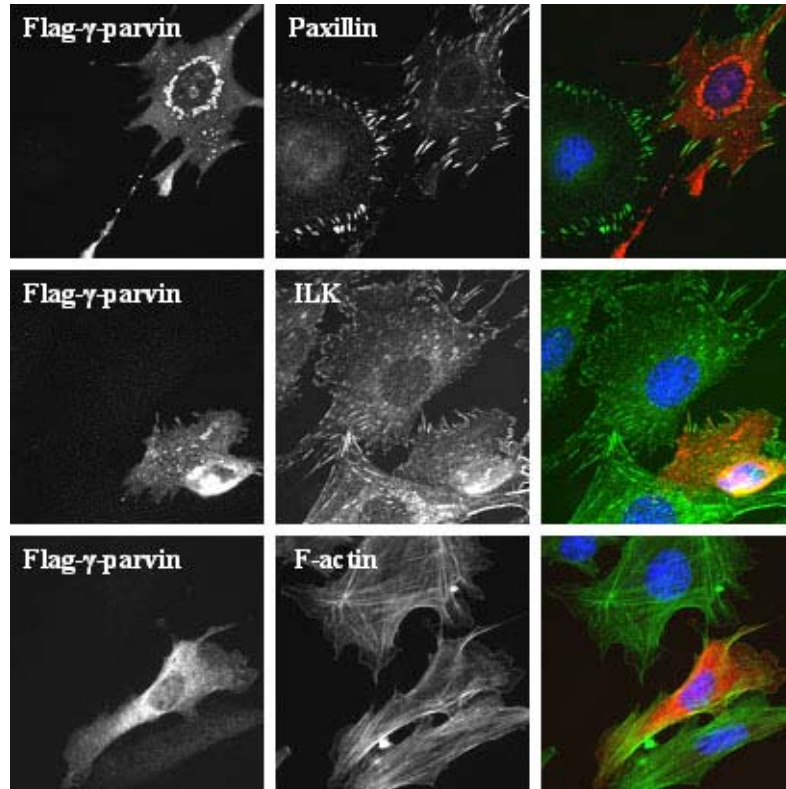


Figure 3.2-4 Subcellular localization of Flag-tagged γ -parvin in fibroblasts. Flag-tagged γ -parvin was absent at focal adhesion site-like structures and distributed in the cytoplasm. Flag-tagged γ -parvin plasmids were transfected into NIH/3T3 cells and stained with rabbit anti-Flag polyclonal antibody and anti-ILK or anti-paxillin antibodies or FITC-conjugated phalloidin. Blue: DAPI staining in the nucleus. Right panels show the merged pictures.

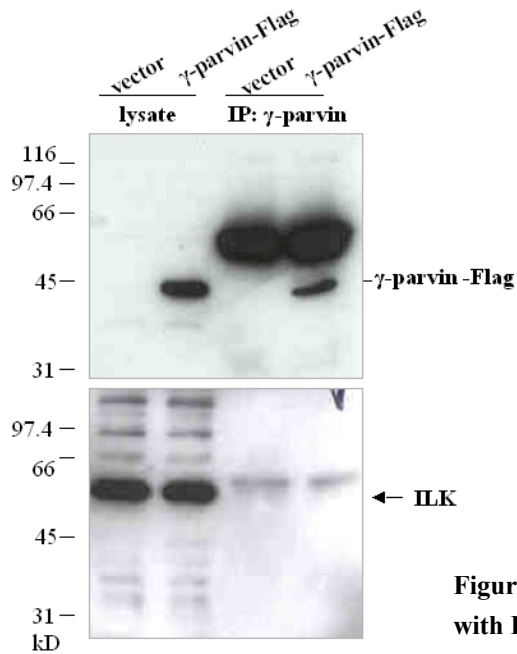


Figure 3.2-5 γ -parvin-Flag was not associated with ILK when expressed in NIH/3T3 cells.

3.2.4 Generation of γ -parvin knockout mice

3.2.4.1 Gene structure, alternative splicing and the targeting strategy

Mouse γ -parvin gene (PARVG) is located on chromosome 15 and is composed of 13 exons. The mouse γ -parvin exons are numbered here according to the published human γ -parvin gene due to the high similarity in their structures (Korenbaum et al., 2001). The exon-intron organization of mouse α -, β - and γ -parvin genes (PARVA, PARVB and PARVG) is summarized in Table 3.2-1. The structures of the mouse γ -parvin gene and protein are shown in Figure 3.2-6. γ -parvin is composed of an N-terminal region followed by two CH domains separated by a linker region. By analysis of the mouse γ -parvin cDNA sequence in the GeneBank Mouse EST database using the NCBI nucleotide BLAST program, two ESTs (BB844229 and AA000543) showed possible alternative splicing of the gene. EST1 was derived from a 6-day neonatal spleen and lacked the first ATG-containing exon (E4), due to a splicing event. There are two additional potential ATGs in exon 6. Thus, the shorter transcript might produce a short γ -parvin protein lacking the amino acids encoded by exon 4 and exon 5. Unfortunately, the translation of this potential short form of γ -parvin could not be investigated with our γ -parvin peptide antibody

Table 3.2-1

Exon-intron organization of mouse alpha, beta, gamma parvin genes

Gene	Exon No	Size	Sequence at exon-intron junction		Intron Size Codon		Amino acid at the splice site	
			5' Splice donor	3' Splice acceptor	bp	phase		
PARVA ch7	1	268	AAGAAG/gtagga	tcttc/TATCCG	\geq 118218	I	V	46
	2	90	TGCTGG/gtaaat	ttacag/TATCCG	466	I	E	76
	3	71	ATGAAG/gtaaga	ctgcag/GTGCTC	2707	O	K/V	99/100
	4	103	TCTTCG/gtagga	ctgcag/AGAAAC	12793	I	E	134
	5	141	TGGATT/gtgagt	tttcag/CTGTTC	7693	I	S	181
	6	116	GTCCAG/gtaaga	ttttag/AAACGA	4992	O	Q/K	219/220
	7	59	CACAGA/gtatgt	ttccag/GGCCCT	2425	II	E	239
	8	20	GGCATG/gtgagt	tttcag/AACGTG	1025	I	E	246
	9	62	AAGAAG/gtgggt	tttcag/ACCCTC	474	O	K/T	266/267
	10	69	ACACAG/gttggt	atgcag/TTTGCA	2651	O	Q/F	289/290
	11	102	CAGAAG/gtaagg	tgccag/GTCCTG	1132	O	K/V	323/324
	12	73	CAGAAG/GTACTT	ccacag/ACATTG	7517	I	D	348
	13	3153	TACAAA					
PARVB ch15	1	\geq 122	GGGAGG/gtgagt	caacag/TGACTG	39044	I	V	39
	2	90	AGATAG/gtacag	tgacag/AGGAGA	2178	I	E	69
	3	71	GTCAAG/gtgagt	caggta/GTGCTT	9192	O	K/V	92/93
	4	103	TTCTGG/gtgagt	ccaccg/AAAAGC	7522	I	E	127
	5	141	TCCACT/gtgagt	Ccgcag/CTATCC	2254	I	S	174
	6	116	GTTCGG/gtgagt	Tttcag/AAGCGA	2659	O	R/K	211/213
	7	59	CACAGA/gtaagt	tcacag/GATCAT	2350	II	E	232
	8	20	GGTTTG/gattga	ctgcag/AGCGGG	5422	I	E	239
	9	62	AAGAAG/gtagat	tgacag/TCTCTC	365	O	K/S	259/260
	10	69	ACCCAG/gtaggc	ctgcag/TTTGCA	4949	O	Q/F	282
	11	102	CAGAAG/gtaagt	tgacag/GTGCAC	3748	O	K/V	316/317
	12	73	CTGAAG/gtaaca	ttgcag/ATGTGG	179	I	D	341
	13	$>$ 356						
PARVG ch15	3	\geq 112	CAGCGG/gtgagt	Ttccag/GGAAGG				
	4	96	CACGAG/gtcctg	cttcca/GGAGGA	1210	I	G	27
	5	65	CAGAAG/gtacgc	cagcag/GTGCTG	504	O	K/V	48/49
	6	103	TGTTCC/gtaagc	tttcag/AGAAGT	1056	I	Q	83
	7	141	TGGAGA/gtatgt	ctctag/CCATCT	815	I	T	131
	8	116	ATTGAG/gtactt	ctgtag/AGCACC	1196	O	E/S	169/170
	9	56	ATGCAA/gtgagg	ctctag/GTCACA	344	II	K	188
	10	23	CTTTAC/gtgagt	ctgcag/AGGACG	1628	I	Q	196
	11	59	CAAGAG/gtaggg	tcttag/GCCATT	185	O	E/A	215/216
	12	69	ACCCAG/gtaggg	ctgcag/TTTGCA	3130	O	Q/F	238/239
	13	102	GAAATG/gtaagc	tcatag/CTGCAC	2967	O	M/L	272/273
	14	73	CTGAAG/gtgagt	ccacag/ATATTG	412	I	D	297
	15	1601	cagttt					

Exon sequences are written in capital letters and intron sequence in lower case letters. Phase 0 refers to introns that do not split codon triplets, Phase I refers to introns inserted after the first nucleotide of the triplet; phase II introns are inserted after the second nucleotide of the triplet.

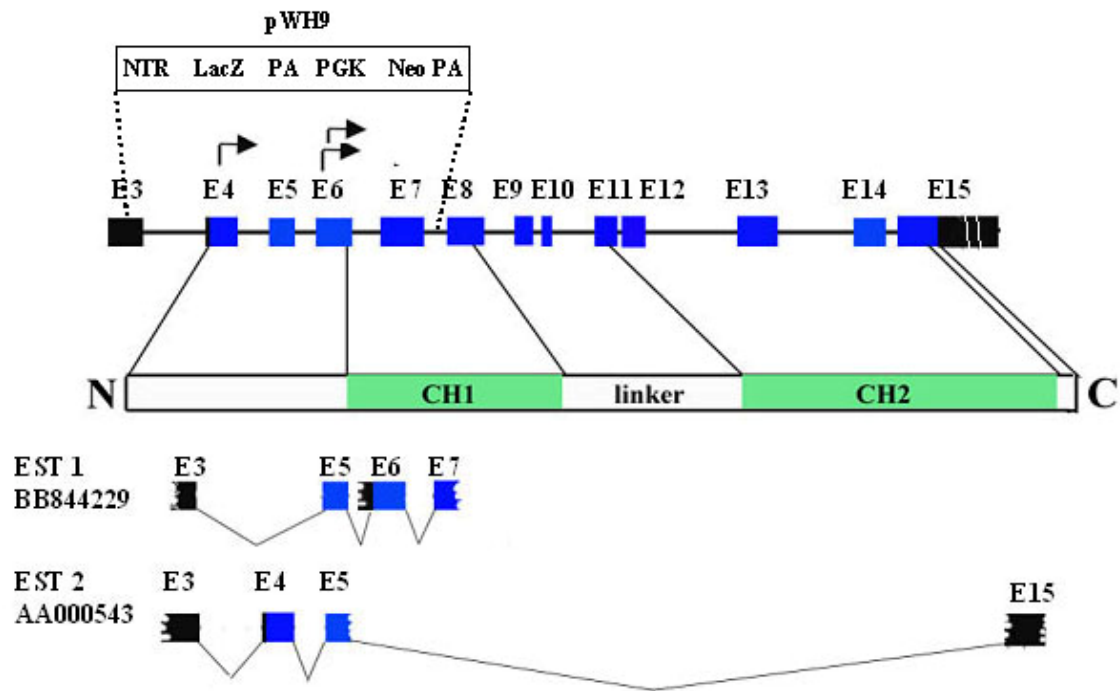


Figure 3.2-6 The scheme of gene and protein structures of γ -parvin, γ -parvin alternative splicing and the gene targeting strategy. γ -parvin is composed of 13 exons encoding a N-terminal region followed by two CH domains separated by a linker region. The first translation start codon ATG lies in exon 4. EST1 shows that exon4 is spliced out indicating that translation may start from two potential ATGs in exon 6. To obtain constitutive γ -parvin gene deletion, the genomic sequence spanning exon 3 to intron 7 encompassing both ATG-containing exons (exon 4 and 6) was replaced by the pWH9 vector. Insertion of NTR (an IRES, Inter Ribosomal Entry Site) to exon 3 leads to the truncation of γ -parvin mRNA translation and expression of LacZ. PA, poly adenine; PGK, PGK promoter; Neo, neomycin resistance gene. Arrow indicates ATG. Black boxes indicate non-coding exons, blue boxes coding exons.

because the peptide sequence used for the antibody generation is encoded by exon 4, which is absent in the short isoforms. Given the low frequency of the shorter transcript (1 among 139 ESTs), the shorter γ -parvin proteins cannot be major isoforms. The product of the other EST (AA000543) would only contain a short amino acid sequence encoded by exon 4 and the part of exon 5, which cannot be a functional protein.

In order to obtain constitutive γ -parvin knockout mice, both exon 4 and exon 6 were deleted. The pWH9 vector was inserted into exon 3 of the γ -parvin gene and replaced the genomic sequence spanning from exon 3 to intron 7 (Figure 3.2-6). This insertion led to the deletion of both ATG-containing exons, exon 4 and exon 6, and, consequently, inactivation of the entire gene. The pWH9 vector contains a reporter gene β -galactosidase (LacZ) and the neomycin resistance gene (Neo). The reporter LacZ gene was designed to study the expression pattern of the targeted gene, especially at the cellular level while there is no

antibody available for cell and tissue immunostaining. The neomycin resistance gene was used for selection of recombinant embryonic stem cell clones after the electroporation of the targeting construct (Sakai et al., 2003).

3.2.4.2 Assembly of the γ -parvin knockout targeting vector

To build the γ -parvin knockout targeting vector, a cDNA fragment spanning exon 5 to exon 13 derived from EST clone AA981356 was sequenced and used as a probe for the hybridisation with the 129/Sv mouse P1-derived artificial chromosome (PAC) library RPCI21. Five positive PAC clones were ordered from the Human Genome Mapping Project Center, Cambridge, United Kingdom, and investigated for the presence of exons 4, 5 and 6. PAC clone 656L16 was used for the construction of the targeting vector. A 15-kb XhoI fragment containing γ -parvin genomic sequence encompassing intron 3 to intron 12 was subcloned into pBlueScript[®]. A 5.5-kb XhoI-SexAI (the SexAI restriction enzyme site lies in exon 3) fragment containing part of exon 3 was subcloned as the 5' flanking arm and a 2.3-kb StuI-ApaLI fragment containing exons 8 and 9 was subcloned as the 3' flanking arm of the targeting construct. The WH9 vector containing a *lacZ* reporter gene and a PKG-driven *neo* gene was ligated with the two arms. A genomic sequence of 5.4 kb spanning exon 3 to intron 7 was deleted in the recombinant allele. A 700-bp SphI/HindIII DNA fragment derived from intron 10 downstream of the 3' flanking arm (marked as a red box in Figure 3.2-8), showed a specific band on Southern blot of genomic DNA when digested with HindIII (7.3 kb) or EcoRV (5.7 kb) (data not shown). The 700-bp DNA fragment was used as an external probe (EP) to identify recombinant ES clones. A 400-bp PCR fragment spanning exon 8 and part of intron 8 sequence was used as an internal probe to exclude random integrations that could not be detected with the external probe. The details of ligation steps are shown in Figure 3.2-7.

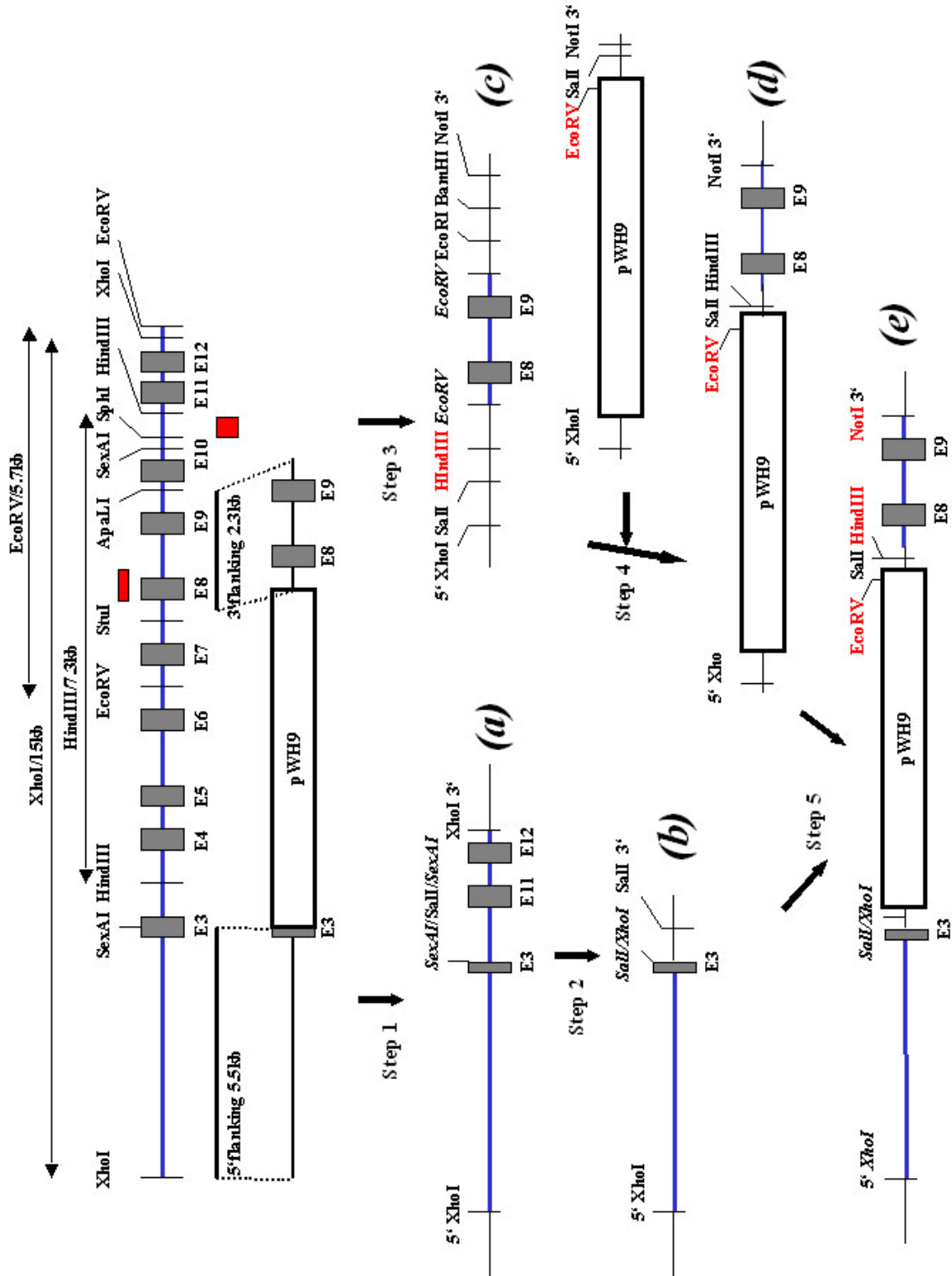


Figure 3.2-7 Cloning steps of construction of γ -parvin targeting vector. A 15-kb XhoI fragment and a 7.3-kb Hind III fragment were subcloned into the pBlueScript[®] and these two DNA plasmids were used for the construction of the targeting vector. In step 1, the 15-kb XhoI plasmid was digested with MabI, SexAI isoschizomer (in exon 3), and the DNA ends were blunted with Klenow and a phosphorylated SalI linker was inserted to obtain a DNA plasmid that contained a part of exon 3, exon 11 and exon 12 (plasmid *a*). In step 2, a XhoI/SalI 5.5-kb fragment (*b*) was isolated from the plasmid *a* and subcloned to the XhoI site of pBlueScript[®] in an orientated direction shown in the figure. In step 3, a StuI/ApaLI 2.3-kb fragment (*c*) was subcloned into the EcoRV site of pBlueScript[®] in an orientated direction with the SalI site at 5' end and NotI site at 3' end. In step 4, the 2.3-kb fragment was isolated with SalI and NotI restriction enzymes and ligated into the SalI and NotI sites of pWH9 vector (*d*). In the final ligation step 5, the 5.5-kb XhoI/SalI fragment was taken out from plasmid *b* and ligated into XhoI site of plasmid *d* in the orientation shown in *e*.

A 700-bp SphI/HindIII fragment (red box) derived from intron 10 was used as an external probe to identify the recombinant ES clones on Southern blot. A 400-bp PCR fragment spanning exon 8 and a part of intron 8, as shown in upper red box, was used as an internal probe to exclude the random integrations of the targeting vector in the recombinant ES clones that could not be detected with the external probe. Exons are shown in grey boxes. The genomic sequence is presented with solid blue line. The thin lines indicate the sequence of the multiple cloning sites of the vectors. The restriction enzyme sites in italic indicate that they were destroyed and not recutable. The restriction enzyme sites shown in red were used for linearization of the targeting vector (NotI, from the pWH9 vector) or genotyping of ES clones and mice (HindIII and EcoRV).

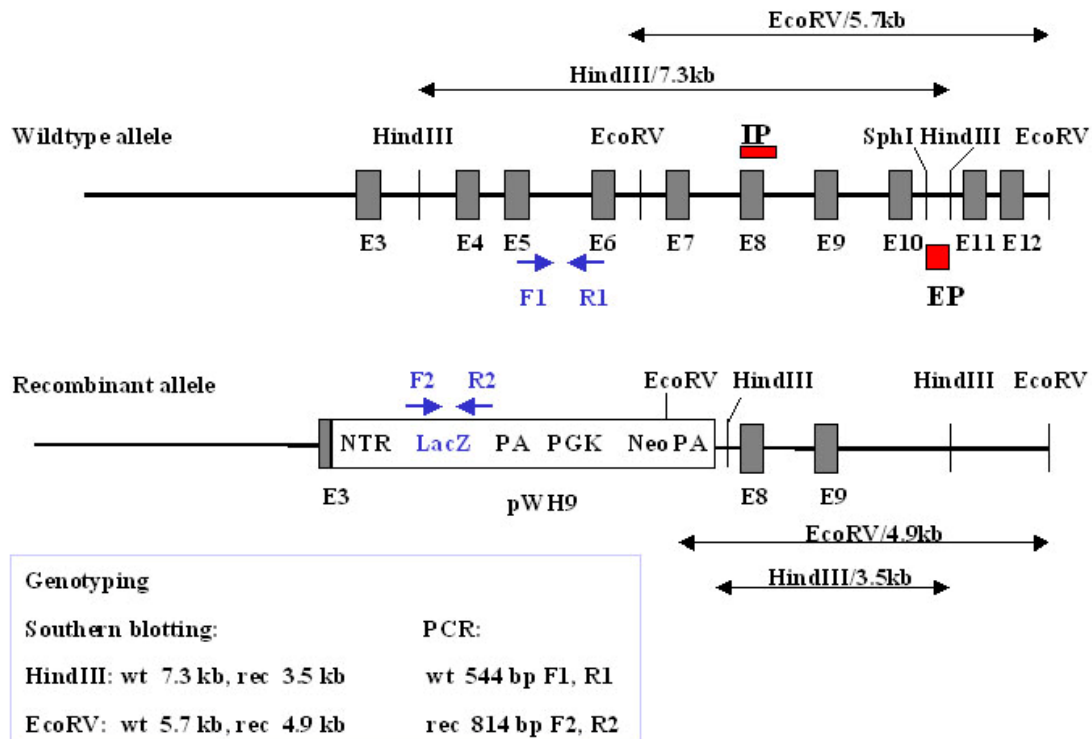


Figure 3.2-8 The genotyping strategy of wildtype and recombinant alleles. Genomic DNA was digested with HindIII or EcoRV and a 700-bp SphI/HindIII fragment was used as an external probe (EP, lower red box) to identify the recombinant allele on Southern blot. A PCR product spanning exon 8 and a part of intron

8 was used as an internal probe of the targeting construct (IP, upper red box) to detect the random integrations. Two pairs of primers (blue arrows) were used for genotyping. F1 was derived from exon 5, R1 from exon 6. F1/R1 amplified the wildtype allele of 544bp that was deleted in the recombinant allele. While F2/R2 amplified a 814-bp fragment of LacZ gene that was only present in the recombinant allele derived from the pWH9 vector.

3.2.4.3 Genotyping strategy for γ -parvin wildtype and recombinant alleles

Figure 3.2-8 shows the strategy for genotyping wildtype and recombinant γ -parvin alleles. Genomic DNA was digested with HindIII or EcoRV. HindIII digestion led to a fragment of 7.3 kb for the wildtype allele and 3.5 kb for the recombinant allele. The EcoRV digestion generated a wildtype fragment of 5.7 kb and a recombinant fragment of 4.9 kb. Using PCR genotyping, a 544-bp fragment spanning exon 5, intron 5 and exon 6 was amplified for the wildtype allele and an 814-bp fragment of the LacZ gene for the recombinant allele which is derived from the pWH9 vector and is absent in the wildtype allele.

3.2.4.4 Generation of γ -parvin chimeric mice

To generate γ -parvin parvin chimeric mice, 100 μ g of linearized targeting vector DNA was electroporated into R1 embryonic stem (ES) cells as described in Materials and Methods. The day following the electroporation, ES clones were selected with G418 for six to eight days and afterwards, 360 G418-resistant ES clones were picked and frozen. The DNA samples of ES clones were analysed by Southern blotting to screen recombinant ES clones with the external probe. Out of 360 G418-resistant ES cell clones, 4 recombinant ES clones were identified (Figure 9A). The recombinant ES clones were further confirmed with the internal probe to exclude random integrations. No random integrations were detected in the recombinant ES clones. The internal probe recognized the fragments of the same sizes as those with the external probe (figure 9B). Two of the four blastocyst microinjected recombinant ES clones gave birth to highly chimeric agouti mice. The chimeric agouti male mice were mated with C57B6 females and the germ-line transmission of the mutated γ -parvin gene in offspring was confirmed by Southern blotting with the external probe (data not shown). γ -parvin heterozygotes were crossed to obtain homozygotes.

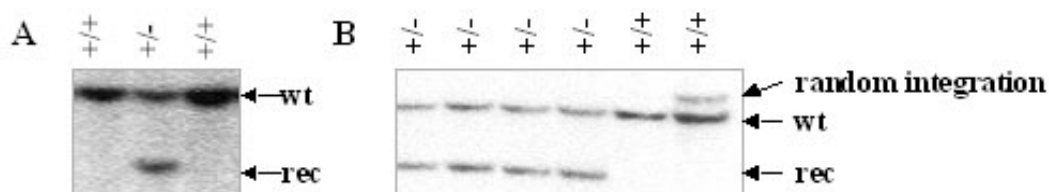


Figure 3.2-9 γ -parvin recombinant ES clones were confirmed by Southern blotting. (A) One of four γ -parvin recombinant ES clones (+/-) was detected with the external probe. (B) No random integrations were found in the four γ -parvin recombinant ES clones. A random integration was detected in one of non-recombinant ES clones with the internal probe. ES cell genomic DNAs were digested with HindIII. Wt, wildtype allele, 7.3 kb; rec, recombinant allele, 3.5 kb.

3.2.4.5 Genetic deletion of γ -parvin

The offspring from γ -parvin heterozygous mating were genotyped by Southern blotting or PCR. The gene deletion of γ -parvin in homozygotes was confirmed by Northern blot at mRNA level and Western blot at protein level (Figure 3.2-10).

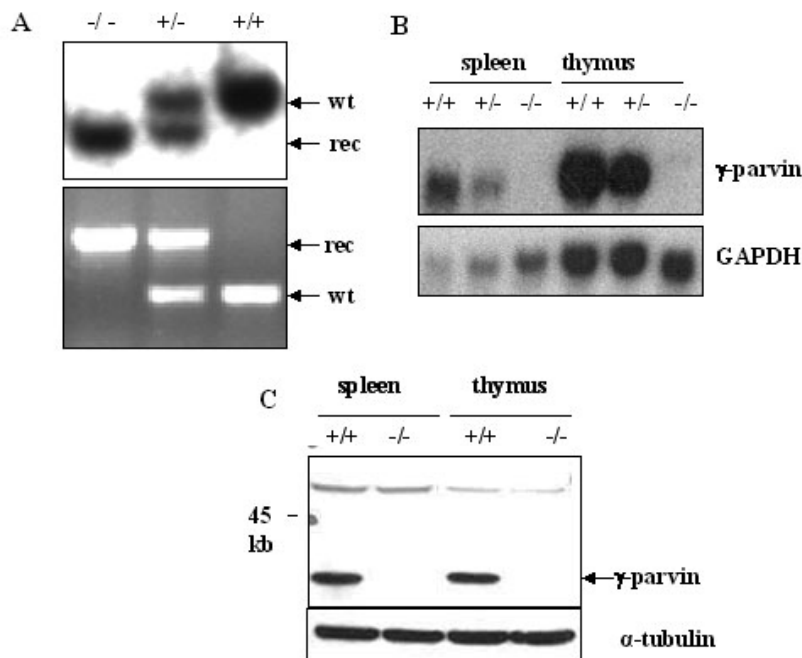


Figure 3.2-10 The genetic deletion of γ -parvin. (A) γ -Parvin homozygous mice were identified by Southern blotting (upper panel) and PCR genotyping (lower panel). The gene deletion of γ -parvin was confirmed by Northern blotting (B) and Western blotting (C). GAPDH and tubulin were used as RNA and protein loading controls, respectively.

3.2.5 Phenotypic analysis of γ -parvin null mice

3.2.5.1 γ -Parvin null mice are viable and fertile and show normal Mendelian distribution

Genotyping of 159 adult offspring derived from heterozygous crosses revealed a normal Mendelian ratio of genotypes (+/+ : 28 %, +/- : 47%, -/- : 25%). Both heterozygotes and mutant mice were viable, fertile and were not distinguishable from their wildtype littermates.

3.2.5.2 ILK and PINCH1 are downregulated in the γ -parvin null hematopoietic cells, while α - and β -parvin(l) expression levels are not changed

The expression of α - and β -parvins and parvin-associated proteins ILK and PINCH1 was investigated in γ -parvin null mice (Figure 3.2-11). ILK and PINCH1 proteins were reduced in the BM, thymus, LN and PP of γ -parvin null mice, but reduced expression was not obvious in the spleen tissue where α - and β -parvins were expressed at higher levels compared to other lymphoid organs. α - and β -parvin(l) expression levels were not changed in the γ -parvin null mice.

BM-derived macrophages and dendritic cells from γ -parvin heterozygotes and γ -parvin null mice were generated as described in Materials and Methods (Figure 3.2-12A, B). The cells derived from both γ -parvin heterozygotes and γ -parvin null mice showed similar purities (85% and 79% respectively for dendritic cells and 98.7% and 98% respectively for macrophages) as analysed by FACS using antibodies against CD11c, MHCII and Gr-1 for dendritic cells and Mac-1, F4/80 for macrophages (Figure 3.2-12A and B). The similar reduction of ILK and PINCH1 was observed in both γ -parvin-null macrophages and dendritic cells as compared to γ -parvin heterozygous cells (Figure 3.2-12C). Consistent with previous observations, α -parvin was not expressed in either cell type. β -parvin(l) was coexpressed with γ -parvin in both cell types, while the protein level of β -parvin(l) was not changed in the absence of γ -parvin.

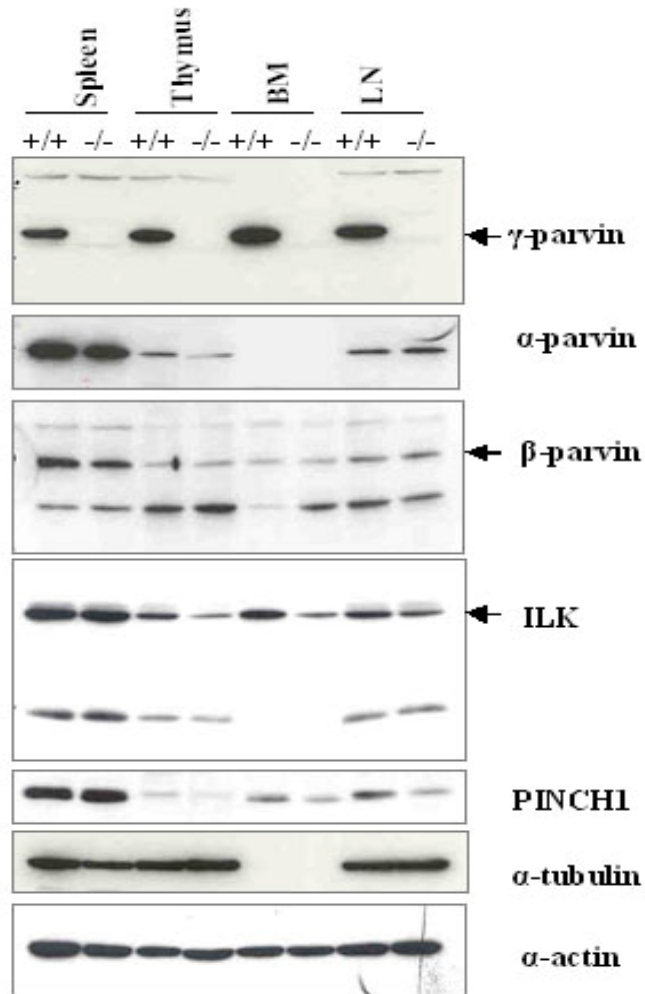


Fig. 3.2-11 ILK and PINCH1 were reduced in the thymus, BM and LN of γ -parvin-null mice, but not in spleen tissue. α - and β -parvin expression levels were not changed.

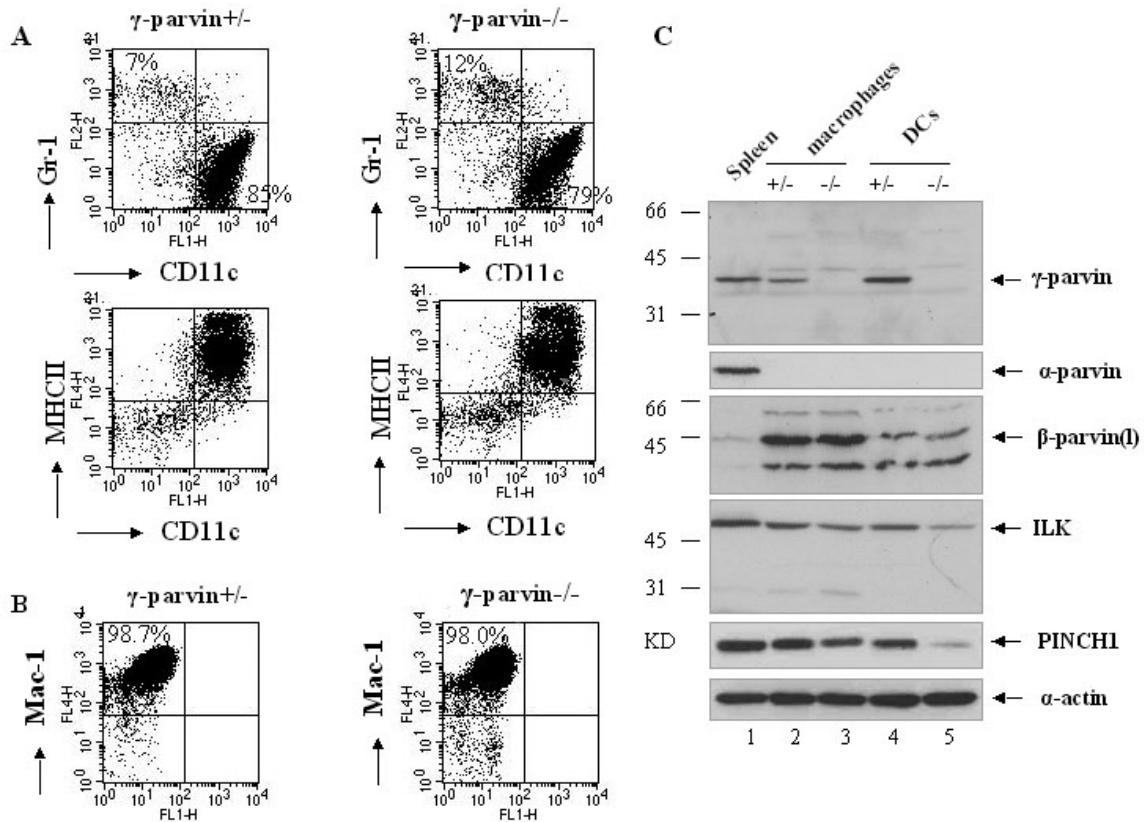


Fig. 3.2-12 ILK and PINCH1 were reduced in γ -parvin-null BM-derived dendritic cells and macrophages. (A, B) BM-derived dendritic cells (A) and macrophages (B) were generated from γ -parvin heterozygotes and γ -parvin null mice and showed similar purities as analysed by FACS (85% and 79% respectively for dendritic cells and 98.7% and 98% respectively for macrophages). (C) Both γ -parvin and β -parvin(l) were expressed in BM-derived dendritic cells and macrophages. ILK and PINCH1 were reduced in both cell types in the absence of γ -parvin as shown by Western blot.

3.2.5.3 γ -Parvin null mice show normal architecture of lymphoid organs

The lymphoid organs, thymus, spleen, LNs and PPs, from γ -parvin null mice were indistinguishable from those of control mice. γ -parvin null mice exhibited normal morphology in thymus, spleen, LN and PP compared to wildtype or heterozygous mice by HE staining (Figure 3.2-13). Immunostaining of spleen, LN, and PP with B cell marker B220 and T cell marker Thy1.2 showed normal T and B cell distribution in γ -parvin null mice compared to controls (Figure 3.2-14).

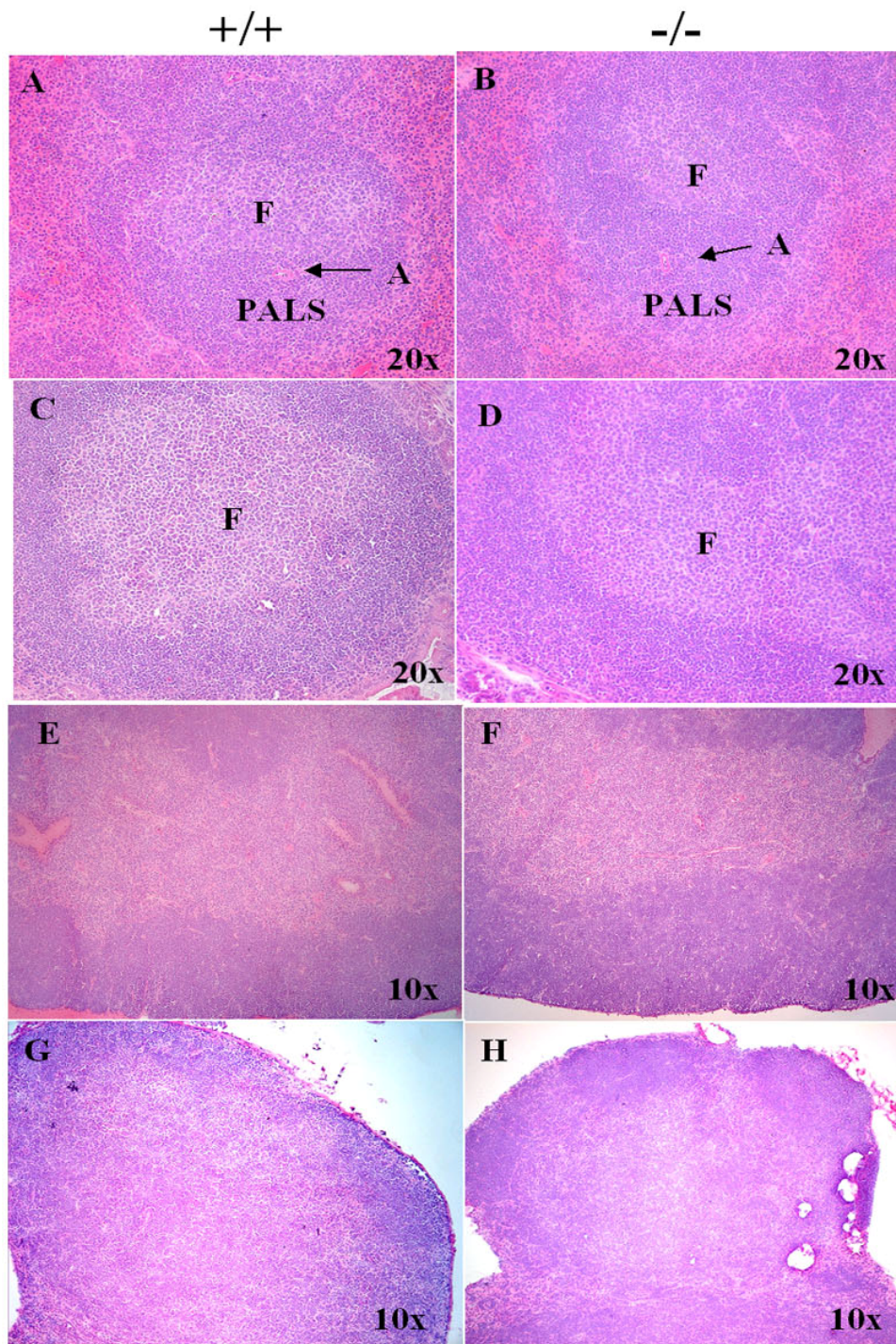


Figure 3.2-13 HE staining of spleen (A, B), PP(C, D), thymus (E, F) and LN (G, H). The γ -parvin null mice (left panel) showed similar morphology of lymphoid organs as controls (right panel). A, central arteriole. F, follicle. PALS, periarteriolar lymphoid sheath. Picture magnifications, 200X (A-D) or 100X (E-H).

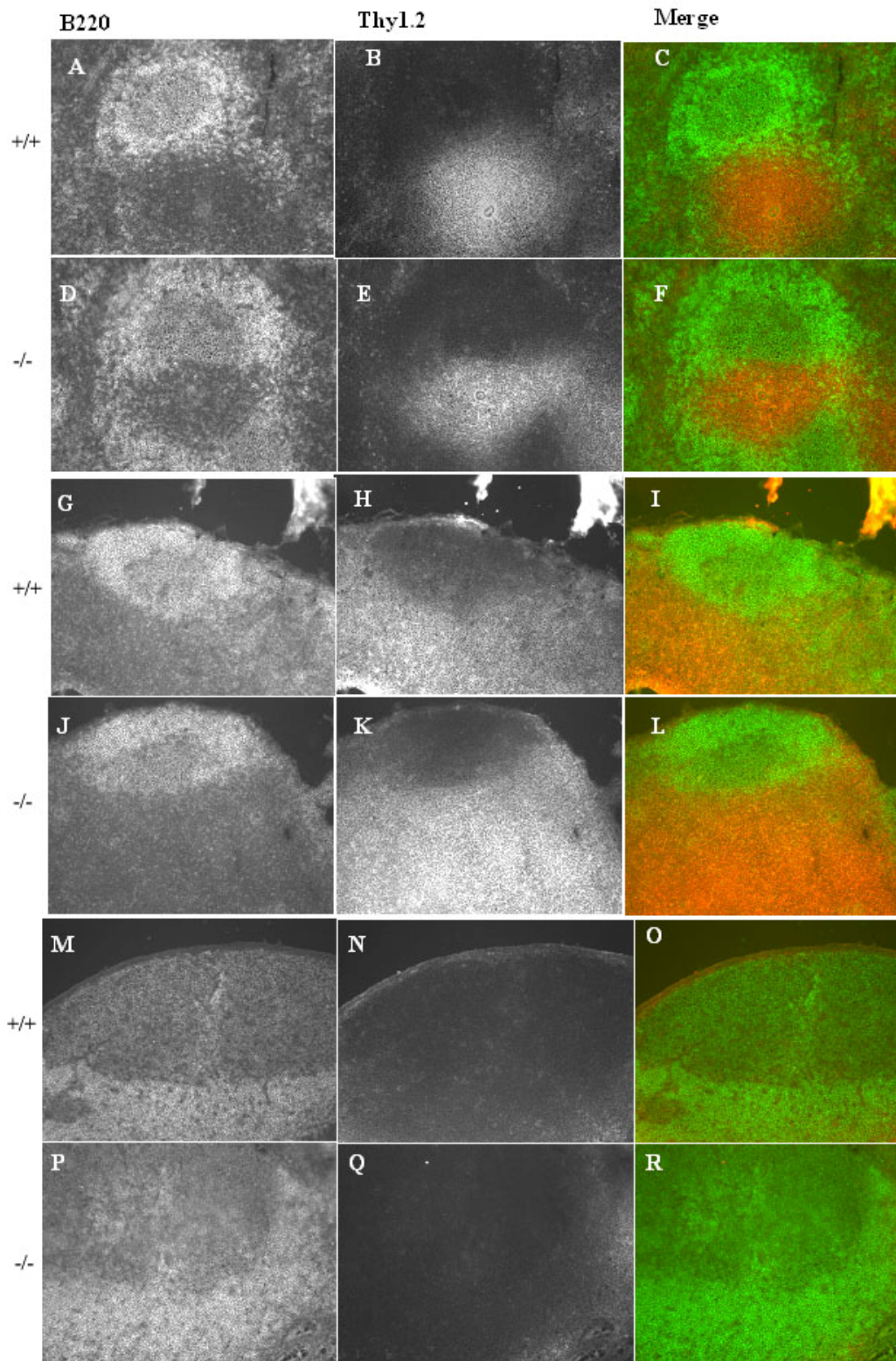


Fig. 3.2-14 γ -parvin null mice showed similar B and T cell distribution in the spleen (A-C, +/+, D-F, -/-), LN (G-I, +/+, J-K, -/-) and PP (M-O, +/+, P-R, -/-) as wildtypes. Tissue cryosections were stained for B cell marker B220 and T cell marker Thy1.2. Picture magnification, 200X.

3.2.5.4 γ -Parvin null mice have normal cellularity of lymphoid organs and show normal hematopoiesis

Hematopoietic cells of lymphoid organs were prepared as described in Materials and Methods. The cellularities of lymphoid organs of γ -parvin null mice were similar to those of control mice. Figure 3.2-15 presents statistics of the cellularities of BM (con: $29.8 \pm 8.1 \times 10^6$, -/-: $35.1 \pm 11.1 \times 10^6$), thymus (con: $37.1 \pm 10.6 \times 10^6$, -/-: $40.2 \pm 12.1 \times 10^6$) and spleen (con: $104.0 \pm 33.5 \times 10^6$, -/-: $107.6 \pm 30.8 \times 10^6$) in 5-month-old control and γ -parvin-null mice.

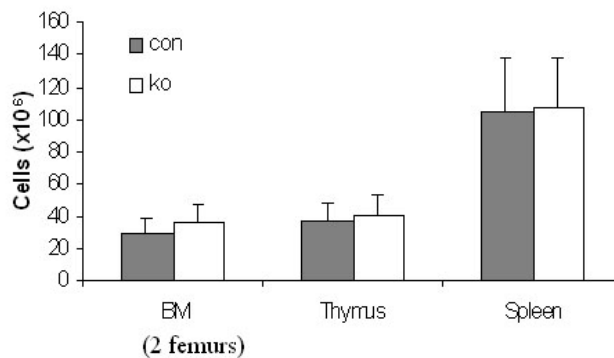


Figure 3.2-15 The cellularities of lymphoid organs (BM, thymus and spleen) from γ -parvin null mice are similar to those from controls (5-month old mice, n=5,5).

As γ -parvin is expressed in lymphoid tissues, and specifically in lymphoid lineages of B and T cells and myeloid lineages of dendritic cells and macrophages (Figure 3.2-2, 12), I investigated whether the deletion of γ -parvin influenced the development of hematopoietic lineages. Hematopoietic cells prepared from lymphoid organs were immunostained with different lineage markers (B cell markers B220, IgM and IgD; T cell markers CD4, CD8 and CD3; erythrocyte marker Ter119; granulocyte marker Gr-1; macrophage marker Mac-1; and natural killer cell markers Dx5 and NK1.1) and analyzed by flow cytometry as described in Materials and Methods. No developmental differences were found between control and γ -parvin null mice in investigated haematopoietic lineages in both central lymphoid organs (BM and thymus, Figure 3.2-16) and in peripheral lymphoid organs (spleen, LN, PP) (5-month-old control and γ -parvin null mice; n=5;5. Figures 3.2-17). Data of CD19 and Dx5/NK1.1 staining are not shown. Normal hematopoiesis of γ -parvin null mice was also demonstrated at earlier developmental stages such as 4- and 8-weeks-old (data not shown).

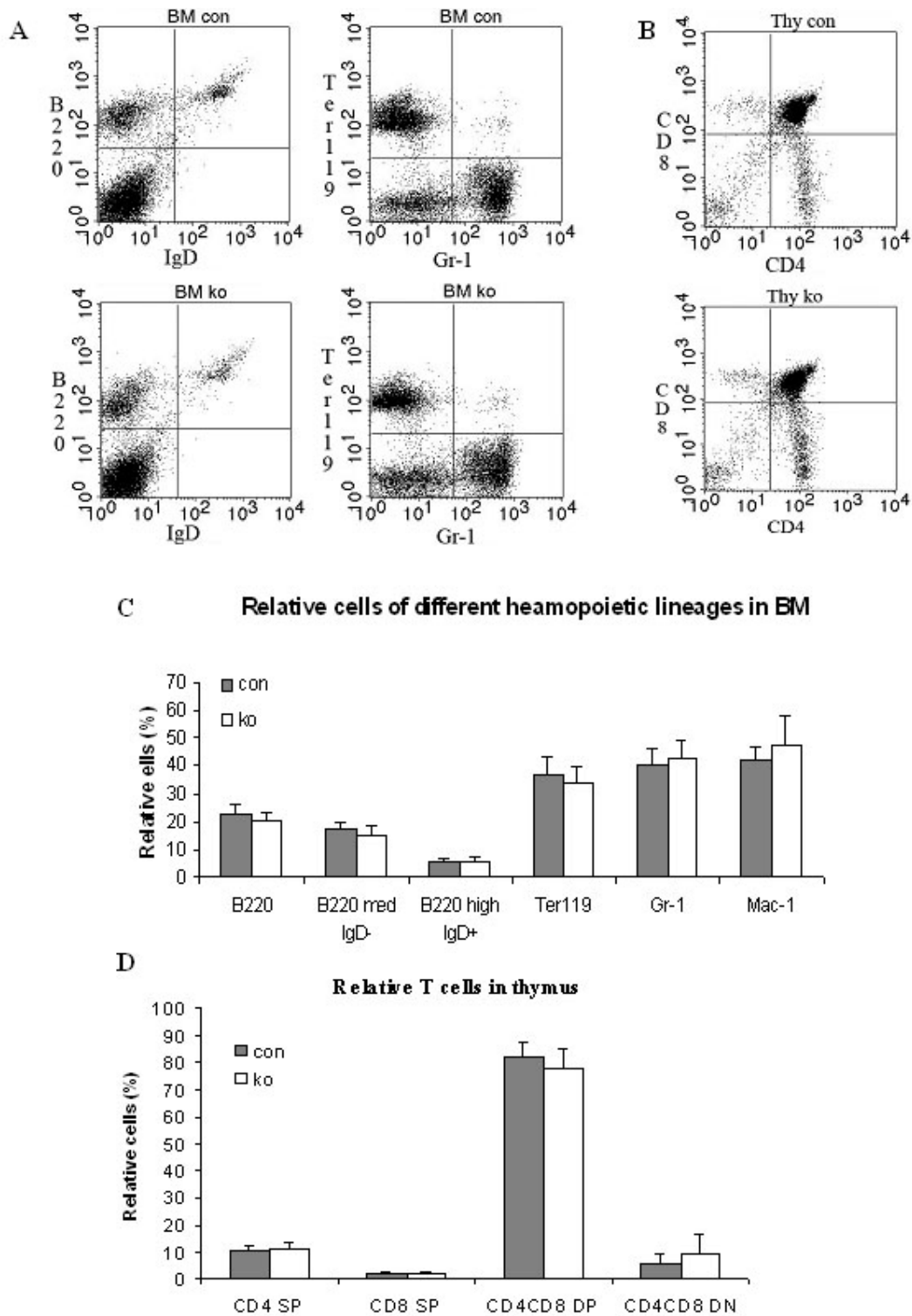


Figure 3.2-16 γ -parvin null mice (ko) showed normal hematopoietic lineage development in BM (A, C) and thymus (B, D) as controls. Hematopoietic cells prepared from BM and thymus were analysed for the expression of B220, IgD, CD4, CD8, Gr-1, Ter-1 and Mac-1 by FACS. Bar graphs present the relative cell number of each population.

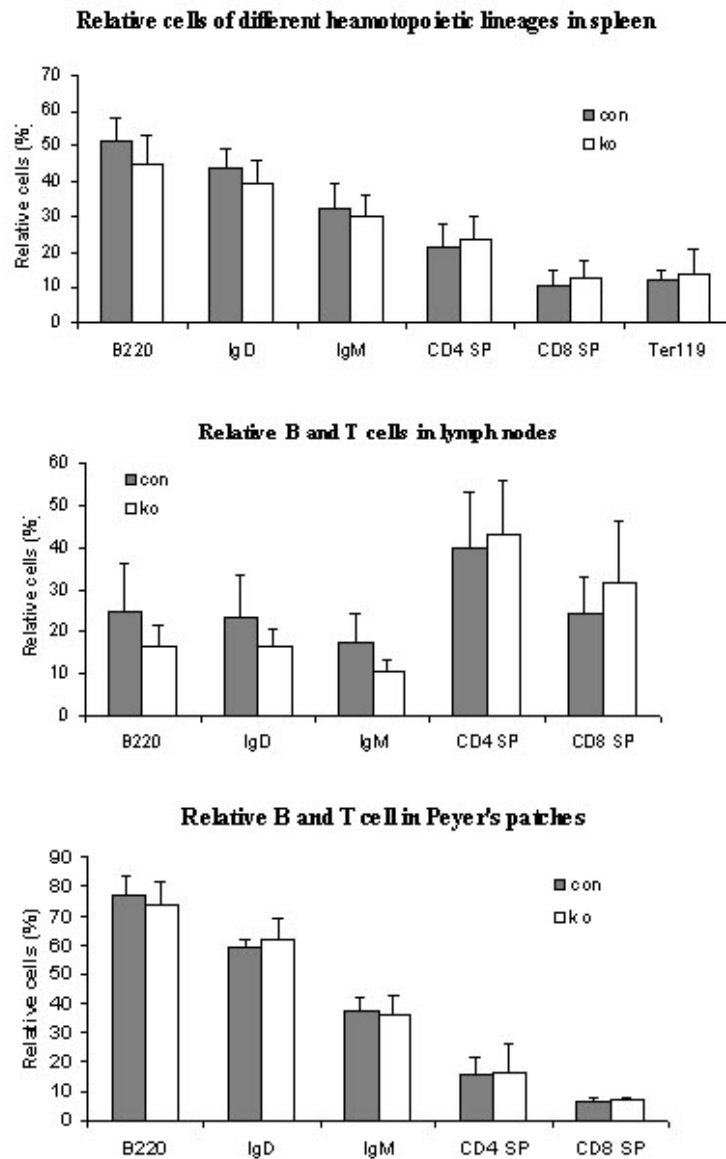


Figure 3.2-17 γ -parvin null mice (ko) showed similar B and T cell development in peripheral lymphoid organs (spleen, lymph nodes and Peyer's patches) (n=5,5; 5-month-old mice).

3.2.5.5 γ -parvin null dendritic cells can mature normally *in vitro*

Since γ -parvin is expressed in dendritic cells, I further investigated whether γ -parvin-null dendritic cells could mature normally upon the stimulation of LPS *in vitro*. γ -parvin null dendritic cells could mature to the same extent as γ -parvin heterozygote cells. A representative experiment is shown in Figure 3.2-18. Both costimulatory molecules CD86 and CD40 (CD40 staining data not shown), as well as MHC II were upregulated after the stimulation in both control and γ -parvin null cells. MHC II CD86⁺ cells increased from

37% before stimulation to 88% after LPS stimulation in control, and from 28% before stimulation to 84% in γ -parvin null dendritic cells.

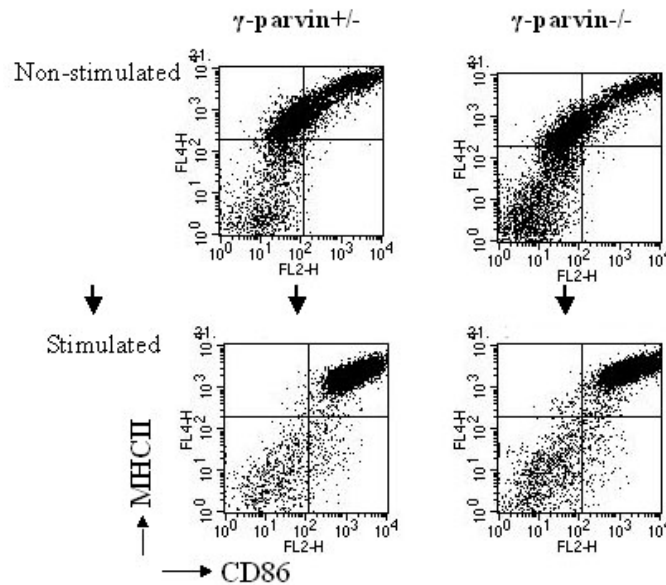
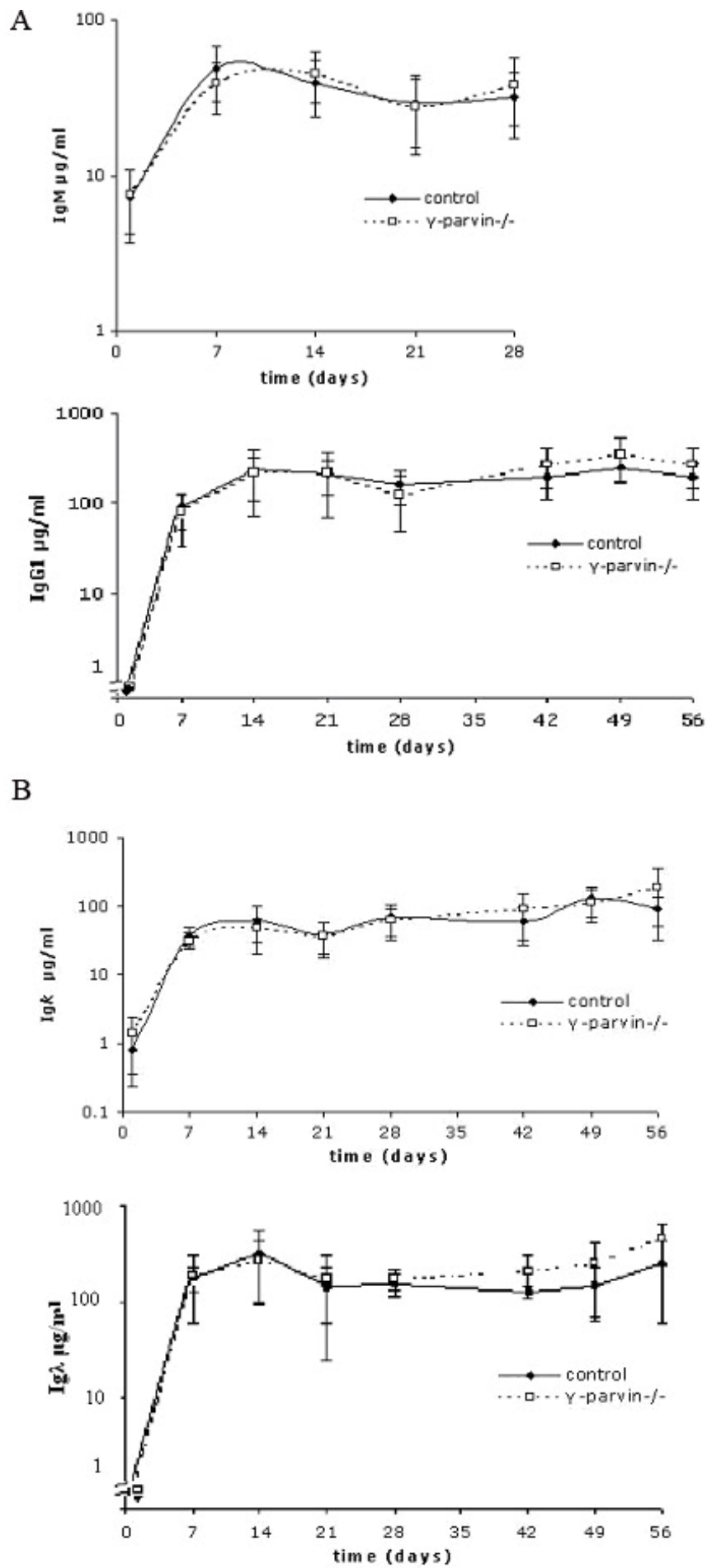


Figure 3.2-18 BM-derived dendritic cells from γ -parvin null mice could mature normally as those from γ -parvin heterozygotes and both CD86 and MHC II were upregulated after the stimulation with LPS overnight.

3.2.5.6 γ -parvin null mice display normal T-cell dependent antibody response

The specific expression of γ -parvin in DC, B and T cells suggested a potential role of the protein in the adaptive immune response. To test this, T-cell dependent antigen NP-CG was used to immunize the mice. The anti-NP antibody isotypes (IgM, IgG1, IgG2a, IgG3, Ig κ and Ig λ) were estimated by ELISA. No significant differences were found in any of all these anti-NP isotypes between γ -parvin null mice and controls (Figure 3.2-19). Anti-NP IgM increased dramatically in the first 7 days and then dropped on day 14. The peak of anti-NP IgG1 appeared on day 14, later than IgM, and remained at a high level during the second immune response. γ -parvin null mice showed slightly higher production of anti-NP IgG1 and Ig λ during the second immune response, but differences were not significant. The production of IgG2a and IgG3 in γ -parvin null mice and controls are also the same (data not shown).

Figure 3.2-19 Normal T-cell dependent antibody responses in γ -parvin null mice. γ -parvin null mice produced similar amount of anti-NP IgM, IgG1 (A) and Ig κ and Ig λ Ig (B) as controls (n=5-7 in each group).



3.3 *In vivo* analysis of α -parvin

3.3.1 Exon2 deletion of α -parvin

3.3.1.1 α -parvin knockout strategy

The mouse α -parvin gene is located on chromosome 7 and composed of 13 exons (Table 3.2-1). No alternative α -parvin mRNA splicing was found in mouse EST database. The translation start codon ATG is in exon 1. To obtain constitutive gene deletion of α -parvin, the pWH9 vector was inserted into exon 2 and part of exon 2 and intron 2 sequence was deleted (Figure 3.3-1). The translation of α -parvin mRNA should be truncated in exon2 when the ribosome encounters NTR.

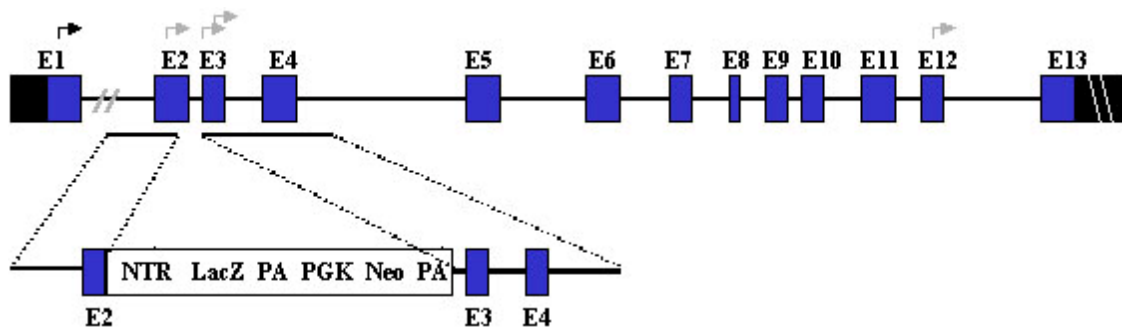


Figure 3.3-1 α -parvin knockout strategy. The pWH9 cassette was inserted into exon 2. The translation of α -parvin mRNA should be truncated when the ribosome encounters NTR and LacZ should get expressed in the locations where α -parvin is expressed. Arrow indicates in-frame ATG. Black box, non-coding sequence of the cDNA; blue box, coding exon.

3.3.1.2 Construction of α -parvin knockout vector

For the construction of the α -parvin targeting vector, a 400-bp α -parvin cDNA fragment corresponding to the coding sequence spanning exons 1,2,3 and 4 derived from α -parvin EST clone AI006605 was used as a probe for the hybridisation of 129/Sv mouse P1-derived artificial chromosome (PAC) library RPCI21. Five positive PAC clones were ordered and clone 486C16 was used for further cloning. Briefly, a 2.7-kb of *SacI/AvaI* fragment (*AvaI* site lies in exon 2) was subcloned as the 5' flanking arm and a 7.4-kb *EcoRI* fragment was subcloned as the 3' flanking arm. The PWH9 vector that contains a *lacZ* reporter gene and a PKG-driven *neo* gene was ligated with the two arms. 150 base pairs encompassing part of exon 2 and intron 2 were deleted from α -parvin gene. The assembly steps of the construct are shown in figure 3.3-2.

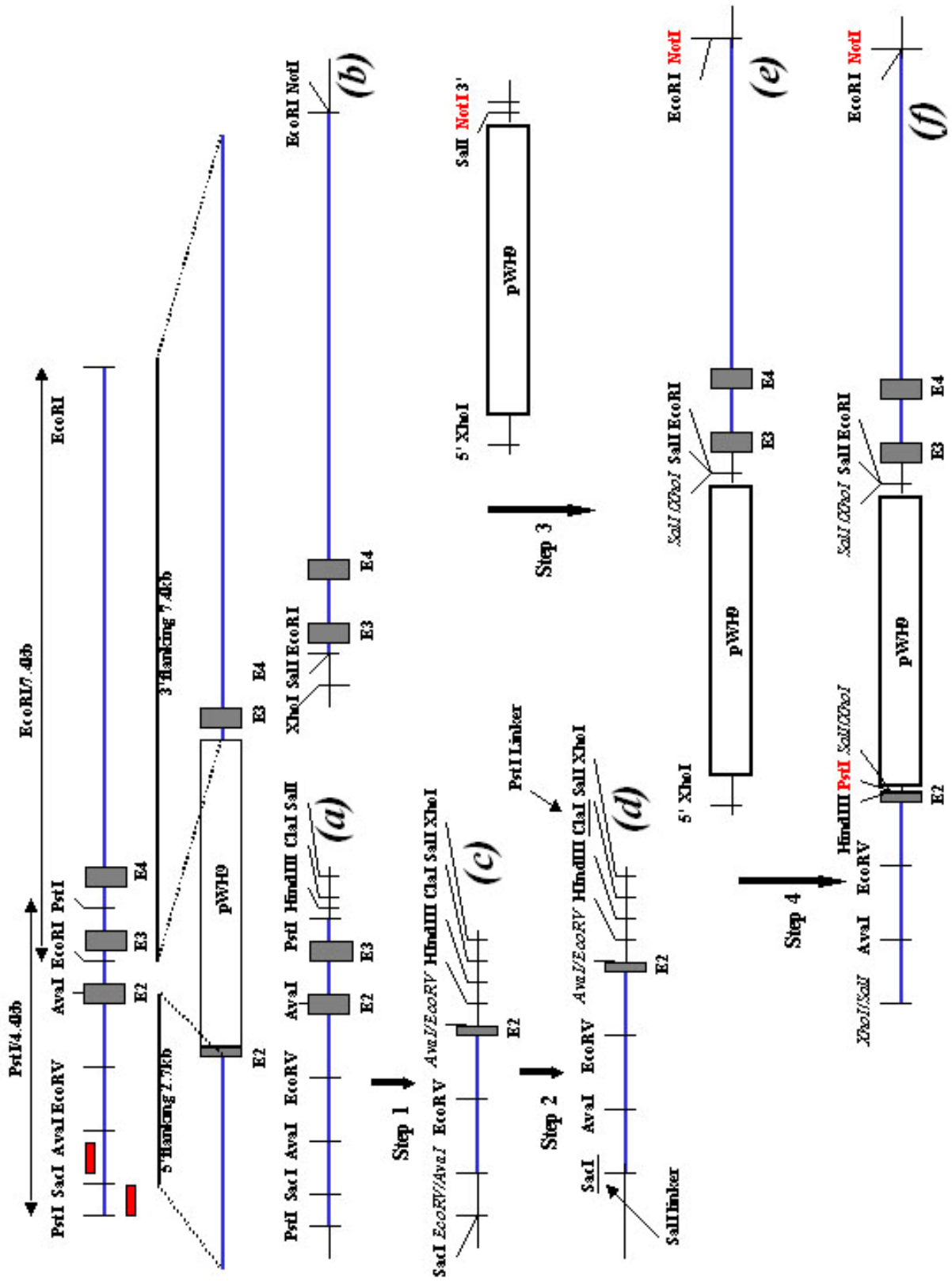


Figure 3.3-2 Assembly steps of α -parvin targeting construct. A 4.4 kb PstI fragment and an EcoRI 7.4 kb fragment were subcloned to the pBlueScript® multiple cloning sites of PstI and EcoRI enzyme sites respectively in the orientated directions shown in the figure (plasmid *a* and *b*). These two DNA plasmids were used for the construction of the targeting vector. In step 1, an AvaI fragment (containing part of exon2) was isolated from the plasmid *a* and subcloned into the blunt EcoRV site in the orientated direction with a SacI site derived from pBlueScript® at 5' end (plasmid *c*). In step 2, a SacI/AvaI fragment isolated from the plasmid *a* was ligated into SacI/EcoRV sites of the plasmid *c* to get a plasmid *d*. A SalI linker was ligated into the SacI site at 5' end of the plasmid *d* and then a PstI linker was ligated into the plasmid *d* through a ClaI site. In step 3, the 7.4 kb EcoRI fragment was taken out with XhoI/NotI enzymes and ligated into the pWH9 vector that was linealized with SalI/NotI enzymes (plasmid *e*). In the final step 4, the SalI fragment from the plasmid *d* (with a SalI linker at 5' end and a PstI site at 3' end) was isolated and ligated into the XhoI site of the plasmid *e* to obtain the final targeting construct - plasmid *f*.

The PstI/SacI 400-bp fragment (lower red box, a sequence upstream of the 5' flanking arm) was used as an external probe to identify the recombinant ES clones for Southern blotting. A 740 bp PCR product amplified from the intron 1 sequence between the SacI and AvaI restriction enzyme sites (shown in upper red box), was used as an internal probe to exclude the random integrations of the targeting construct in the recombinant ES clones that could not be detected with the external probe. The grey boxes show exons. The solid blue lines present genomic sequence of the gene. The thin lines indicate the short sequences of the multiple cloning sites of the vectors. The restriction enzyme sites shown in italic indicate that they are destroyed and not recutable. The restriction enzymes shown in red were important enzymes that would be used for the linearization of targeting construct for the electroporation into ES cells (NotI, from pWH9 vector) and genotype identification of ES clones and mice (PstI).

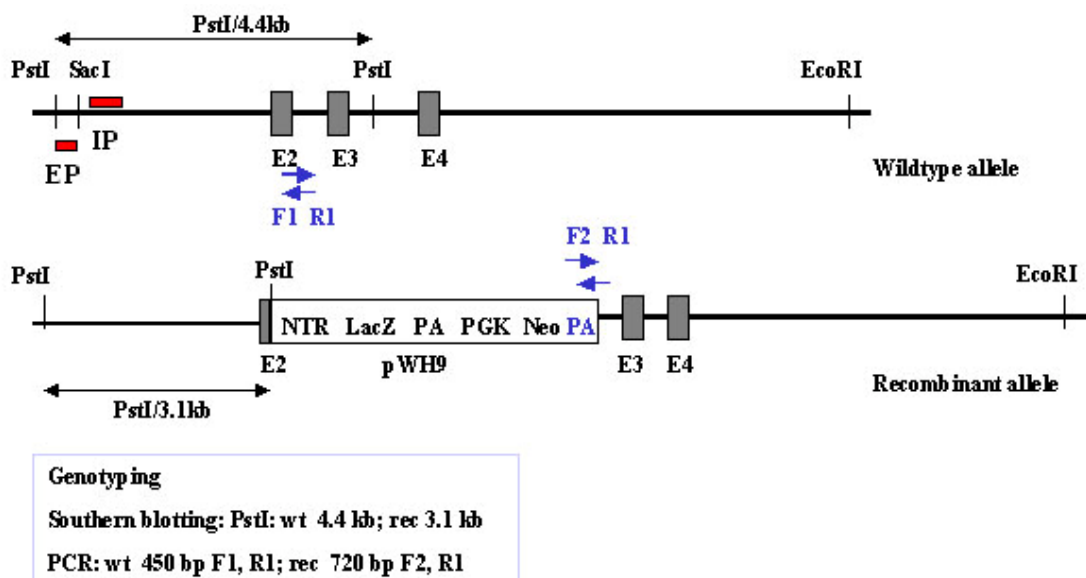


Figure 3.3-3 The genotyping strategy for wildtype and recombinant alleles of α -parvin. The wildtype and recombinant alleles were detected by PstI digestion for Southern blotting. A 400bp PstI/SacI fragment derived from intron 1, which was upstream of the 5' flanking arm of targeting construct, was used as an external probe (EP, lower red box) to identify recombinant ES clones and mice genotyping on Southern blot. A PCR product

amplified from the intron was used as an internal probe (IP, upper red box) to detect the random integrations in the recombinant ES clones. Three-primer PCR system (blue arrows) was used for genotyping. F1 was derived from exon 2, R1 from intron 2. Both F1 and R1 primers were present in targeted construct. F1/R1 amplified a 450 bp fragment on wildtype allele, but no product on recombinant allele. F2 was derived from PGK poly adenine sequence of the pWH9 vector and was absent in wildtype allele. F2/R1 amplified part of the PGK Poly A sequence and part of the intron 2 sequence and gave a PCR product around 720 bp.

3.3.1.3 Genotyping strategy of wildtype and recombinant alleles of α -parvin

Figure 3.3-3 shows the genotyping strategy for identification of wildtype and recombinant alleles. Genomic DNA was digested with PstI and the wildtype allele produced a fragment of 4.4 kb and recombinant allele of 3.1 kb on Southern blot detected with the external probe. A three-primer PCR genotyping system was also established for mice genotyping.

3.3.1.4 Generation of α -parvin chimeric mice

To generate α -parvin chimeric mice, targeting construct DNA was linearized and electroporated into R1 ES cells as described in Materials and Methods. ES clones were selected with G418 and the clones were picked. DNA of ES clones was analysed by Southern blotting with the external probe (a 400bp PstI/SacI fragment derived from intron 1, Figure 3.3-3). Out of 350 G418-resistant ES cell clones, 47 recombinant ES clones were identified (recombination rate 13%, Figure 3.3-4). The recombinant ES clones were further confirmed with the internal probe to exclude random integrations that could not be detected by the external probe. The internal probe gave bands of exactly the same size as the external probe and no random integrations were detected in all recombinant ES clones (data not shown). The ES clones with equal density of both wildtype and recombinant alleles on Southern blot were chosen for blastocyst microinjections. One of four injected clones (clone 19) gave birth to highly chimeric agouti mice. The chimeric agouti male mice were mated with C57B6 females and the pups were genotyped to confirm the germ-line transmission of the mutated α -parvin gene by Southern blotting with the external probe (data not shown). α -parvin heterozygotes were crossed to obtain homozygous mice.

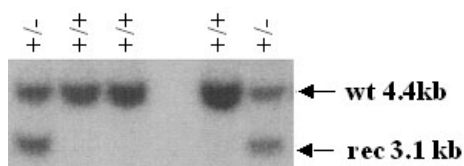


Figure 3.3-4 Two of α -parvin recombinant ES clones were shown on Southern blot.

3.3.1.5 Exon 2 deletion of α -parvin

The offspring from α -parvin heterozygote crosses were genotyped by Southern blotting and PCR genotyping to identify homozygotes (Figure 3.3-5). The mRNA expression of α -parvin mutant mice was investigated by Northern blotting with two cDNA probes (Figure 3.3-6A). The probe1 derived from coding sequence corresponding to α -parvin N-terminus, CH1 domain and linker region was

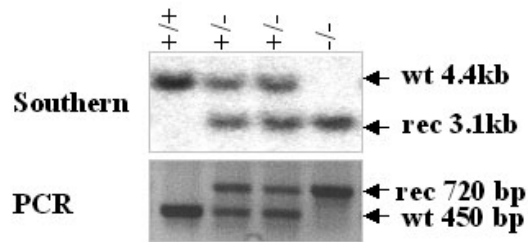


Figure 3.3-5 α -parvin mutant homozygotes were identified by Southern blotting and PCR genotyping according to the strategy shown in Figure 3.3-3.

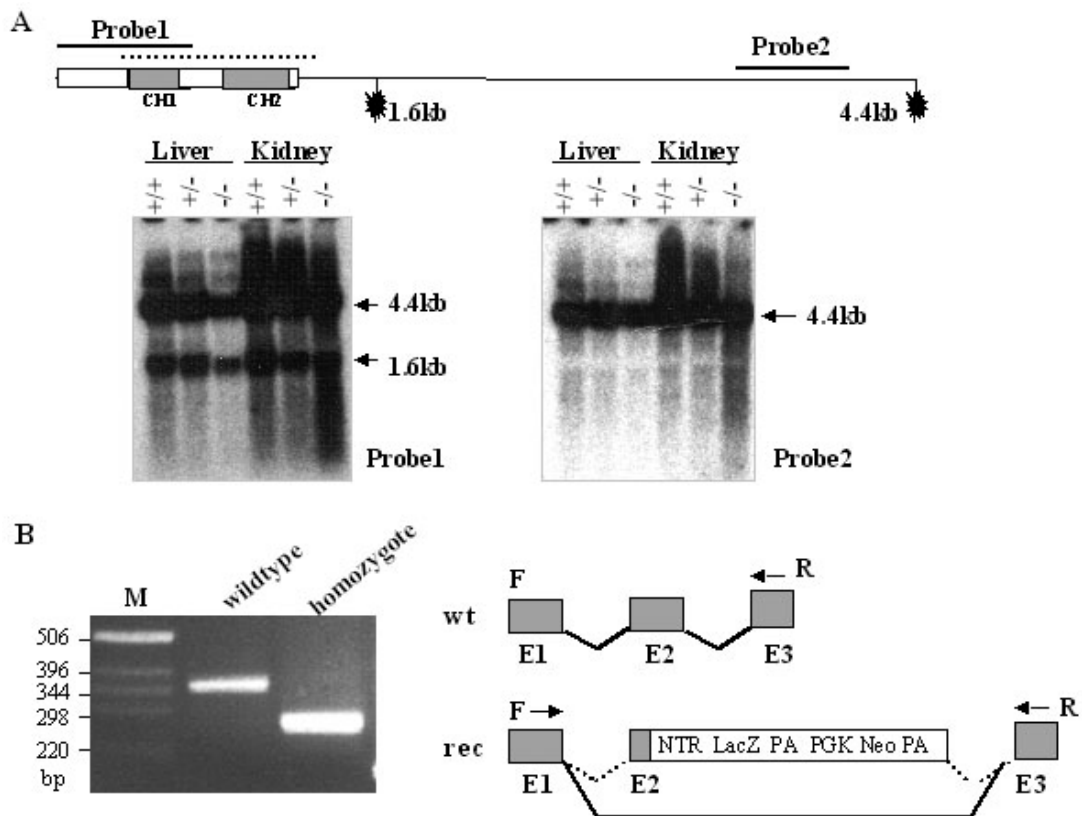


Figure 3.3-6 (A) Both α -parvin probes derived from cDNA and 3'UTR sequences respectively, gave signals of transcripts on Northern blots of liver and kidney tissues of α -parvin homozygous mouse. (B) α -Parvin homozygous mouse gave a shorter RT-PCR product in liver compared to that in wildtype mouse.

hybridised with the β -parvin cDNA sequence corresponding to β -parvin CH1, linker region and CH2 domains (dotted line in Figure 3.2-6A) to exclude possible cross-reactions. Probe1 gave two transcripts of 4.4 kb and 1.6 kb in liver and kidney tissues of wildtype mice. Probe 2 derived from α -parvin 3' UTR sequence gave a 4.4 kb transcript. This is consistent with the published data (Olski et al., 2001). Surprisingly, the homozygous mouse also gave similar pattern as wildtype and heterozygote on Northern blot. RT-PCR product amplified using primers derived from exon 1 and exon 3 was around 90bp shorter in homozygote than that from the wildtype (Figure 3.3-6B). The sequencing of the RT-PCR product showed that exon 2 was spliced out in the homozygotes.

The truncated transcript produced an α -parvin mutant protein of 39 kD, lacking 30 amino acids encoded by exon 2. The protein sequence encoded by exon 2 lies between the N-terminal 2nd NLS signal and CH1 domain. The expression of truncated α -parvin E2 Δ/Δ protein was confirmed with the α -parvin peptide polyclonal antibody. The mutant protein was expressed at a similar level to that in wildtype mouse (Figure 3.3-7).

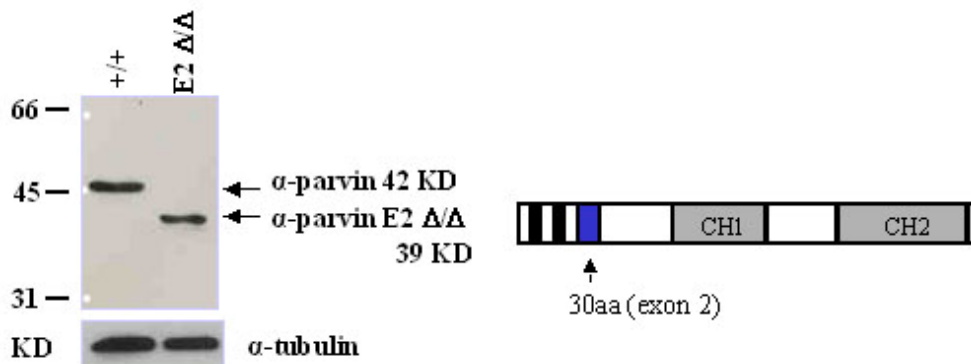


Figure 3.3-7 (A) Western blot of α -parvin exon2 deletion protein and (B) the scheme of α -parvin protein structure. Blue box indicates exon 2 coding sequence. Black box indicates the putative NLS.

There are two polyA signals in the pWH9 cassette. The absence of exon 2 in homozygotes and the failure of detection of LacZ signal in both the heterozygote and the homozygote (data not shown) indicated the inserted pWH9 cassette was also spliced out together with exon 2. Since exon 2 harbours the same codon phase I as exon 1, the transcript was still in frame and gave a partial-deletion α -parvin protein. Thus, the second targeting strategy was designed to obtain complete deletion of α -parvin.

3.3.2 Preliminary phenotypic analysis of α -parvin E2 Δ /E2 Δ mice

A total 263 offspring from α -parvin⁺/E2 Δ crosses were genotyped. α -parvin exon 2 deletion homozygous mice are viable and fertile. Newborn offspring from α -parvin ⁺/E2 Δ mice crosses showed the normal Mendelian distribution (Table 3.3-1), while when genotyped at 3-4 weeks age, only 20% mice offspring were α -parvin E2 Δ /E2 Δ and 5% mutants were missing.

Table 3.3-1 The ratio of genotyped mice.

	total mice	+/+	+/E2 Δ	E2 Δ /E2 Δ
expected		25%	50%	25%
genotyped (3-4w)	195	29.2%	50.8%	20%
genotyped (new-born)	68	22.1%	52.9%	25%

3.3.2.1 α -parvin E2 Δ /E2 Δ mice are smaller

Although α -parvin E2 Δ /E2 Δ mice could develop to adult and were fertile, they were smaller than their littermates. The average body length of α -parvin E2 Δ /E2 Δ female mice was significantly shorter than control mice at 1 day, 1-week, 2- and 3-weeks-old ($P < 0.05$, $n = 6$ to 9 in each group; Figure 3.3-8). α -parvin E2 Δ /E2 Δ mice had lower body weight than control mice and the differences were significant at 4-weeks of age. At 4-week-old, the average body weight of α -parvin E2 Δ /E2 Δ female was around 75% of the control (Female mice: control 14.6 ± 1.3 g ($n = 28$), E2 Δ /E2 Δ 10.9 ± 3.2 g ($n = 14$); $P < 0.0001$. Male mice: con 15.5 ± 1.9 g ($n = 24$), E2 Δ /E2 Δ 11.8 ± 1.5 g ($n = 5$); $P < 0.0001$; Figure 3.3-9). The significantly shorter length of α -parvin E2 Δ /E2 Δ mice at newborn (P1) stage indicates that the deletion of exon 2 retards normal embryonic development. The reduction in body weight may be a second defect.

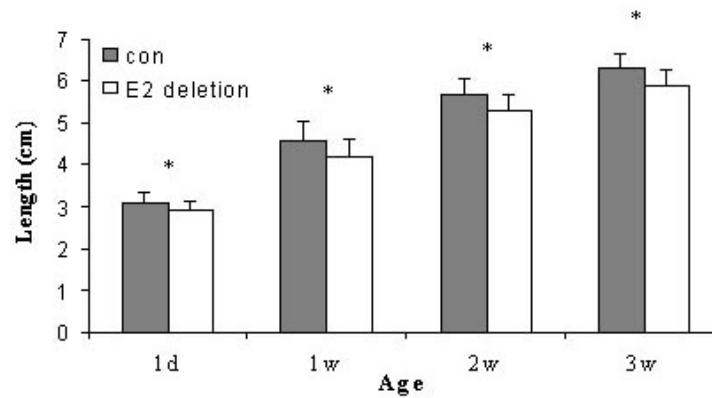


Figure 3.3-8 α -parvin E2 Δ /E2 Δ female mice have significantly shorter body length compared to control mice at 1-day, 1-week-, 2-weeks-and 3-weeks age (* $P < 0.05$, $n = 6$ to 9 in each group).

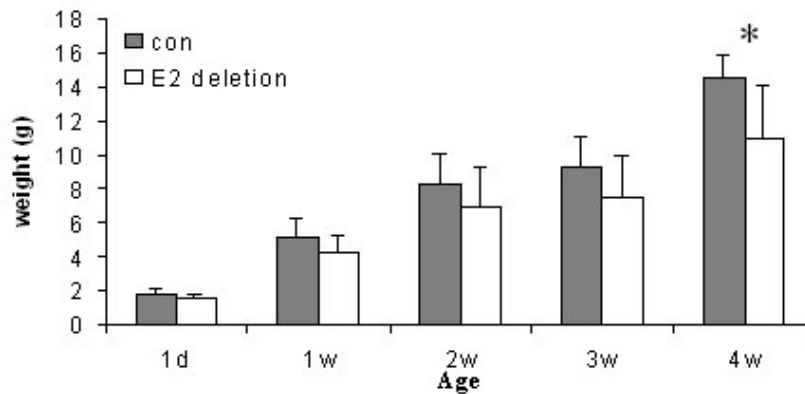


Figure 3.3-9 α -parvin E2 Δ /E2 Δ female mice have less body weight compared to control mice and the difference is significantly at 4-weeks- old age (* $P < 0.05$, $n = 6$ to 28 in each group).

3.3.2.2 α -Parvin E2 Δ /E2 Δ protein can localize to focal adhesion sites

To investigate whether α -parvin E2 Δ /E2 Δ protein can localize to focal adhesion sites as wildtype protein, cells isolated from the cartilage of newborn were stained with anti- α -parvin and paxillin antibodies. α -parvin E2 Δ /E2 Δ protein showed co-localization with paxillin (Figure 3.3-10).

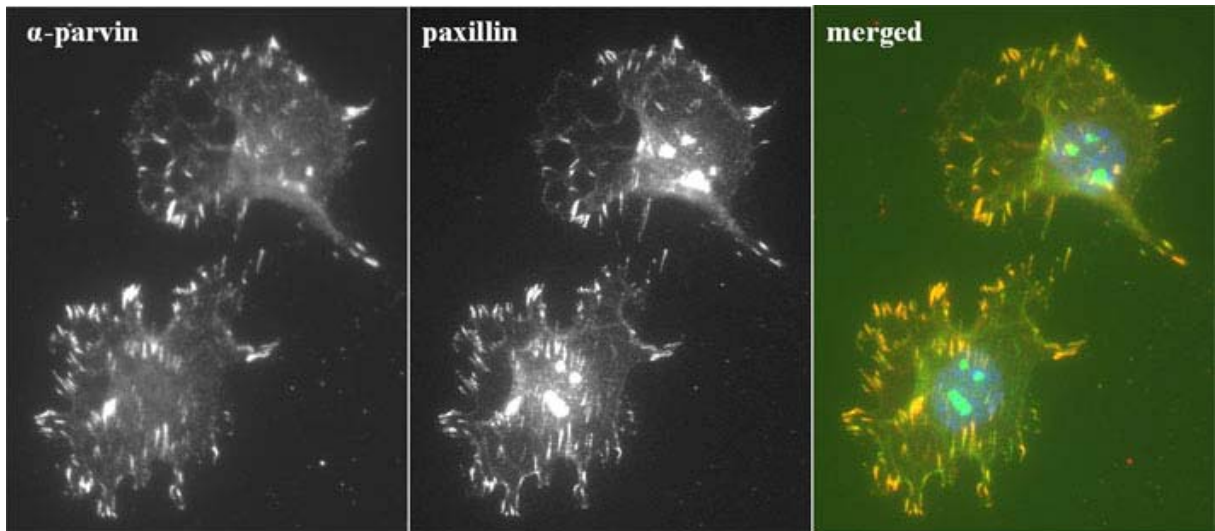


Figure 3.3-10 α -Parvin E2 Δ /E2 Δ protein can localize to FAs with paxillin. Cells isolated from the cartilage of an α -parvin E2 Δ /E2 Δ newborn mouse were stained with anti- α -parvin and paxillin antibodies. Blue, DAPI staining in the nucleus.

3.3.3 Generation of α -parvin null mice

To obtain α -parvin null mice, a second α -parvin knockout strategy was designed as shown in Figure 3.3-11. The pWH9 cassette was inserted into exon 2 and part of exon 2, intron 2 and part of exon 3 were deleted. This insertion should disrupt the gene and lead to no protein production. Even if the inserted cassette would be spliced out as happened in the first strategy, exon 1 would be spliced to exon 4, the transcript would be out of frame and give no functional peptide, since exon 1 harbors codon phase I while exon 3 displays a codon phase O (Table 3.2-1).

The second α -parvin targeting vector was built based on the first construct as shown in Figure 3.3-12. The 2nd targeting construct was electroporated into ES cells and the same experimental procedures were followed as for the first targeting construct. Three hundred sixty G418 ES clones were picked and 14% recombinant clones were identified with the external probe by Southern blot. No random integrations were detected with the internal probe in the recombinant ES clones (data not shown). One of the three blastocyst-microinjected ES clones (clone 28) gave highly chimeric mice and the chimeric male mice were mated with C57B6 females to obtain heterozygotes. The germline contribution of ES clones was confirmed by Southern blot (data not shown).

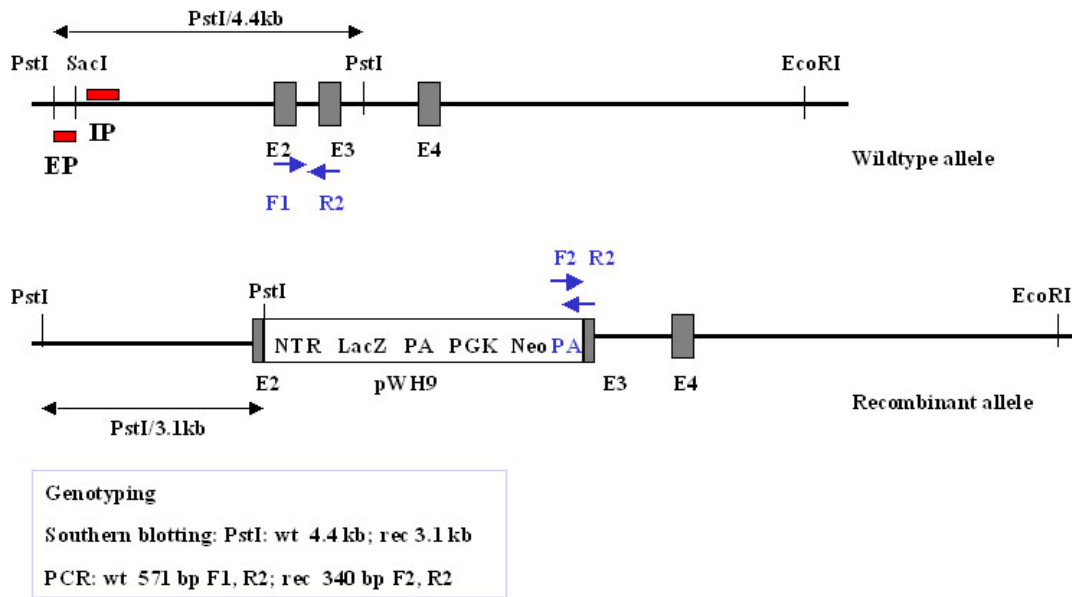
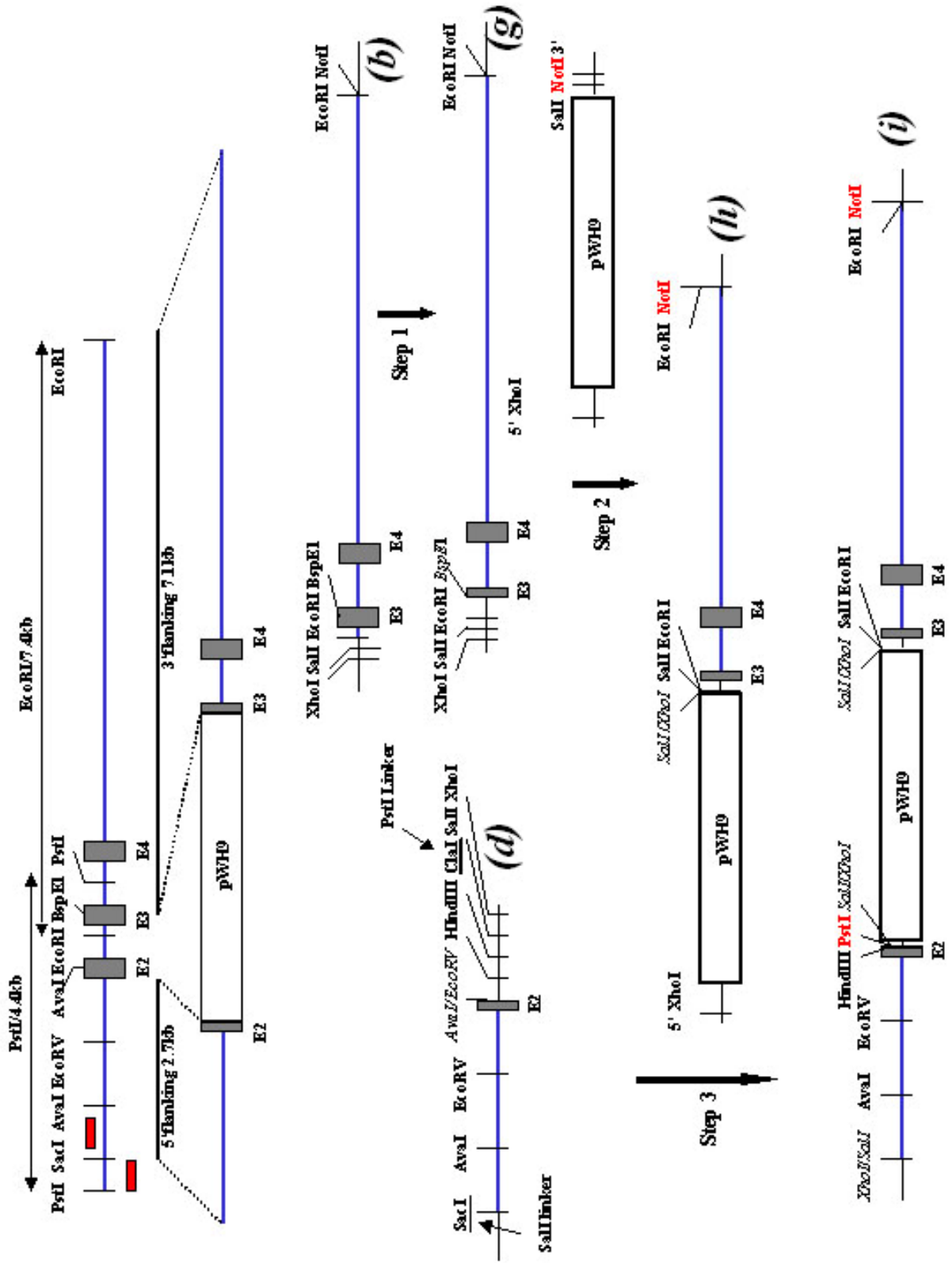


Figure 3.3-11 The 2nd α -parvin targeting strategy and genotyping strategy. The pWH9 cassette was inserted into exon 2 and part of exon 2, intron 2 and part of exon 3 were deleted. The genotyping for wildtype and recombinant alleles by Southern blotting was same as that for the first α -parvin targeting construct (figure 3). A three-primer PCR system (blue arrows) was used for genotyping. Primers F1 and F2 are as same as those used for the first construct. R3 primer was derived from exon 3 sequence (see Materials and Methods). F1/R2 amplified a 571-bp fragment on wildtype allele. F2/R2 amplified a 340-bp fragment that contains part of PGK PolyA and part of exon 3 sequence.

Figure 3.3-12 (next page) The 2nd α -parvin targeting strategy and the assembly steps for the targeting construct. The α -parvin 2nd targeting construct was modified based on the first construct (figure 2). In step 1, the plasmid *b* containing a 7.4 kb EcoRI fragments was digested with BspE1 and the DNA fragment ends were blunted with klenow and re-ligated (plasmid *g*). Thus part of exon 3 was deleted. In step 2, a 7.1kb XhoI/NotI fragment was removed with XhoI/enzymes from the plasmid *g* and ligated into the pWH9 vector that was linealized with SalI/NotI enzymes (plasmid *h*). In the final step 3, the SalI fragment from plasmid *d* (with a SalI linker at 5' end and a PstI enzyme site at 3' end) was isolated and ligated into the XhoI site of the plasmid *h* to get the final targeting construct - plasmid *i*.

The external and internal probes were as same as those of the first α -parvin targeting strategy (Figure 3.3-2). The grey boxes show exons. The solid blue lines stand for the genomic sequences of the gene. The thin lines indicate the short sequence of the multiple cloning sites of the vector. The restriction enzymes sites in italic indicate they were destroyed. The restriction enzymes in red were important enzymes that would be used for the linearization of targeting construct for the electroporation into ES cells (NotI, from pWH9 vector) and for genotyping of recombinant ES clones and mice (PstI).



3.3.4 α -parvin null mice are embryonic lethal

The offspring from α -parvin heterozygotes crossing were genotyped by Southern blot and PCR to identify α -parvin null mice. Among 108 offspring, no α -parvin homozygotes were identified. The ratio of heterozygotes to wildtype mice is close to 2:1 (Figure 3.3-13). This indicates α -parvin null mice are embryonic lethal.

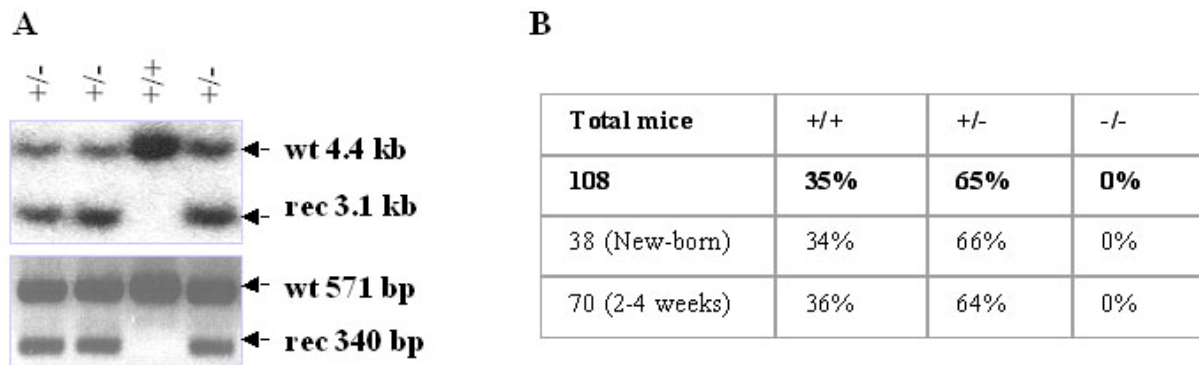


Figure 3.3-13 α -parvin homozygotes are embryonic lethal. (A) Offspring derived from α -parvin heterozygotes crossing were genotyped by Southern blotting (A, upper panel) and PCR genotyping (A, lower panel). (B) The ratio of genotyped offspring from α -parvin heterozygotes crossing.

4. Discussion and perspectives

4.1 Parvin peptide antibodies

Several parvin antibodies exist in the literature. For example, α -parvin full-length fusion proteins have been expressed to generate polyclonal and monoclonal antibodies (GST- α -actopaxin, Nikolopoulos et al., 2000; His-tagged α -parvin, Olski et al., 2001). Monoclonal antibodies were also produced using α -parvin residues 29-372 (GST-CH-ILKBP residues 29-372, Tu et al., 2001). An anti- β -parvin polyclonal antibody has also been generated by using human β -parvin(ss) as the antigen (GST-ss-affixin; Yamaji et al., 2001). Recently, the group of Wu generated another β -parvin monoclonal antibody using N-terminal residues 1-91 (Zhang et al., 2004). However, none of these reported antibodies are commercially available and no γ -parvin antibody has been reported so far.

Therefore, we generated our own anti-parvin peptide antibodies. This method was chosen for two reasons. First, the production of peptide antibodies is much less time consuming than other methods and, more importantly peptide antisera are extremely specific. This is an important issue due to the similarity of the three parvin proteins. The β -parvin monoclonal antibody generated against residues 1-92 aa of the protein also recognizes α -parvin when α -parvin is enriched in the lysate (Zhang et al., 2004), which is mostly likely due to the homology between the long N-terminal sequences of the two proteins. This can be avoided with peptide antibody production.

The disadvantage of peptide antibodies is the risk that they will not recognize the native proteins in immunohistochemistry staining or immunoprecipitation assays as the short peptides contain fewer possible epitopes than the full-length proteins. This disadvantage was realized in our β -parvin peptide antiserum which did not recognize native protein in MEF cells. Additionally, our β -parvin peptide antibody was unable to recognize β -parvin(s) and β -parvin(ss), since the corresponding peptide sequence is absent in the two shorter isoforms (Figure 3.1-3, spleen tissue). An antibody generated using a full-length fusion protein of the human β -parvin short form was shown to cross-react with mouse β -parvin and detected all three β -parvin isoforms (Yamaji et al., 2001). No such comparisons can be made for the γ -parvin antibody. One mouse γ -parvin EST lacks exon 4, so the translation may start from one of the ATGs in exon 6 (Figure 3.2-1). The γ -parvin peptide we used for antibody generation was encoded by exon 4. Therefore, the γ -parvin peptide antibody would not be able to recognize the putative short form of γ -parvin. In order to generate

antibodies that can detect all isoforms of β - and γ -parvins, we also used peptides derived from the C-terminus of β - and γ -parvins to generate antibodies. Unfortunately, both C-terminal peptide antisera failed to give specific signals on Western blot.

4.2 Expression profile of parvins and their associated proteins ILK and PINCH1 in the hematopoietic system

I confirmed the expression of the putative γ -parvin protein in the hematopoietic system on Western blot using our γ -parvin peptide polyclonal antibody. γ -parvin is highly expressed in, and relatively restricted to, lymphoid tissues such as BM, thymus, spleen, LN and PP, with the highest expression level in BM. Further, γ -parvin is specifically expressed at least in B220+, CD4+ and CD8+ cells, BM-derived macrophages and dendritic cells.

α -parvin is expressed in neither BM nor spleen single cell preps, nor in B220+ cells, CD4+ and CD8+ T cells, BM-derived macrophages and dendritic cells. These results indicate that α -parvin is not expressed in hematopoietic cells. The expression of α -parvin in lymphoid tissues arises from the stroma cells.

There are three β -parvin isoforms expressed in mouse (Yamaji et al., 2001). Our β -parvin antibody only detects β -parvin(l). The expression of β -parvin(l) in BM-derived macrophages and dendritic cells, but not in B220+, CD4+ and CD8+ subpopulations, indicates β -parvin(l) is expressed in myeloid lineages, but not in lymphoid lineages.

Three mouse β -parvin isoforms arise from different initiation codons on a single transcript and not from alternative splicing (Yamaji et al., 2001). The expression of β -parvin(l) and β -parvin(s) seems to be always coupled and they are co-expressed in the same tissue and same cell, and further, transfection of cells with β -parvin(l) cDNA leads to the expression of both β -parvin(l) and β -parvin(s) (Yamaji et al., 2001; Zhang et al., 2004). This suggests that the first two initiation codons are simultaneously active. The third initiation codon seems to be specifically active in spleen, as β -parvin(ss) is the major isoform expressed in spleen, and consistently, the predominant isoform in platelet (Yamaji et al., 2001; 2004).

Given the simultaneous activation of the first two initiation codons, the expression of β -parvin(l) may represent the expression of both β -parvin(l) and β -parvin(s), while β -parvin(ss) may also express in other hematopoietic cell types, in addition to platelets. A more complete expression profile of β -parvin in different hematopoietic cell types may be obtained by Northern blotting or RT-PCR, while the transcript cannot distinguish β -parvin isoforms. We are trying to express β -parvin-fusion proteins as antigens to generate new β -

parvin antibodies that should recognize all isoforms (Yamaji et al., 2001; Zhang et al., 2004).

ILK protein, an α - and β -parvin binding partner, is widely expressed at similar levels in lymphoid organs of BM, thymus, spleen, LN and PP. Like γ -parvin, ILK is expressed in B220+, CD4+, CD8+ cells, macrophages and dendritic cells. PINCH1 is expressed in macrophages and dendritic cells, weakly in B220+ cells, but not in CD4+ and CD8+ T cells. PINCH2 is not detectable in lymphoid tissues.

4.3 Subcellular localization of γ -parvin in fibroblasts

γ -parvin is not expressed in fibroblasts such as NIH/3T3 cells (Figure 3.1-3). Exogenously expressed C- or N-terminal Flag-tagged γ -parvins in NIH/3T3 cells displayed a cytoplasmic distribution and did not localize to FAs with ILK or paxillin (Figure 3.2-4). γ -parvin can form complexes with ILK and PINCH1 in spleen cells *in vivo* (Figure 3.1-8). ILK and PINCH1 have been found both in the cytoplasm and FAs (Pasquet et al., 2002; Campana et al., 2003; C. Grashoff and R. Fässler, unpublished data). The cytoplasmic ILK in platelets can be translocated to the membrane upon ADP or PMA stimulation and this translocation correlates with a transient increase in ILK kinase activity (Pasquet et al., 2002). The subcellular localization of PINCH1 also has been shown to shuttle between cytoplasm, nucleus and membrane (Campana et al., 2003). Therefore, it is possible that, like ILK and PINCH1, γ -parvin may localize in the cytoplasm.

The ILK-parvin interaction has been shown to be important to stabilize α -parvin (Fukuda et al., 2003), β -parvin (our unpublished data) and γ -parvin (Figure 3.2-11). Furthermore, the ILK- α -parvin interaction is important for both proteins to localize to FAs (Zhang et al., 2002). Therefore, it was important to check whether exogenously expressed γ -parvin also forms complexes with ILK and whether the binding of γ -parvin to ILK may facilitate its FA localization. However, only γ -parvin, but not ILK, was detected in the γ -parvin-Flag transfected NIH/3T3 cells with γ -parvin antibody in the immunoprecipitation assay, which indicates that γ -parvin-Flag cannot bind to ILK. The failure of γ -parvin to bind to ILK may explain the absence of γ -parvin at FAs in NIH/3T3 cells.

Both α - and β -parvins localize to FAs with ILK (Tu et al., 2001; Yamaji et al., 2001). Interaction of ILK with α - and β -parvin are mutually exclusive and the complexes formation between α -parvin and ILK is negatively regulated by β -parvin (Zhang et al., 2004). The amount of ILK that bound to α - or β -parvin (FA targeted ILK pool) seems constant, as overexpressing β -parvin did not immunoprecipitate more ILK compared to

expressing normal level of β -parvin, while the ILK that bound to α -parvin decreased (Zhang et al., 2004). Therefore, it is possible that the failure of γ -parvin to bind to ILK may be due to its lower binding affinity to ILK compared to α - and β -parvins, exogenously expressed γ -parvin cannot compete with endogenous α - and β -parvin for ILK binding and localizing to FAs. Cells that do not express α - and β -parvins will be used to further test this hypothesis. It has been shown that the interaction between α -parvin and ILK is essential, though not sufficient, for their efficient localization to cell-ECM adhesions (Zhang et al., 2002). Interactions with other proteins, such as paxillin are also essential for α -parvin targeting to FAs (Nikolopoulos and Turner). Thus, the association of γ -parvin with ILK and probably other proteins(s) may be essential to localize γ -parvin to FAs.

4.4 ILK-PINCH-parvin complexes

γ -parvin can form complexes with ILK and PINCH1 (Figure 3.1-12; 3.2-2). The ablation of γ -parvin downregulated both ILK and PINCH1 protein in lymphoid organs including BM, thymus, LN, and PP, where γ -parvin is the predominant parvin member, but not in spleen. In spleen, β -parvin(l) is expressed much more abundantly than in other lymphoid tissues (Figure 3.2-1). Furthermore, in spleen but not in thymus, β -parvin(ss) is expressed as the predominant β -parvin isoform at a much higher level than β -parvin(l) and β -parvin(s) (Yamaji et al., 2001). Therefore, like α -parvin, γ -parvin is important for maintenance of ILK and PINCH1, especially in cells where γ -parvin is the predominant parvin member. This is consistent with the published data showing that assembly of ILK-PINCH- α -parvin complexes promotes the stability of the proteins, a common function shared by different IPP complexes (Fukuda et al., 2003; Zhang et al., 2004).

ILK deletion in macrophages results in a strong inhibition of PKB/Akt phosphorylation on Ser473 associated with the ILK kinase activity. The inhibition of PKB/Akt activity promoted apoptosis (Troussard et al., 2003). Loss of ILK results in a dramatic reduction of α -parvin and β -parvin(l) (Zhang et al., 2003; our observation, data not shown). Considering the mutual dependence of IPP complexes, γ -parvin is probably reduced in the ILK-deficient hematopoietic cells. The phenotype of ILK-deficient macrophages is probably partially due to the decrease of both ILK-PINCH1- γ -parvin and ILK-PINCH1- β -parvin complexes, as γ - and β -parvin are co-expressed in macrophages (Figure 3.2-12).

4.5 γ -parvin is dispensable for normal hematopoiesis

γ -parvin is predominantly and specifically expressed in the hematopoietic system, including BM, thymus, spleen, LN and PP. Furthermore, γ -parvin expression starts at E7, and possibly even earlier (Korenbaum et al., 2001). That is the time when hematopoiesis begins in the yolk sac outside the embryo proper and HSCs migrate to the PAS/AGM (Morrison et al., 1995). This spatio-temporal expression pattern indicates that γ -parvin may play a role in the development of the hematopoietic system. However, no differences were found in the organization and distribution of B cells/T cells, and the cellularity of both central and peripheral lymphoid organs between control and γ -parvin null mice (Figure 3.2-13, 14, 15). FACS analysis using different hematopoietic lineage markers showed that γ -parvin null mice display normal development of hematopoietic lineages of B cells, T cells, granulocytes/macrophages, erythrocytes, and NK cells (NK cell data not shown), as compared to control mice. Further IgD and IgM stainings showed the normal development of B cells at different stages. Thus γ -parvin is dispensable for hematopoiesis. The formation of ILK-PINCH1- γ -parvin complexes is not crucial for hematopoiesis, since PINCH1 is only weakly expressed in B cells and absent in T cells (Figure 3.2-2). Although ILK is downregulated in γ -parvin null hematopoietic cells, the expression of β 1 and β 3 integrin was not changed (data not shown). Several experimental evidence suggested that β 1 integrin-mediated adhesion of HSC is important for their function in the BM (Potocnik et al., 2000). It has also been shown that β 1 integrin is not essential for HSC retention in the BM, for hematopoiesis or trafficking of lymphocytes (Brakebusch et al., 2002). γ -parvin null macrophages exhibit the same behavior of movement as control cells in an *in vitro* migration assay (data not shown).

4.6 γ -parvin is dispensable for T-cell dependent antibody response

γ -parvin transcription was reduced under certain pathological conditions, such as in Burkitt's lymphoma and leukemias, as well as colorectal adenocarcinoma (Korenbaum et al., 2001). The specific expression of γ -parvin in dendritic cells, macrophages, B and T cells suggests a potential role of the protein in the adaptive immune response.

Dendritic cells (DC) are extremely efficient APC at initiating primary T cell responses because they express high levels of MHC class II molecules, costimulatory molecules such as CD40 and B7 (CD86 and CD80) and other adhesion molecules. B cells share several important characteristics with other APC and also act as APC for CD4 T cells. CD40 on the B cell plays a critical role in isotype switching via an interaction with the CD40 ligand CD154. We observed similar maturation of γ -parvin null DCs and control cells *in vitro*

upon the stimulation of LPS. T-cell dependent antigen NP-CG requires interaction with T_H cells to stimulate B cells for antibody production. No significant differences were found in the anti-NP-CG antibody production between γ -parvin null mice and controls. γ -parvin null mice showed slightly, but not significant, increase in IgG1 and Ig λ production during the second immune response (Figure 3.2-19). We are currently determining the total amount of different immunoglobulins under physiologic conditions in γ -parvin null mice compared to controls to estimate their general ability to produce antibodies.

These data suggest a functional redundancy of γ -parvin, which may compensate for β -parvin. The phenotypic analysis of β/γ -parvin double knockout mice will deepen our understanding of these two proteins in the hematopoietic system. β -parvin and γ -parvin are located on the same chromosome and the distance between the two genes is less than 12 kb. Therefore we could not obtain β - and γ -parvin double knockout mouse by breeding crosses. Instead, we are trying to generate a β -parvin-null/ γ -parvin-floxed allele in ES cells. We built a γ -parvin exon 6 floxed construct. The deletion of exon 6 should lead to ablation of γ -parvin (Figure 3.2-6). The γ -parvin-floxed recombinant ES clones were microinjected to blastocysts check the germ-line transmission. The γ -parvin-floxed recombinant ES clones that went into the germ line were chosen for the electroporation of the β -parvin targeting construct and a single β -parvin recombinant clone was identified. We are currently breeding the β/γ -parvin chimeric mice for germline transmission.

4.7 α -parvin is critical for mouse embryo development

α -parvin null mice are embryonic lethal, which is consistent with the *in vivo* study of α -parvin/PAT-6, the sole parvin homolog in *C. elegans*. PAT-6 null worms die of a lethal defect in the assembly of muscle dense bodies that attach actin filaments to the sarcolemma (Lin et al., 2003). ILK-PINCH1- α -parvin complexes provide crucial physical linkages between integrins and the actin cytoskeleton and transduce diverse signals from the ECM to intracellular effectors and play important roles in many biological processes (Wu, 2004). ILK null mouse embryos die during the peri-implantation stage (Sakai et al., 2003), and PINCH1 null mice also die around embryonic stage E5.5-6.5 (R. Bordoy, A. Braun, R. Fässler, unpublished data). PINCH2 null mice do not show obvious phenotypes and no obvious upregulation of PINCH2 was observed in PINCH1-deficient MEF cells (F. Stanchi, R. Fässler, unpublished data). β -parvin null mice are viable and fertile (I. Thievessen, H. Chu, R. Fässler, unpublished data). β -parvin is upregulated in α -parvin-depleted cells (Zhang et al., 2004). The phenotype of α -parvin null mice may be the combined

consequence of the loss of α -parvin and increase in β -parvin, since ILK-PINCH1- β -parvin complexes are suggested to function as a pro-apoptosis mediator, contrast to the anti-apoptotic function of α -parvin.

Conditional deletion of ILK in chondrocytes leads to skeletal growth retardations characterized by abnormal chondrocyte shape and decreased proliferation *in vivo*, and diminished chondrocyte spreading on ECM and reduced stress fiber formation *in vitro* (Grashoff et al., 2003; Terpstra et al., 2003). The phenotype of the reduced chondrocyte proliferation in the absence of ILK is, at least partially, caused by the loss of ILK-PINCH1- α -parvin complexes, and probably other IPP complexes. A conditional deletion of α -parvin in chondrocytes will provide a valuable model to understand the mechanism of action of ILK in chondrocytes, and to dissect the distinct roles between the different components of the IPP complexes.

Thus, the analysis of α -parvin null mice will add valuable knowledge to functions of both parvins and the IPP complexes. I am currently trying to find out when α -parvin-null embryos die and to establish α -parvin-deficient cell lines for the study of the cellular functions of α -parvin.

4.8 Intact α -parvin is indispensable for normal embryo development

α -parvin E2-deletion mice are significantly smaller than their littermates, and show a reduction of the body length at birth. The mechanism underlying the phenotype is not clear yet. At 3-4 weeks old, 5% of the mutant mice die, and the weight of the mutant mice is significant lower than control mice after 4 weeks, which is probably a secondary defect, probably due to that the mutant mice cannot compete with the wildtype or heterozygote littermates for milk or defect in food absorption in the intestine. α -parvin is widely expressed in intestine, skin, lung, muscle and chondrocytes (Figure 3.1-6 and data not shown). The α -parvin E2-deletion protein can localize to FAs with paxillin as well as the wildtype protein (Figure 3.3-10). It is likely that the α -parvin E2-deletion protein binds to ILK through its intact CH2 domain (Zhang et al., 2004). α - and β -parvins are coexpressed in many tissues and cell types (Nikolopoulos and Turner, 2000; Yamaji et al., 2001). In MEF cells, α -parvin E2-deletion protein is expressed at a similar level as the full length protein in wildtype mice, while β -parvin(1) expression level in MEFs is not changed (data not shown). The normal FA localization of the α -parvin E2-deletion protein indicates that the defect during mutant mouse embryonic development is probably not directly related to the function of the IPP complexes, but due to other protein interactions with the N-terminus

of α -parvin, where 30 amino acids encoded by exon 2 are missing. These 30 amino acids contain a putative SH3 binding site (PLSP) and a putative serine (S19) phosphorylation site (Olski et al., 2001; Curtis et al., 2002). The N-terminus of α -parvin is phosphorylated by cyclin B1/cdc2 during mitosis and dephosphorylation occurs after mitosis in an adhesion-independent manner. There is evidence suggesting that yet unknown proteins may bind to the N-terminus and/or the CH1 region of α -parvin and/or β -parvin (Zhang et al., 2004; Yamaji et al., 2004). The new binding partner(s) of α -parvin may be identified by immunoprecipitation with our α -parvin polyclonal antibody.

4.9 Distinct roles of parvin paralogues

The structurally similar parvin paralogues have distinct roles both *in vitro* and *in vivo*, although they share some common features. α - and β -parvins have an identical domain architecture and share a high level of sequence similarity, yet play distinct and even contrasting roles in regulation of cell behavior. For example, α -parvin functions as an important anti-apoptotic protein, while β -parvin functions as a pro-apoptotic protein (Zhang et al., 2004). Consistent with this, recently Mongroo et al (2004) reported that the expression level of β -parvin, but not α -parvin, was downregulated in certain breast cancer cell lines and tumors, and the downregulation of β -parvin was suggested to contribute to the upregulation of ILK signalling. The functions of α - and β -parvin in cell shape modulation are also different (Fukuda et al., 2002; Zhang et al., 2004). Both α - and β -parvins, but not γ -parvin, localize to FAs in NIH/3T3 fibroblasts (Olski et al., 2001; Yamaji et al., 2001 and Figure 3.2-4).

The distinct roles of parvins are shown by our *in vivo* studies. α -parvin null mice die during embryonic development and the intact α -parvin protein is important for normal embryo development, while β -parvin null mice are viable and fertile (our unpublished data). The mice with the ablation of γ -parvin, which is specifically expressed in hematopoietic cells, show normal architectures in lymphoid organs and normal hematopoiesis. Thus, β - and γ -parvins that probably appear during evolution by gene duplication events are dispensable for embryogenesis.

The regulations between structurally similar parvin paralogues have been observed between α - and β -parvins and the regulations are at least partially through the IPP complexes. For example, interactions of α - and β -parvin with ILK are mutually exclusive and competitive (Zhang et al., 2004). α -parvin is absent in hematopoietic cells. β -parvin(1) is co-expressed with γ -parvin in certain hematopoietic cells, such as dendritic cells and

macrophages (Figures 3.2-12). However, no regulated change in expression was observed between β - and γ -parvin. Even in the β - and γ -parvins co-expressing dendritic cells and macrophages, β -parvin(l) expression levels were not changed in the absence of γ -parvin. Similarly, the expression γ -parvin protein in the β -parvin null lymphoid organs was not changed compared to wildtypes (I. Thievessen, H. Chu, R. Fässler, unpublished data). β -parvin may compensate the lost function of γ -parvin in those β - and γ -parvin co-expressing cells.

With its restricted expression profiles in hematopoietic cells, γ -parvin functions differently than α - and β -parvin. The studies presented in this thesis indicate γ -parvin is a functionally redundant parvin member, although structurally it promotes stability of ILK and PINCH1 in hematopoietic cells. β -/ γ -parvin double knockout in hematopoietic cells may reveal additional functions of γ -parvin.

5 Summary/Zusammenfassung

Cell interactions with extracellular matrix (ECM) are essential for various biological processes, including cell migration, proliferation, differentiation, regulation of gene expression and cell survival. The interactions mainly involve the integrin family, which links ECM to the actin cytoskeleton. The link between integrin and actin is mediated by cytoplasmic molecules. Among them, a novel family of focal adhesion associated proteins, parvins (α -, β - and γ -parvins), have been described. α - and β -parvins bind to integrin-linked kinase (ILK) and link integrins to the actin cytoskeleton.

With the parvin paralogue-specific peptide polyclonal antibodies we generated, I could show the expression profiles of parvins in the hematopoietic system. α -Parvin is absent in hematopoietic cells. The longest β -parvin isoform (β -parvin(l)) is expressed in hematopoietic cells, but not in B220+, CD4+ and CD8+ cells. γ -Parvin is highly expressed in lymphoid organs and specifically in B220+, CD4+ and CD8+ T cells. And both β -parvin(l) and γ -parvin are expressed in dendritic cells and macrophages. γ -Parvin can form ternary complexes with ILK and PINCH1 in spleen cells. However, unlike α and β -parvin, Flag-tagged γ -parvin expressed in NIH/3T3 fibroblasts displays a cytoplasmic distribution with no colocalization with paxillin, ILK or the tips of actin stress fibers. Further immunoprecipitation assays show that the Flag-tagged γ -parvin could not bind to ILK.

To analyze parvin functions *in vivo*, α - and γ -parvin mutant mice were generated by a genetic approach and the phenotypes of the mutant mice were analysed.

(1) γ -Parvin null mice are viable and fertile, and show normal architecture of lymphoid organs as demonstrated by HE staining and B and T cell immunostainings. The mutant mice have normal cellularity of lymphoid organs and FACS analyses show normal hematopoiesis in the mutant mice as compared to control mice. γ -parvin null mice exhibit similar T-cell dependent antibody responses as control mice. γ -parvin null BM-derived dendritic cells can mature normally *in vitro* as control cells. Both ILK and PINCH1 are downregulated in γ -parvin null hematopoietic cells compared to control cells, while the expression levels of α -parvin and β -parvin(l) are not changed in the absence of γ -parvin.

(2) No α -parvin null mice are identified from the offspring of heterozygote crosses, which suggests that α -parvin is critical for mouse embryogenesis.

(3) α -Parvin exon 2 deletion mutant mice are viable, but they are smaller and the new-born mutants have significant shorter body length compared to control littermates, although the

mutant protein can localize to focal adhesion sites with paxillin as well as the wildtype protein. Thus, an intact α -parvin is important for normal embryo development.

In summary, different parvin members seem to have distinct roles. The embryonic lethal phenotype of α -parvin-null mice indicates that β -parvin cannot take over the function of α -parvin during embryogenesis. β -parvin may compensate the loss of function of γ -parvin in the hematopoietic system. Alternatively, γ -parvin might be a functional redundant parvin member in the hematopoietic system.

Zusammenfassung

Die Interaktion von Zellen mit der extrazellulären Matrix (ECM) ist essentiell für viele biologische Prozesse. Dazu zählen Migration, Proliferation, Differenzierung, Regulation der Genexpression oder das Überleben der Zelle. Diese Interaktion wird hauptsächlich durch Proteine der Integrinfamilie vermittelt, welche die ECM mit dem Aktin-Zytoskelett verbinden. Die Verbindung zwischen Integrinen und Aktin wird durch zytoplasmatische Proteine hergestellt. Unter diesen befindet sich eine neue Familie von Proteinen, die mit fokalen Adhäsionskontakten assoziiert sind, die Parvine. Es sind 3 Isoformen, α -, β - und γ -Parvin beschrieben. α - und β -Parvin binden ILK (integrin linked kinase) und verbinden so Integrine mit dem Aktin-Zytoskelett.

Mit den von uns generierten Parvin subtyp-spezifischen polyklonalen Peptidantikörpern konnte ich das Expressionsprofil der einzelnen Parvine im hämatopoetischen System analysieren. α -Parvin fehlt in hämatopoetischen Zellen. Die längste von drei β -Parvin Isoformen ist in hämatopoetischen Zellen exprimiert, nicht jedoch in B220, CD4 und CD8 positiven Zellen. Im Gegensatz zu α - und β -Parvin ist γ Parvin fast ausschließlich in lymphoiden Organen und besonders in B220, CD4 und CD8 positiven Subpopulationen vertreten. In dendritischen Zellen und Makrophagen wird neben γ -Parvin auch β -parvin(l) exprimiert. γ -Parvin kann in Milzzellen einen ternären Komplex mit ILK und PINCH1 bilden. Im Gegensatz zu α - und β - Parvin zeigt ein in NIH/3T3 Fibroblasten exprimiertes, Flag-markiertes γ -Parvin zytoplasmatische Lokalisation. Eine Kolo-kalisation mit Paxillin, ILK oder den Spitzen von Aktin-Stressfasern konnte nicht beobachtet werden. In Ko-Immunopräzipitationsexperimenten konnte gezeigt werden, dass Flag-markiertes γ -Parvin nicht an ILK bindet.

Um *in vivo* Funktionen zu analysieren wurden α - und γ -Parvin defiziente Mäuse generiert und ihre Phänotypen analysiert.

(1) γ -Parvin knock-out Mäuse sind lebensfähig und fertil. Auch konnte in HE Färbungen und Immunfärbungen von B und T Zellen ein normaler Aufbau der lymphoiden Organe beobachtet werden. Die lymphoiden Organe der mutierten Mäuse zeigten normale Zellularität. In FACS-Experimenten wurde eine normale Hämatopoese der mutierten Mäuse beobachtet. Verglichen mit Kontrolltieren γ -Parvin null Mäuse zeigten keinen Unterschied in der Antikörperproduktion nach Stimulierung der T-Zellen. Auch zeigten γ -Parvin defiziente, vom Knochenmark gewonnene dendritische Zellen eine normale *in vitro* Reifung. Während ILK und PINCH1 in lymphoiden Organen von γ -Parvin defizienten Mäusen geringer exprimiert wurden als in Wildtypmäusen, konnte keine Änderung in der Expression von α - und β -Parvin beobachtet werden.

(2) Das Fehlen von homozygoten α -Parvin defizienten Nachkommen aus Verpaarungen von heterozygoten Mäusen lässt auf eine wichtige Rolle von α -Parvin in der Mausembryogenese schließen.

(3) Mäuse in denen das Exon 2 von α -Parvin deletiert wurde sind lebensfähig, aber kleiner als ihre wildtypischen Geschwister, obwohl das mutierte Protein ebenso mit Paxillin in fokalen Adhäsionen lokalisiert wie das Wildtypprotein. Ein intaktes α -Parvin ist daher wichtig für eine normale Embryonalentwicklung.

Zusammenfassend scheinen verschiedene Parvine unterschiedliche Funktionen zu haben. Der embryonal lethale Phänotyp der α -Parvin null Mäuse lässt vermuten, dass β -Parvin nicht dessen Funktion in der Embryogenese ersetzen kann. Den Verlust γ -Parvins im Hämatopoetischen System jedoch kann möglicherweise durch β -Parvin funktionell kompensiert werden. Alternativ kann eine funktionelle Redundanz zwischen β und γ -Parvin im hämatopoetischen System nicht ausgeschlossen werden.

6 ACKNOWLEDGEMENTS

The work presented in this thesis was initiated at the Department of Experimental Pathology at the University of Lund, Sweden in November 2001. Since January of 2002, the work was performed at the Max-Planck-Institute of Biochemistry in Martinsried, Germany. The work was carried out under the direction of Prof. Dr. Reinhard Fässler in the Max Planck Institute of Biochemistry in Martinsried and the supervision of Prof. Dr. Angelika Anna Noegel at the Center for Biochemistry, University of Cologne, Germany.

The work would have never been possible without many people to whom I am grateful. I wish to express my sincere gratitude to:

My supervisor **Prof. Dr. Reinhard Fässler**, for giving me the opportunity to be a PhD student in his group and introducing me to the field of integrin-related adhesion and signaling field, and for sharing his knowledge and providing stimulating guidance, and generous support through my PhD study.

My supervisor **Prof. Dr. Angelika Anna Noegel**, for the supervision and support and always being willing to listen, and for sharing with me her knowledge and ideas about the actin cytoskeleton.

Dr. Attila Braun, my “young supervisor”, for teaching me molecular cloning techniques. He initiated the parvin projects and screened the parvin positive PAC clones.

Ingo Thievensen, my co-worker of our “parvin family”, for his great contribution to the generation of the parvin antibodies, for the “family” discussions and for being a friend.

Dr. Michael Sixt for helping with the generation of dendritic cells and macrophages, macrophage in vitro migration assay and for stimulating discussions. Dr. Markus Moser for microinjection of α -parvin ES clones.

Dr. Cord Brakebusch for stimulating discussions. Gerd Bungartz, Tatjana Dorn, Sebastian Stiller, for sharing me their expertise in FACS and for being friends.

Drs. Günter Koster and Walter Göring, for the microscopy technique support, computer and laboratory support.

Mrs. Bettina Lauss, for helping with administrative matters in the University of Cologne.

Dr. Ari Waisman and Claudia Uthoff-Hachenberg in University of Cologne for helping with ELISA assay.

Drs. Kathryn Rodgers, Kyle Legate for careful reading and excellent English revision of this thesis. Drs. Ramin Massoumi and Martina Bauer for critical reading.

All members of the Department of Molecular Medicine, MPI, for their concern and help.

Finally, the most important persons in my life, my Mother, my Father and my Sister, for always showing their concern for me - I am grateful forever.

7 References list

- Attwell, S., Mills, J., Troussard, A., Wu, C., Dedhar, S. (2003) Integration of cell attachment, cytoskeletal localization, and signaling by integrin-linked kinase (ILK), CH-ILKBP, and the tumor suppressor PTEN. *Mol Biol Cell*. 14(12):4813-25.
- Brakebusch, C., Fillatreau, S., Potocnik, A.J, Bungartz, G., Wilhelm, P., Svensson, M., Kearney, P., Korner, H., Gray D, Fassler, R. (2002) Beta1 integrin is not essential for hematopoiesis but is necessary for the T cell-dependent IgM antibody response. *Immunity*. 16(3):465-77.
- Brakebusch, C., Fassler, R. (2003) The integrin-actin connection, an eternal love affair. *EMBO J*. 22(10):2324-33.
- Braun, A., Bordoy, R., Stanchi, F, Moser, M., Kostka, G., Ehler, E., Brandau, O., Fassler, R. (2003) PINCH2 is a new five LIM domain protein, homologous to PINCH and localized to focal adhesions. *Exp Cell Res*. 284(2):239-50.
- Brown, M.C., Turner, C.E. (2002) Roles for the tubulin- and PTP-PEST-binding paxillin LIM domains in cell adhesion and motility. *Int J Biochem Cell Biol*. 34(7):855-63.
- Brown, M.C., Turner, C.E. (2004) Paxillin: Adapting to Change. *Physiol Rev* 84:1315-1339.
- Campana, W.M., Myers, R.R., Rearden, A. (2003) Identification of PINCH in Schwann cells and DRG neurons: shuttling and signaling after nerve injury. *Glia*. 41(3):213-23.
- Cantley, L.C. (2002) The phosphoinositide 3-kinase pathway. 296(5573):1655-7.
- Cary, L.A., Han, D.C., Polte, T.R., Hanks, S.K., Guan, J.L. (1998) Identification of p130Cas as a mediator of focal adhesion kinase-promoted cell migration. *J Cell Biol*. 1998 Jan 12;140(1):211-21.
- Clark, K.A., McGrail, M., Beckerle, M.C. (2003) Analysis of PINCH function in Drosophila demonstrates its requirement in integrin-dependent cellular processes. *Development*. 130(12):2611-21.
- Clarke, D.M., Brown, M.C., LaLonde, D.P., Turner, C.E. (2004) Phosphorylation of actopaxin regulates cell spreading and migration. *J Cell Biol*. 166(6):901-12.
- Cohen, P., Frame, S. (2001) The renaissance of GSK3. *Nat Rev Mol Cell Biol*. 2(10): 769-76.
- Curtis, M., Nikolopoulos, S.N., Turner, C.E. (2002) Actopaxin is phosphorylated during mitosis and is a substrate for cyclin B1/cdc2 kinase. *Biochem J*. 363(Pt 2):233-42.
- Delcommenne, M., Tan, C., Gray, V., Rue, L., Woodgett, J., Dedhar, S. (1998) Phosphoinositide-3-OH kinase-dependent regulation of glycogen synthase kinase 3 and protein kinase B/AKT by the integrin-linked kinase. *Proc Natl Acad Sci U S A*. 95(19):11211-6.
- Delcommenne et al induce phosphorylation of the protein kinases PKB/Akt and GSK-3 β in cells overexpressing ILK.
- Downward, J. (1998) Mechanisms and consequences of activation of protein kinase B/Akt. *Curr Opin Cell Biol*. 10(2):262-7.
- Etienne-Manneville, S., Hall, A. (2002) Rho GTPases in cell biology. *Nature*. 420(6916):629-35.

Fukuda, T., Guo, L., Shi, X., Wu, C. (2003a) CH-ILKBP regulates cell survival by facilitating the membrane translocation of protein kinase B/Akt. *J Cell Biol.* 160(7):1001-8.

Fukuda, T., Chen, K., Shi, X., Wu, C. (2003b) PINCH-1 is an obligate partner of integrin-linked kinase (ILK) functioning in cell shape modulation, motility, and survival. *J Biol Chem.* 278(51):51324-33.

Geiger, B., Bershadsky, A., Pankov, R., Yamada, K.M. (2001) Transmembrane crosstalk between the extracellular matrix—cytoskeleton crosstalk. *Nat Rev Mol Cell Biol.* 2(11):793-805.

Gimona, M., Djinovic-Carugo, K., Kranewitter, W.J., Winder, S.J. (2002) Functional plasticity of CH domains. *FEBS Lett.* 513(1):98-106.

Gulbranson-Judge A, Tybulewicz VL, Walters AE, Toellner KM, MacLennan IC, Turner M. (1999) Defective immunoglobulin class switching in Vav-deficient mice is attributable to compromised T cell help. *Eur J Immunol.* 29(2):477-87.

Guo, L., Wu, C. (2002) Regulation of fibronectin matrix deposition and cell proliferation by the PINCH-ILK-CH-ILKBP complex. *FASEB J.* 16(10):1298-300.

Guo, W. and Giancotti, F.G. (2004) Integrin signalling during tumour progression. *Nat Rev Mol Cell Biol.* (10):816-26.

Grashoff C, Aszodi A, Sakai T, Hunziker EB, Fassler R (2003) Integrin-linked kinase regulates chondrocyte shape and proliferation. *EMBO Rep,* 4: 432-438.

Grashoff, C., Thievensen, I., Lorenz, K., Ussar, S., Fassler, R. (2004) Integrin-linked kinase: integrin's mysterious partner. *Curr Opin Cell Biol.* 16(5):565-71.

Greene, D.K., Tumova, S., Couchman, J.R., Woods, A. (2003) Syndecan-4 associates with alpha-actinin. *J Biol Chem.* 278(9):7617-23.

Hall, A. (1998) Rho GTPases and the actin cytoskeleton. *Science.* 279(5350):509-14.

Hannigan GE, Leung-Hagesteijn C, Fitz-Gibbon L, Coppolino MG, Radeva G, Filmus J, Bell JC, Dedhar S. (1996) Regulation of cell adhesion and anchorage-dependent growth by a new beta 1-integrin-linked protein kinase. *Nature.* 379(6560):91-6.

Hu, Y., Cascone, P.J., Cheng, L., Sun, D., Nambu, J.R., Schwartz, L.M. (1999) Lepidopteran DALP, and its mammalian ortholog HIC-5, function as negative regulators of muscle differentiation. *Proc Natl Acad Sci U S A.* 96(18):10218-23

Huang, Y., Wu, C. (1998) Integrin-linked kinase and associated proteins (review). *Int J Mol Med.* 3(6):563-72.

Hobert, O., Moerman, D.G., Clark, K.A., Beckerle, M.C., Ruvkun, G. (1999) A conserved LIM protein that affects muscular adherens junction integrity and mechanosensory function in *Caenorhabditis elegans*. *J Cell Biol.* 144(1):45-57.

Hynes, R.O. (2002) Integrins: bidirectional, allosteric signaling machines. *Cell.* 110(6):673-87.

Ishibe, S., Joly, D., Zhu, X., Cantley, L.G. (2003) Phosphorylation-dependent paxillin-ERK association mediates hepatocyte growth factor-stimulated epithelial morphogenesis. *Mol Cell.* 12(5):1275-85.

Janeway, Charles A. Immunobiology : the immune system in health and disease / Janeway, Jr. ... [et al.].-- 5th ed.

Kawabe, T., Naka, T., Yoshida, K., Tanaka, T., Fujiwara, H., Suematsu, S., Yoshida, N., Kishimoto, T., Kikutani, H. (1994) The immune responses in CD40-deficient mice: impaired immunoglobulin class switching and germinal center formation. *Immunity*. 1(3):167-78.

Kilmartin, J.V., Wrigh, B., Milstein, C. (1982) Rat monoclonal antitubulin antibodies derived by using a new nonsecreting rat cell line. *J Cell Biol*. 93(3):576-82.

Kim, U., Qin, X.F., Gong, S., Stevens, S., Luo, Y., Nussenzweig, M., Roeder, R.G. (1996) The B-cell-specific transcription coactivator OCA-B/OBF-1/Bob-1 is essential for normal production of immunoglobulin isotypes. *Nature*. 383(6600):542-7.

Korenbaum, E., Olski, T.M., Noegel, A.A. (2001) Genomic organization and expression profile of the parvin family of focal adhesion proteins in mice and humans. *Gene*. 279(1):69-79.

Kutsche K, Yntema H, Brandt A, Jantke I, Nothwang HG, Orth U, Boavida MG, David D, Chelly J, Fryns JP, Moraine C, Ropers HH, Hamel BC, van Bokhoven H, Gal A. (2000) Mutations in ARHGEF6, encoding a guanine nucleotide exchange factor for Rho GTPases, in patients with X-linked mental retardation. *Nat Genet*. 26(2):247-50.

Laird, P.W., Zijderveld, A., Linders, K., Rudnicki, M.A., Jaenisch, R., and Berns, A. Simplified mammalian DNA isolation procedure. (1991) *Nucleic Acids Res* 19(15):4293.

Lawlor, M.A., Alessi, D.R. (2001) PKB/Akt: a key mediator of cell proliferation, survival and insulin responses? *J Cell Sci*. 2001 Aug;114(Pt 16):2903-10.

Lee, J.W., Juliano, R. (2004) Mitogenic signal transduction by integrin- and growth factor receptor-mediated pathways. *Mol Cells*. 17(2):188-202.

Leung-Hagesteijn, C., Mahendra, A., Naruszewicz, I., Hannigan, G.E. (2001) Modulation of integrin signal transduction by ILKAP, a protein phosphatase 2C associating with the integrin-linked kinase, ILK1. *EMBO J*. 20(9):2160-70.

Li, B., Trueb, B. (2001) Analysis of the alpha-actinin/zyxin interaction. *J Biol Chem*. 276(36):33328-35.

Lin, X., Qadota, H., Moerman, D.G., Williams, B.D. (2003) *C. elegans* PAT-6/actopaxin plays a critical role in the assembly of integrin adhesion complexes in vivo. *Curr Biol*. 13(11):922-32.

Liu, S., Kiosses, W.B., Rose, D.M., Slepak, M., Salgia, R., Griffin, J.D., Turner, C.E., Schwartz, M.A., Ginsberg, M.H. (2002) A fragment of paxillin binds the alpha 4 integrin cytoplasmic domain (tail) and selectively inhibits alpha 4-mediated cell migration. *J Biol Chem*. 277(23):20887-94

Liu, S., Slepak, M., Ginsberg, M.H. (2001) Binding of Paxillin to the alpha 9 Integrin Cytoplasmic Domain Inhibits Cell Spreading. *J Biol Chem*. 276(40):37086-92.

Lutz et al., (1999) *J Immun Methods* 223:77-92.

Mackinnon AC, Qadota H, Norman KR, Moerman DG, Williams B.D (2002) *C. elegans* PAT-4/ILK functions as an adaptor protein within integrin adhesion complexes. *Curr Biol* 12(10):787-97.

- McGregor, A., Blanchard, A.D., Rowe, A.J., Critchley, D.R. (1994) Identification of the vinculin-binding site in the cytoskeletal protein alpha-actinin. *Biochem J.* 301 (Pt 1):225-33.
- Mishima, W., Suzuki, A., Yamaji, S., Yoshimi, R., Ueda, A., Kaneko, T., Tanaka, J., Miwa, Y., Ohno, S., Ishigatsubo, Y. (2004) The first CH domain of affixin activates Cdc42 and Rac1 through alphaPIX, a Cdc42/Rac1-specific guanine nucleotide exchanging factor. *Genes Cells.* 9(3):193-204.
- Morrison, S.J., Uchida, N., Weissman, I.L. (1995) The biology of hematopoietic stem cells. *Annu Rev Cell Dev Biol.* 11:35-71.
- Nikolopoulos, S.N., Turner, C.E. (2000) Actopaxin, a new focal adhesion protein that binds paxillin LD motifs and actin and regulates cell adhesion. *J Cell Biol.* 151(7):1435-48.
- Nikolopoulos, S.N., Turner, C.E. (2001) Integrin-linked kinase (ILK) binding to paxillin LD1 motif regulates ILK localization to focal adhesions. *J Biol Chem.* 276(26):23499-505.
- Nikolopoulos, S.N., Turner, C.E. (2002) Molecular dissection of actopaxin-integrin-linked kinase-Paxillin interactions and their role in subcellular localization. *J Biol Chem.* 277 (2): 1568-75.
- Nishiya, N., Tachibana, K., Shibamura, M., Mashimo, J.I., Nose, K. (2001) Hic-5-reduced cell spreading on fibronectin: competitive effects between paxillin and Hic-5 through interaction with focal adhesion kinase. *Mol Cell Biol.* 21(16):5332-45.
- Novak, A., Dedhar, S. (1999) Signaling through beta-catenin and Lef/Tcf. *Cell Mol Life Sci.* 56(5-6):523-37.
- Olski, T.M., Noegel, A.A., Korenbaum, E. (2001) Parvin, a 42 kDa focal adhesion protein, related to the alpha-actinin superfamily *J Cell Sci.* 114(Pt 3):525-38.
- Otey, C.A., Vasquez, G.B., Burridge, K., Erickson, B.W. (1993) Mapping of the alpha-actinin binding site within the beta 1 integrin cytoplasmic domain. *J Biol Chem.* 268(28):21193-7.
- Pavalko, F.M., Otey, C.A., Simon, K.O., Burridge, K. (1991) Alpha-actinin: a direct link between actin and integrins. *Biochem Soc Trans.* 19(4):1065-9.
- Pasquet, J.M., Noury, M., Nurden, A.T. (2002) Evidence that the platelet integrin alphaIIb beta3 is regulated by the integrin-linked kinase, ILK, in a PI3-kinase dependent pathway. *Thromb Haemost.* 88(1):115-22.
- Playford, M.P., Schaller, M.D. (2004) The interplay between Src and integrins in normal and tumor biology. *Oncogene.* 23(48):7928-46.
- Potocnik, A.J., Brakebusch, C., Fassler, R (2000). Fetal and adult hematopoietic stem cells require beta1 integrin function for colonizing fetal liver, spleen, and bone marrow. *Immunity.* 12(6):653-63.
- Prosper, F., Verfaillie, C.M. (2001) Regulation of hematopoiesis through adhesion receptors. *J Leukoc Biol.* 69(3):307-16.
- Reiske, H.R., Kao, S.C., Cary, L.A., Guan, J.L., Lai, J.F., Chen, H.C. (1999) Requirement of phosphatidylinositol 3-kinase in focal adhesion kinase-promoted cell migration. *J Biol Chem.* 274(18):12361-6.

Rosenberger, G., Jantke, I., Gal, A., Kutsche, K. (2003) Interaction of alphaPIX (ARHGEF6) with beta-parvin (PARVB) suggests an involvement of alphaPIX in integrin-mediated signaling. *Hum Mol Genet.* 12(2):155-67.

Ronty, M., Taivainen, A., Moza, M., Otey, C.A., Carpen, O. (2004) Molecular analysis of the interaction between palladin and alpha-actinin. *FEBS Lett.* 566(1-3):30-4.

Sakai, T., Li, S., Docheva, D., Grashoff, C., Sakai, K., Kostka, G., Braun, A., Pfeifer, A., Yurchenco, P.D., Fassler, R. (2003) Integrin-linked kinase (ILK) is required for polarizing the epiblast, cell adhesion, and controlling actin accumulation. *Genes Dev* 17(7):926-40.

Sastry, S.K., Burridge, K.(2000) Focal adhesions: a nexus for intracellular signaling and cytoskeletal dynamics. *Exp Cell Res.* 261(1):25-36. Review.

Shibanuma, M., Mochizuki, E., Maniwa, R., Mashimo, J., Nishiya, N., Imai, S., Takano, T., Oshimura, M., Nose, K. (1997) Induction of senescence-like phenotypes by forced expression of hic-5, which encodes a novel LIM motif protein, in immortalized human fibroblasts. *Mol Cell Biol.* 17(3):1224-35.

Sieg, D.J., Hauck, C.R., Ilic, D., Klingbeil, C.K., Schaefer, E., Damsky, C.H., Schlaepfer, D.D. FAK integrates growth-factor and integrin signals to promote cell migration. *Nat Cell Biol.* 2000 May;2(5):249-56.

Siegel DH, Ashton GH, Penagos HG, Lee JV, Feiler HS, Wilhelmsen KC, South AP, Smith FJ, Prescott AR, Wessagowit V, Oyama N, Akiyama M, Al About D, Al About K, Al Githami A, Al Hawsawi K, Al Ismaily A, Al-Suwaid R, Atherton DJ, Caputo R, Fine JD, Frieden IJ, Fuchs E, Haber RM, Harada T, Kitajima Y, Mallory SB, Ogawa H, Sahin S, Shimizu H, Suga Y, Tadini G, Tsuchiya K, Wiebe CB, Wojnarowska F, Zaghoul AB, Hamada T, Mallipeddi R, Eady RA, McLean WH, McGrath JA, Epstein EH. (2003) Loss of kindlin-1, a human homolog of the *Caenorhabditis elegans* actin-extracellular-matrix linker protein UNC-112, causes Kindler syndrome. *Am J Hum Genet.* 73(1):174-87.

Talts, J.F., Brakebusch, C., and Fässler, R. From: *Methods in Molecular Biology*, vol. 129: *Integrin Protocols*. Edited by: A.R. Howlett. Humana Press Inc., Totowa, NJ

Terpstra L, Prud'homme J, Arabian A, Takeda S, Karsenty G, Dedhar S, St-Arnaud R (2003) : Reduced chondrocyte proliferation and chondrodysplasia in mice lacking the integrin-linked kinase in chondrocytes. *J Cell Biol.* 162: 139-148.

Tong, X., Howley, .PM. (1997)The bovine papillomavirus E6 oncoprotein interacts with paxillin and disrupts the actin cytoskeleton. *Proc Natl Acad Sci U S A.* 94(9):4412-7.

Troussard, A.A., Mawji, NM., Ong, C., Mui, A., St -Arnaud, R., Dedhar, S (2003) Conditional knock-out of integrin-linked kinase demonstrates an essential role in protein kinase B/Akt activation. *J Biol Chem,* 278: 22374-22378.

Tu, Y., Li, F., Goicoechea, S., Wu, C. (1999) The LIM-only protein PINCH directly interacts with integrin-linked kinase and is recruited to integrin-rich sites in spreading cells. *Mol Cell Biol.* 19(3):2425-34.

Tu, Y., Huang, Y., Zhang, Y., Hua, Y., Wu, C. (2001) A new focal adhesion protein that interacts with integrin-linked kinase and regulates cell adhesion and spreading. *J Cell Biol.* 153(3):585-98.

- Tu Y, Wu S, Shi X, Chen K, Wu C. (2003). Migfilin and Mig-2 link focal adhesions to filamin and the actin cytoskeleton and function in cell shape modulation *Cell*. 113(1):37-47.
- Tumbarello DA, Brown MC, Turner CE. (2002) The paxillin LD motifs. *FEBS Lett*. 513(1):114-8
- Turner, C.E. (2000) Paxillin interactions. *J Cell Sci*. 113 Pt 23:4139-40.
- Turner CE *Nat Cell Biol*. 2000 Paxillin and focal adhesion signalling. 2(12):E231-6.
- Velyvis A, Vaynberg J, Yang Y, Vinogradova O, Zhang Y, Wu C, Qin J (2003) Structural and functional insights into PINCH LIM4 domain-mediated integrin signaling. *Nat Struct Biol*, 10: 558-564.
- Watton, S.J., Downward, J. (1999) Akt/PKB localisation and 3' phosphoinositide generation at sites of epithelial cell-matrix and cell-cell interaction. *Curr Biol*. 9(8):433-6.
- Webb, D.J., Donais, K., Whitmore, L.A., Thomas, S.M., Turner, C.E., Parsons, J.T., Horwitz, A.F. (2004) FAK-Src signalling through paxillin, ERK and MLCK regulates adhesion disassembly. *Nat Cell Biol*. 6(2):154-61.
- Wehland, J., Schroder, H.C., Weber, K. (1984) Amino acid sequence requirements in the epitope recognized by the alpha-tubulin-specific rat monoclonal antibody YL 1/2. *EMBO J*. 3(6):1295-300
- Weissman, I.L., Anderson, D.J., Gage, F. (2001) Stem and progenitor cells: origins, phenotypes, lineage commitments, and transdifferentiations. *Annu Rev Cell Dev Biol*. 17:387-403.
- Westhoff, M.A., Serrels, B., Fincham, V.J., Frame, M.C., Carragher, N.O. (2004) SRC-mediated phosphorylation of focal adhesion kinase couples actin and adhesion dynamics to survival signaling. *Mol Cell Biol*. 24(18):8113-33.
- Wu, C. (2004) The PINCH-ILK-parvin complexes: assembly, functions and regulation. *Biochim Biophys Acta*. 1692(2-3):55-62.
- Wu, C., Dedhar, S. (2001) Integrin-linked kinase (ILK) and its interactors: a new paradigm for the coupling of extracellular matrix to actin cytoskeleton and signaling complexes. *J Cell Biol*. 155(4):505-10. Epub 2001 Nov 05.
- Yamaji, S., Suzuki, A., Kanamori, H., Mishima, W., Yoshimi, R., Takasaki, H., Takabayashi, M., Fujimaki, K., Fujisawa, S., Ohno, S., Ishigatsubo, Y. (2004) Affixin interacts with alpha-actinin and mediates integrin signaling for reorganization of F-actin induced by initial cell-substrate interaction. *J Cell Biol*. 165(4):539-51.
- Yamaji, S., Suzuki, A., Kanamori, H., Mishima, W., Takabayashi, M., Fujimaki, K., Tomita, N., Fujisawa, S., Ohno, S., Ishigatsubo, Y. (2002) Possible role of ILK-affixin complex in integrin-cytoskeleton linkage during platelet aggregation. *Biochem Biophys Res Commun*. 297(5):1324-31.
- Yamaji, S., Suzuki, A., Sugiyama, Y., Koide, Y., Yoshida, M., Kanamori, H., Mohri, H., Ohno, S., Ishigatsubo, Y. (2001) A novel integrin-linked kinase-binding protein, affixin, is involved in the early stage of cell-substrate interaction. *J Cell Biol*. 153(6):1251-64.
- Zamir, E., and Geiger, B. (2001) Molecular complexity and dynamics of cell-matrix adhesions. *J Cell Sci*. 114:3583-3590.
- Zervas CG, Gregory SL, Brown NH. (2001) Drosophila integrin-linked kinase is required at sites of integrin adhesion to link the cytoskeleton to the plasma membrane. *J Cell Biol*. 152(5):1007-18.

Zervas CG, Brown NH (2002) Integrin adhesion: when is a kinase a kinase? *Curr Biol.* 12(10):R350-1.

Zhang, J., Zhang, L.X., Meltzer, P.S., Barrett, J.C., Trent, J.M. (2000) Molecular cloning of human Hic-5, a potential regulator involved in signal transduction and cellular senescence. *Mol Carcinog.* 27(3):177-83.

Zhang, Y., Chen, K., Guo, L., Wu, C. (2002a) Characterization of PINCH-2, a new focal adhesion protein that regulates the PINCH-1-ILK interaction, cell spreading, and migration. *J Biol Chem,* 277: 38328-38338.

Zhang, Y., Guo, L., Chen, K., Wu, C. (2002b) A critical role of the PINCH-integrin-linked kinase interaction in the regulation of cell shape change and migration. *J Biol Chem.* 277(1):318-26. Epub 2001 Nov 01.

Zhang, Y., Chen, K., Tu, Y., Velyvis, A., Yang, Y., Qin, J., Wu, C. (2002c) Assembly of the PINCH-ILK-CH-ILKBP complex precedes and is essential for localization of each component to cell-matrix adhesion sites. *J Cell Sci.* 115(Pt 24):4777-86.

Zhang, Y., Chen, K., Tu, Y., Wu, C. (2004) Distinct roles of two structurally closely related focal adhesion proteins, alpha-parvins and beta-parvins, in regulation of cell morphology and survival. *J Biol Chem.* 279(40):41695-705.

Erklärung/Statement

Ich versichere, dass ich die von mir vorgelegte Dissertation selbständig angefertigt, die benutzten Quellen and Hilfsmittel vollständig angegeben und die Stellen der Arbeit - einschließlich Tabellen und Abbildungen -, die anderen Werken im Wortlaut oder dem Sinn nach entnommen sind, in jedem Einzelfall als Entlehnung kenntlich gemacht habe; dass diese Dissertation noch keiner anderen Fakultät oder Universität zur Prüfung vorgelegen hat; dass sie – abgesehen von unten angegebenen beantragen Teilpublikationen – noch nicht veröffentlicht ist, sowie, dass ich eine Veröffentlichung vor Abschluss des Promotionsverfahrens nicht vornehmen werde. Die Bestimmungen dieser Promotionsordnung sind mir bekannt. Die von mir vorgelegte Dissertation ist von Professor Dr. Angelika Anna Noegel und Professor Dr. Reinhard Fässler betreut worden.

Martinsried bei München, den 25.01.2005

Haiyan Chu

The work contribution to the generation of β -parvin knockout and β/γ -parvin double knockout strains is not included in this thesis.

Curriculum Vitae

Haiyan Chu

Doctoral student
Prof. Dr. Reinhard Fässler's lab
Max Planck Institute of Biochemistry
Am Klopferspitz 18a
D-82152 Martinsried
Germany
Tel: +49-89-8578-2112
Fax: +49-89-8578-2422
Email: chu@biochem.mpg.de



Personal data

Date of birth: 7.1.1974
Place of birth: Jiangsu, China
Nationality: Chinese
Address: Am Klopferspitz 14c, D-82152 Martinsried, Germany

Education

Sept 1980 - July 1985 Primary school
Sept 1985 - July 1988 Primary Middle school
Sept 1988 - July 1991 High school

University Education

Sept 1991 - July 1996 Bachelor degree of Medicine, School of Public health,
Nanjing Medical University, China. Major: Preventive Medicine.

Graduate Education

Sept 1996 - July 2000 Master degree of Medical Science, Obstetrics and Gynaecology Hospital,
Medical School of Fudan University, Shanghai, China.

Research Orientation: Gynaecological Oncology
Supervisor: Prof. Youji Feng

Sept 2000- July 2001 Research student at Research Laboratory of Department of Obstetrics and
Gynaecology, Lund University, Sweden. Supervisor: Dr. Bertil Casslen

Aug 2001 - Dec 2001 Ph.D student at Department of Experimental Pathology, University of Lund,
Sweden. Supervisor: Prof. Dr. Reinhard Fässler

Doctoral study

Jan 2002 - Present Ph.D student at Department of Molecular Medicine, Max Planck Institute
of Biochemistry, Martinsried, Germany.

Project: *In vivo* analysis of parvins, a family of focal adhesion proteins
Supervisor: Prof. Dr. Angelika A. Noegel
Co-supervisor: Prof. Dr. Reinhard Fässler

Lebenslauf

Haiyan Chu

Doktorandin
Prof. Dr. Reinhard Fässlers Labor
Max-Planck-Institut für Biochemie
Am Klopferspitz 18a
D-82152 Martinsried
Deutschland
Tel: +49-89-8578-2112
Fax: +49-89-8578-2422
Email: chu@biochem.mpg.de

Personalangaben

Geburtsdatum: 7.1.1974
Geburtsort : Jiangsu, China
Staatsangehörigkeit: chinesisch
Adresse: Am Klopferspitz 14c, D-82152 Martinsried, Deutschland

Schulausbildung

Sept 1980 - July 1985 Grundschule
Sept 1985 - July 1988 Mittelschule
Sept 1988 - July 1991 Gymnasium

Studium

Sept 1991 - July 1996 Bachelor in Medizin, "School of Public health",
Medizinische Universität Nanjing, China. Hauptfach: Präventive Medizin.

Graduate Education

Sept 1996 - July 2000 Master der medizinischen Wissenschaften, "Obstetrics and Gynaecology Hospital" der medizinischen Hochschule der Universität Fudan, Shanghai, China. Forschungsschwerpunkt: Gynäkologische Onkologie. Betreuer: Prof. Youji Feng

Sept 2000- July 2001 Gaststudent am "Research Laboratory of Department of Obstetrics and Gynaecology", Universität Lund, Schweden. Betreuer: Dr. Bertil Casslen

Aug 2001-Dec 2001 Doktorandin am Universität Lund, Schweden.
Betreuer: Prof. Dr. Reinhard Fässler;

Promotionsstudium

Seit Jan 2002 Doktorandin am Max-Planck-Institut für Biochemie, Abteilung für Molekulare Medizin, Martinsried, Deutschland. Thema: *In vivo* Analyse von Parvinen, einer neuen Familie von fokalen Adhäsionsproteinen.
Betreuer: Prof. Dr. Reinhard Fässler;
Dissertationsbetreuer: Prof. Dr. Angelika A. Noegel

Martinsried bei München, 18.12.2004

Haiyan Chu